Short-term sediment resuspension on the continental slope and geochemical implications: the Faeroe-Shetland Channel

Jérôme BONNIN

Short-term sediment resuspension on the continental slope and geochemical implications: the Faeroe-Shetland Channel

Kortedurige sediment resuspensie op de continentale helling en de geochemische gevolgen hiervan: de Faeroe-Shetland Geul

(met een samenvatting in het Nederlands)

Remise en suspension des sédiments au niveau de la pente continentale liée à des processus rapides et les implications géochimiques: le Canal Faeroe-Shetland

(avec un résumé en Français)

Proefschrift

ter verkrijging van de graad van doctor
aan de Universiteit Utrecht,
op gezag van de Rector Magnificus Prof. Dr. W. H. Gispen
ingevolge het besluit van het College voor Promoties
in het openbaar te verdedigen
op vrijdag 6 Februari 2004 des middags te 12.45 uur

door

Jérôme BONNIN
Geboren op 10 Juni 1973, te Libourne, Frankrijk

Promotor: **Prof. Dr. P. Van Cappellen**
Department of Geochemistry
Utrecht University
Utrecht, The Netherlands

Co-promotores: **Dr. W. van Raaphorst†**
Department of Marine Chemistry and Geology
Royal Netherland Institute for Sea Research
Texel, The Netherlands

Dr. G.-J. A. Brummer
Department of Marine Chemistry and Geology
Royal Netherland Institute for Sea Research
Texel, The Netherlands

Dr. H. G. Epping
Department of Marine Chemistry and Geology
Royal Netherland Institute for Sea Research
Texel, The Netherlands

**In memory of Wim van Raaphorst
without whom this thesis would still
rest on the bottom of the Faeroe-
Shetland Channel**

Members of the dissertation committee

Contents

SAMENVATTING

Het onderzoek zoals beschreven in dit proefschrift is uitgevoerd om beter inzicht te krijgen in de samenhang tussen de samenstelling van het oppervlakte sediment op de continentale helling en de waterbeweging direct boven de bodem. Met name werd de invloed van sediment resuspensie onderzocht op de zonering van biogene en niet biogene deeltjes langs de helling. Tot dusver hebben de meeste studies op het gebied van sediment resuspensie zich gericht op de variaties in stroming die optreden op tijdschalen van seizoenen tot jaren. Het onderhavige onderzoek heeft zich juist gericht op de kortdurende mechanismen, die plaatsvinden op een tijdschaal van maximaal enkele uren. Het vernieuwende van deze studie bestaat uit de toegepaste combinatie van sedimentvallen, stroommeters en troebelheidssensoren, geplaatst op een continentale helling in een hoog-energetische omgeving. Omdat de instrumenten gegevens verzamelden met een zeer hoge tijdsresolutie (1 minuut voor de stroommeters) kon er waardevolle informatie worden verkregen over de kortdurende processen die samenhangen met de resuspensie van sediment. Aan deze kortdurende processen werd in het verleden weinig aandacht besteed omdat ze zo moeilijk te bestuderen zijn.

De continentale helling is een belangrijke, maar tevens complexe zone in de overgang van de diepe oceaan naar de ondiepe kustzee. Om te kunnen begrijpen wat er gebeurt met biogene deeltjes die met name in de kustzee worden geproduceerd is het noodzakelijk om de processen die tot resuspensie van sediment op de continentale helling leiden in meer detail te bestuderen. De grote multi-disciplinaire programma's die in de laatste twee decennia zijn uitgevoerd hebben aangetoond dat het transport van deeltjes langs de helling met name wordt veroorzaakt door de grote stroomsnelheid op het sediment-water-grensvlak. Kortdurende processen, zoals de inslag van interne golven op de continentale helling, zijn vaak genoemd om het optreden van sediment resuspensie en lateraal transport van deeltjes te verklaren. Slechts enkele *in situ* studies echter hebben daadwerkelijk het belang aangetoond van deze kortdurende processen voor sediment resuspensie en transport langs de helling. Een van deze studies wordt in dit proefschrift beschreven.

Hoofdstuk 2 beschrijft een serie verankeringen, uitgerust met sedimentvallen, troebelheidssensoren en stroommeters, die werd uitgezet op een transect loodrecht op de zuidoostelijke continentale helling van de Faroer-Shetland Geul. Zowel de hoeveelheden sediment die in de sedimentvallen werden opgevangen als de gemeten troebelheid van het water lieten duidelijk zien dat resuspensie processen verantwoordelijk waren voor de troebeling van het water en de hoeveelheid sediment dat in de sedimentvallen werd teruggevonden. Dichtbij de bodem werden hoge stroomsnelheden gemeten, wat op waterdieptes groter dan 470 m doorlopend tot resuspensie leidde. Ondieper dan 470 m werd geen resuspensie waargenomen omdat de ondergrond hier bestond uit vaste, grove zanden en zwerfkeien die nauwelijks geresuspendeerd kunnen worden. De sterkste resuspensie werd waargenomen op het middelste gedeelte van de helling (700-800 m). Op deze diepte

kon een enkele, intense resuspensie gebeurtenis worden waargenomen die in verband kon worden gebracht met een snelle verandering in zowel temperatuur als stroomsnelheid.

De massale sedimentstromen zoals die werden waargenomen op het middelste gedeelte van de helling, bleken veroorzaakt te worden door een plotseling, dwz binnen een minuut, omkeren van de stromingsrichting op de helling (hoofdstuk 3). Het passeren van interne, niet-lineaire golven ("solibores") bevorderde het ontstaan van grootschalige resuspensie. Gezien de periodiciteit van ongeveer 4 dagen wordt de solibore niet aangedreven door het getij, maar door atmosferische stormen. In dit hoofdstuk wordt aangetoond dat de wisselwerking van een dergelijk atmosferisch verschijnsel met de zeebodem een extra, mogelijk belangrijk, mechanisme kan zijn om sediment over de continentale helling naar de diepe oceaan te transporteren.

Hoofdstuk 4 beschrijft de verrijking met opgelost silicaat van het water dat de van de Faroer-Shetland Geul in zuidwestelijke richting passeert. Tijdens die passage blijkt de concentratie van opgelost silicaat in het water sterker toe te nemen dan uit het oplossen van neerregenend biogeen silicaat alleen (30-120 µmol m^{-2} d^{-1}) verklaard kan worden. Om de bijdrage van de sedimenten op de continentale helling aan dit proces vast te stellen werden de fluxen van opgelost silicaat berekend door de waterkolom heen en van vanuit het sediment naar het bovenstaande water toe. De hoogste silicaatfluxen, 1700 µmol m^{-2} d^{-1}, werden gevonden op het middelste gedeelte van de helling, tussen 600 en 800 meter, in een zone waar verhoogde sedimentafzetting plaatsvindt en het gehalte aan biogeen silicaat verhoogd is ten opzichte van diepere en ondiepere sedimenten langs de helling. Periodiek optredende resuspensie van bodemsediment lijkt te leiden tot een hogere concentratie van opgelost silicaat in het diepe water van de Faroer-Shetland Geul. Onze resultaten suggereren verder dat de geomorfologische vorm van het bekken, ondiep en met een trechtervorm, in combinatie met een sterke stroming de afzetting van relatief vers materiaal op het middelste deel van de helling bevorderd. Passerende watermassa's kunnen vervolgens vanuit het sediment worden verrijkt met opgelost silicaat.

In hoofdstuk 5 wordt een statistische analyse beschreven die werd uitgevoerd op de element concentraties die gemeten werden in monsters van sedimentvallen en oppervlaktesediment. De analyse laat zien dat het materiaal in de sedimentval een overeenkomst vertoont met het oppervlakte sediment van dieper dan 550 meter. Dit wijst erop dat deeltjes die door advectie van de continentale helling loskomen mogelijk niet afkomstig zijn van het bovenste deel van de helling of van het continentaal plat, maar een diepere bron hebben. Tussen monsters die zijn genomen op verschillende tijdstippen tijdens de resuspensie blijken duidelijke verschillen te bestaan in chemische samenstelling. Dat zou het gevolg kunnen zijn van de intensiteit van de resuspensie, maar het is ook mogelijk dat het brongebied van het materiaal anders is. De homogeniteit van de sedimenten en het ontbreken van duidelijk identificeerbare aanvoerbronnen maakt het moeilijk om te bepalen waar het geresuspendeerde sediment vandaan komt.

RESUME

Cette thèse a pour objectif de mieux comprendre les interactions entre les courants de fond et la remise en suspension des sédiments marins au niveau de la pente continentale d'une part et d'autre part d'évaluer l'impact de ces remises en suspension sur la distribution des éléments biogènes. Alors que la plupart des études portant sur le transfert des particules au niveau des marges océaniques se sont concentrées sur le rôle des variations saisonnières ou inter-annuelles du régime des courants, cette thèse se concentre tout particulièrement sur les processus rapides à l'origine des phénomènes de resuspension massive des sédiments de surface. L'aspect novateur de cette étude repose également sur la combinaison de résultats provenant de pièges à sédiments déployés près du fond, de néphélomètres et courantomètres échantillonnant avec une haute résolution et de sédiments de surface. Ainsi, ces données fournissent des informations précieuses sur les processus rapides qui, du fait de leur difficulté à être échantillonnés, ont été peu étudié.

Les pentes continentales sont des régions complexes qui connectent les mers marginales et l'océan profond. Une part importante de la productivité primaire globale se trouve au niveau des ces marges et rend l'étude de ces zones et des processus liés à la remise en suspension du matériel sédimentaire primordiale pour une meilleure connaissance du devenir de la matière particulaire et biogène dans les océans. Lors des deux dernières décennies, plusieurs programmes multidisciplinaires conduits sur diverses marges continentales ont montré que l'advection latérale, depuis le plateau continental jusqu'à la pente et les fonds abyssaux, contribuait de manière substantielle, au flux de matière biogène au niveau des sédiments de la pente. Ces études ont mis en évidence le rôle des grands courants de contour dans le transport des particules. Les processus à court-termes, tels que les tempêtes abyssales ou les frictions issues des interactions entre les ondes internes et les fonds sédimentaires, ont été souvent évoqués pour expliquer la création de niveaux très turbides et le transport latéral de ces matières en suspension vers le large. Toutefois, peu d'études réalisées *in situ* ont permis de montrer l'impact réel de ces processus sur la remise en suspension et la re-distribution des sédiments au niveau de la pente.

Avec pour objectif d'approfondir ces connaissances, des lignes de mouillage équipées de pièges à particules sédimentaires, de néphélomètres et de courantomètres ont été déployés à quelques mètres du fond le long d'une radiale perpendiculaire à la pente sud-est du Canal Faeroe-Shetland. Les résultats présentés dans le chapitre 2 indiquent clairement que le matériel récolté par les pièges à particules provient principalement de remise en suspension. La resuspension des particules sédimentaires est observée durant l'intégralité de la période d'échantillonnage pour les profondeurs supérieures à 470 m et est liée en partie aux forts courants de fonds. Pour le haut de la pente, bien que les courants soient élevés, peu ou pas de remise en suspension n'a été observée ce qui est du à la nature même du substrat, essentiellement composé de sables grossiers et consolidés, ainsi que de blocs erratiques d'origine glaciaire impossibles à éroder sous la seule action des courants. A la mi-pente (700-800m), la remise en suspension des sédiments est largement plus marquée où un événement particulièrement intense et abrupt associé à des changements rapides de

température et des courants des fonds a été enregistré. Ces changements hydrodynamiques, qui se sont produits en moins d'une heure, ont permis la resuspension massive des particules sédimentaires pendant plusieurs jours. Basé sur le contenu en carbone organique du matériel récolté dans les pièges ainsi que sur celui des sédiments de surface, un modèle multi-sources est utilisé pour reconstituer la composition relative du matériel à diverses profondeurs de la pente. Les résultats de ce modèle montrent que pendant les périodes de faible resuspension, les particules collectées correspondent à un mélange de débris issus de la production primaire (provenant de la couche photique) et de particules ayant déjà été en contact avec le fond avant d'être remis en suspension ('rebound particles'). Lors des périodes de forte resuspension, le matériel intercepté correspond à un mélange des deux sources précédemment décrites auxquelles s'ajoutent des particules plus réfractaires et lithogéniques grossières venant des sédiments plus anciens et plus profonds.

Dans le chapitre 3, une étude détaillée plus approfondie révèle que la remise en suspension des sédiments est liée à une inversion abrupte des courants vers le haut de la pente. La remise en suspension massive de sédiments décrite dans le chapitre 2, est associée au passage d'ondes internes se propageant vers le haut de la pente ('solibore'). L'érosion et le transport des sédiments sont plus précisément dus à l'intensification quasi instantanée de la vitesse verticale au niveau du front de ces ondes internes. Celle-ci résultant d'un cisaillement entre la vitesse de propagation de l'onde et la vitesse de la masse d'eau. Le forçage de ce phénomène semble être de nature non tidale et plutôt lié à des tempêtes atmosphériques. Même si l'origine de ce type d'événement est encore floue, nos résultats montrent que des processus à court-terme peuvent générer de forte remise en suspension des sédiments et occasionner leur transport vers le haut de la pente et ainsi limiter le transfert par gravité de matériel sédimentaire vers le bas de la pente.

Le chapitre 4 décrit une augmentation de la concentration de la silice dissoute (DSi) au niveau des eaux de fond dans le Canal Faeroe-Shetland qui, du fait de forts courants et de sa morphologie, a le potentiel de modifier les caractéristiques des masses d'eaux qui le traverse. Le recyclage de la silice biogène à l'interface eau-sédiment ainsi que dans la colonne d'eau a été estimé et les résultats indiquent que les sédiments de surface constituent la source principale de l'enrichissement en DSi et que la contribution de la dissolution des particules de silice biogène qui sédimentent est mineure. Il est aussi montré que la remise en suspension récurrente de sédiments de surface sous des conditions fortement turbulentes contribue à enrichir des eaux de fonds en DSi. Ces résultats révèlent aussi l'importance de la géomorphologie du basin. Avec sa forme en entonnoir, une forte stratification et des forts courants de fonds légèrement orientés vers le haut de la pente, il agit comme un piège à sédiments naturel et favorise le dépôt des sédiments et les flux de DSi à la mi-pente.

Dans le chapitre 5, l'analyse géochimique des sédiments de surface ainsi que des particules récoltées dans les pièges à sédiments à divers périodes d'échantillonnage montre que les particules remises en suspension ont une composition proche de celle des sédiments de surface prélevés à des profondeurs supérieures à 550 m. Cette analyse suggère par ailleurs que sur la pente SE du Canal Faeroe-Shetland les particules advectées ne proviennent pas du plateau ou de la partie supérieure de la pente mais d'une zone plus profonde. L'analyse multi-variables de la composition chimique des particules, issues de resuspension massive et interceptées à différentes périodes indiquent des caractéristiques

différentes suivant les périodes. Ces différences sont interprétées comme le résultat de l'intensité du mécanisme de remise en suspension qui toucherait des sédiments plus ou moins profonds bien qu'il ne soit pas exclu que les sédiments puissent venir de sources différentes. Toutefois, l'homogénéité de la composition des sédiments sur la pente, principalement due à des dépôts glaciaires ubiquistes, à de forts courants de fonds et à l'absence d'apports continentaux clairement identifiables, rend la localisation des sources des sédiments remis en suspension dans le Canal Faeroe-Shetland particulièrement difficile.

SUMMARY

The objectives of the study described in this thesis were to better understand the interactions between near-bottom currents and surface sediments of the continental slope, and to assess the impact of sediment resuspension on the cross-slope redistribution of biogenic and non-biogenic particles. While most of the studies conducted on sediment resuspension on continental margins have investigated the role of seasonal to inter-annual variations of the near-bottom currents, this thesis particularly focuses on short-term (tidal to sub-tidal) mechanisms. The novel aspect of this work lies in the combination of fast sampling near-bottom sediment traps, turbidity sensors and current meters moored on a high-energy continental slope. High-resolution studies have the potential to provide valuable information on the short-term processes involved in sediment resuspension, which, due to their difficulty to be resolved, have not received much attention, yet.

Continental slopes are important and complex regions that connect shallow shelf seas with the deep ocean. Since a large part of the global primary productivity takes place on the continental margins, knowledge on sediment resuspension and associated processes on the continental slope is crucial to understand the fate of particles, including biogenic debris. During the last two decades, large multidisciplinary programmes conducted on continental margins have shown that cross-slope advection caused by strong boundary currents contribute substantially to the flux of biogenic debris to the slope sediment. Short-term processes, such as internal waves impinging on the slope, have often been invoked to explain sediment resuspension and lateral particle transport but few *in situ*, studies have provided direct evidence of the impact of these processes on resuspension and transport of sediments across the slopes.

Chapter 2 describes an array of moorings equipped with near-bottom sediment traps, turbidity sensors and current meters that were deployed on a section perpendicular to the south-eastern continental slope of the Faeroe-Shetland Channel. Both total mass flux and the turbidity record near the bottom indicated that the material collected in the traps was associated with sediment resuspended from the seabed. Sediment resuspension was observed at all times at depths greater than 470 m, and was related to the high bottom-current speeds measured in the study area. At depths above 470 m little or no resuspension was observed, although currents measured near the bottom were strong. This absence of resuspension is attributed to the nature of the substrate, essentially composed of coarse and consolidated sand as well as glacial boulders that are not likely to be eroded under the action of currents. Sediment resuspension was most pronounced at mid-slope depths (700-800 m) where an exceptionally intense event was observed in association with rapid changes, both in temperature and near-bottom current velocity. These changes in hydrodynamics occurred within one tidal cycle and resulted in particles being kept in suspension for several days. Based on the organic carbon content of the material intercepted in the sediment trap samples and the surface sediments, a simple end-member model was used to assess the relative composition of the resuspended material in the traps at various depths across the slope. Results suggest that during periods of low resuspension

(background sediment flux) the material intercepted in the near-bottom traps is a mixture of debris from primary production settling through the water column and rebound particles that have already encountered the seabed before being resuspended. During the period of maximum resuspension, the intercepted material is a mixture of three end-members, the two observed for low resuspension plus the sediment proper made up of coarse and refractory particles that can constitute up to 70% of the flux.

In chapter 3, a detailed study shows that the observed massive sediment fluxes at mid-slope were associated with a sudden reversal of the current from down to up slope occurring within a minute. Massive sediment resuspension was facilitated by the passage of internal non-linear waves ("solibore") travelling up the slope. Sediment was resuspended by strong vertical velocities at the leading edge of the solibore and entrained upward in turbulent waves as previously suggested by laboratory and numerical experiments. The forcing of the solibore appeared not to be of tidal origin, as it had a ~4-day period, but rather to be related to atmospheric storms. This chapter shows that the interaction of such a phenomenon with the seabed can provide a potentially dominant mechanism for upward transport of sediment over continental slopes that may counteract downward avalanching of material by gravity.

Chapter 4 describes the enhanced refuelling of silicic acid (DSi) in the narrow Faeroe-Shetland Channel (FSC), which has the potential to substantially affect characteristics of passing water masses due to its "bottleneck-like" geomorphology. To establish the contribution of t slope sediments to this refuelling, fluxes of DSi in the water column were calculated from the DSi concentration gradient and the vertical eddy diffusion coefficient. Fluxes showed a maximum at mid-slope (600-800 m) with values reaching up to 1700 µmol m^{-2} d^{-1} near the seabed. The mere dissolution of settling biogenic silica, estimated at 30-120 µmol m^{-2} d^{-1} cannot account for this refuelling of the deep-waters of the FSC with DSi. Benthic DSi efflux on the slope, obtained from incubations and from modeled pore water DSi profiles, both indicated highest fluxes at mid-depth corresponding to a zone of enhanced deposition and higher biogenic silica content. Benthic fluxes of DSi at mid-depth are on the order of 1000 µmol m^{-2} d^{-1} and can for most part explain the calculated flux in the water column at around 700 m. Furthermore, we estimated that the recurrent resuspension of bottom material as observed at mid-slope associated with turbulent flow contributes to increase the DSi concentration in the deep water of the FSC. Our data emphasizes the importance of the geomorphological setting of the basin which, with its shallow depth and funnel shape combined with strong currents slightly oriented up the slope favors the accumulation of relatively fresh sediments at mid-slope depths, hence facilitating refuelling of passing waters with DSi from the benthic boundary layer and the sediment.

In chapter 5, statistical analyses of multi-elemental concentrations from surface sediments and sediment trap material indicate that the intercepted material has a composition similar to that of surface sediments from depths greater than 550 m. This suggests that on the SE slope of the Faeroe-Shetland Channel particles advected on the slope do not originate from the upper slope or shelf edge but from a deeper source area. Multi-elemental and grain size analysis from samples collected during distinct resuspension events showed differences among samples. These differences are interpreted as the result of

the intensity of the resuspension mechanism although it cannot be excluded that they originate from different source areas (e.g., due to a different resuspension mechanism). The lack of clearly identifiable continental input sources, the homogeneity of the surface sediments, mainly uniform glacial debris deposits, the high-energy currents, and the high frequency of intense resuspension, make the identification of the source area of resuspended material a particularly difficult task.

The results presented in this thesis show the importance of the short-term processes in the resuspension of sediment on the slope and in the transfer of biogenic materials from the shelf to the deep ocean. This transfer may have significant implications for organic matter recycling along the ocean margins. This work represents the first step towards a better understanding of these potentially very active processes. Clearly, further investigations are needed, particularly for the highly productive ocean margins such as areas with high continental input or coastal upwelling regions, which are also receiving much attention in terms of their paleo-climatological significance. Furthermore, high-energy processes as described in Chapter 3 and the associated massive sediment transport and organic matter recycling illustrated in Chapters 2, 4 and 5 may create major perturbations of the sedimentary signal and lead to erroneous interpretation of proxy data.

CHAPTER 1

Introduction

Sediment resuspension and the transport of particulate matter on continental slopes: A case study of the Faeroe-Shetland Channel.

Ocean margins and slopes constitute important and complex regions that connect the shallow highly productive shelves influenced by strong continental input with the deep ocean (Wollast, 1991). The quantification of the fluxes of dissolved and particulate matter across these margins is therefore necessary to evaluate the global biogeochemical cycles of carbon and associated elements in the oceans. Such quantification requires an understanding of the dominant transport and conversion mechanisms occurring on the slopes.

During the past decade, several multidisciplinary programmes on continental margins have shown that organic matter originating from primary production on the shelf is exported to the slope and the abyssal regions. These programmes include SEEP I and II in the Middle Atlantic Bight (Walsh et al., 1988, Biscaye et al., 1994, Biscaye and Anderson, 1994), OMEX I at the Goban Spur (Van Weering et al. 1998; Wollast and Chou, 2001; Van Weering et al., 2001) and OMEX II at the western Iberian margin (Antia and Peinert, 1999; Herman et al., 2001; Epping et al., 2002) and ECOMARGE in the Gulf of Lions (Monaco et al., 1990). These studies have pointed out that vertical settling of primary particles, as determined by sediment trap analysis, is not sufficient to balance total mass and carbon budgets and lateral advection of particulate matter was invoked (Fig. 1). Lateral transport of particles along the margins and from the shelves to the deep ocean mainly takes place within layers of enhanced turbidity that are confined near the seabed (Jahnke et al., 1990; Anderson et al., 1994).

In the original hypothesis of Walsh (1981) large quantities of shelf-produced material are exported across the shelf edge and deposited on the slope. Results from the SEEP I experiment suggested that preferential deposition occurred on those sites of the slope where the turbulent kinetic energy density in the bottom water is sufficiently low (Csanady, 1988; Biscaye et al., 1988), the so-called "depocenters" (Walsh, 1988). Although the results from SEEP II (Biscaye et al., 1994) and OMEX I and II did not provide evidence of the presence of organic-rich depocenters on the slope, they indicated accumulation of refractory material originating from relict sources on the slope (Van Weering et al. 1998; Wollast et al., 2001; Van Weering and McCave, 2002). The results of the OMEX I at the Goban Spur have indicated that there is a clear relation between the strong boundary currents occurring in this area and the distribution of particles derived from the shelf edge by resuspension (Van Weering et al., 1998, 2002). Under the action of these strong boundary currents, fine particles are resuspended to form bottom nepheloid layers (McCave, 1986; Dickson and McCave, 1986; Biscaye and Anderson, 1994; Van Weering et

al., 1998; Monaco et al., 1999; Durrieu de Madron et al., 1999). Resuspended particles have also been shown to detach from the bottom on the outer shelf, the shelf break or the upper slope and to spread off the slope along isopycnal surfaces (Fig. 2) to form intermediate nepheloid layers (McCave, 1986; Walsh and Nittrouer, 1999; McCave et al., 2001). Recently, some studies have shown the importance of short-duration processes for the creation of sediment resuspension and intermediate nepheloid layers. Heavy wind-induced storms on the shelf (Churchill et al., 1994; Brunner and Biscaye, 1997; Chang et al., 2001; Vitorino et al., 2002), breaking of internal tides on the sloping bottom (Cacchione and Drake, 1986; Dickson and McCave, 1986; Thorpe and White, 1988; Atzetsu-Scott et al., 1995; Wang et al., 2001; Moum et al., 2002), or propagation of internal solitary waves (e.g., Bogucki et al., 1997) have been invoked to explain sediment resuspension. Furthermore, the results of ECOMARGE in the Gulf of Lions (Monaco et al., 1999; Durrieu de Madron et al., 2000) and OMEX II on the Iberian margin (Epping et al., 2002) have illustrated the importance of particle transfer to the deep ocean by way of submarine canyons. Gardner (1989a, b) has shown that focussing of internal waves in submarine canyons can substantially contribute to erosion, resuspension and down-slope transport of particulate matter.
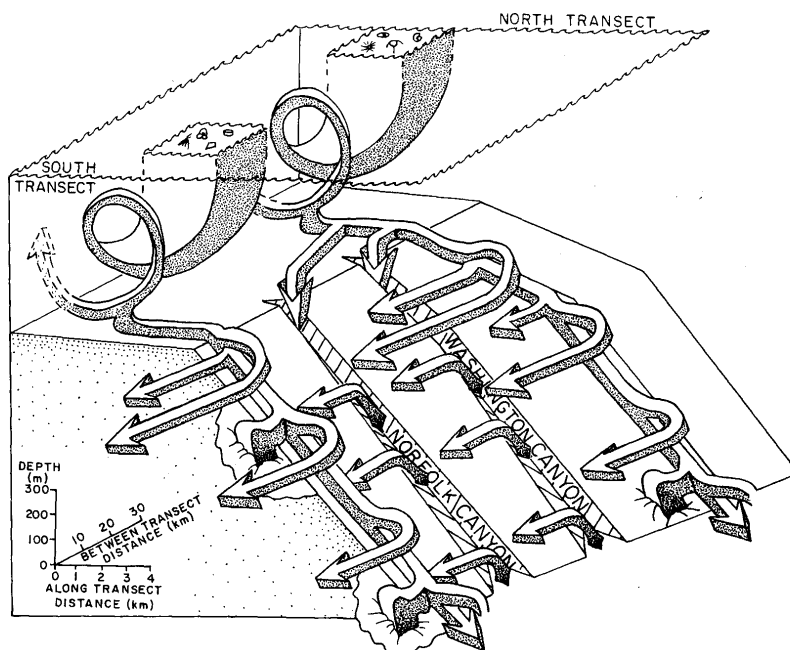
Fig. 1. Schematic diagram illustrating the importance of lateral advection and boundary currents in influencing the transport and fate of particles to and through the SEEP area. Reprinted from Biscaye and Anderson, 1994, Deep-Sea Research, Vol 41, p 493, with permission from Elsevier Science.

Most of the information obtained on the behaviour of internal tides and waves however originate from theoretical or laboratory studies. Detailed measurements of resuspension fluxes on the continental slope are scarce and very few have been able to observe *in situ* the impacts of these short-term features on sediment resuspension. Furthermore, nepheloid layers observed on the continental margins are snap-shot distributions of highly variable suspended matter concentrations which are difficult to relate to the weekly integrated mass fluxes normally measured with sediment traps and it is even more difficult to compare with long-term sediment accumulation rates. The intermittent nature of the nepheloid layers indicates that the mechanisms responsible for their generation are related to short-term but highly energetic processes.
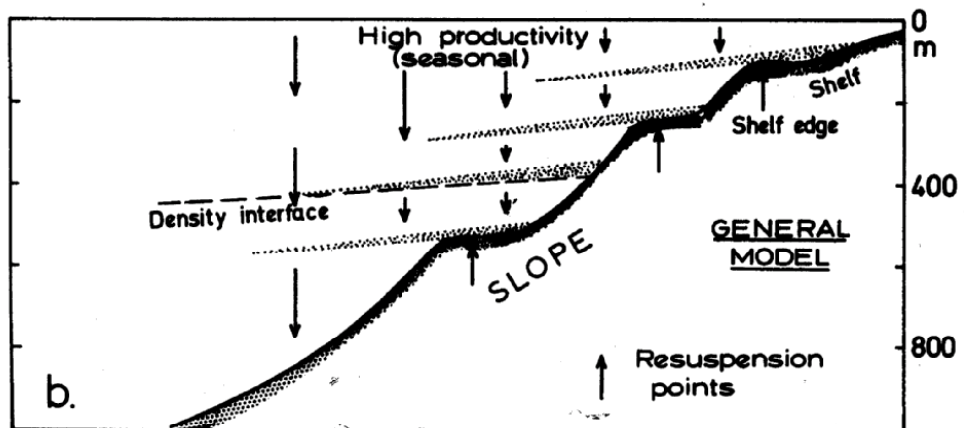
Fig. 2. *Sketch showing the formation of intermediate nepheloid layers (INL) and spreading seawards along density interface (isopycnal surfaces). It also illustrates the down-slope transport of particulate matter within the bottom nepheloid layer (BNL). Reprinted from Dickson and McCave, 1986, Deep-Sea Research, Vol 33, p 816, with permission from Elsevier Science.*

Few studies carried out on sediment distribution, particulate matter transfer and recycling of organic matter on continental slopes have investigated the role of such processes (e.g., Dickson and McCave, 1986; Gardner, 1989a; Chang and Dickey, 2001) and to our knowledge none of them combined high-resolution near-bottom sediment fluxes with current speed data. Furthermore, understanding the short-term processes and the forcing mechanisms of cross-slope transport of particles is of primary importance for better quantification and modelling of the fate of organic carbon.

In a pilot study of the PROCS (PROcesses at the Continental Slope) programme, Van Raaphorst et al. (2001) showed that critical reflection of internal waves may sustain sediment resuspension and subsequent down-slope transport in a benthic nepheloid layer. Bearing this in mind, we deployed within the framework of PROCS an array of moorings combining near-bottom high-resolution sampling sediment traps with high frequency observation of current meters and turbidity sensors (OBS).

The PROCS programme is an integrated study on the SE continental slope of the Faeroe-Shetland Channel combining physical, sedimentological, geochemical and biological investigations. The main objectives of PROCS were to determine the relation between the short-term variability of the hydrodynamic conditions and the cross-slope transport and fluxes of particulate biogenic matter and to assess the impact of these processes on the distribution of benthic fauna across the slope. A driving idea behind the project was that repeated critical reflections of internal waves (i.e. when the angle of the slope equals the angle of the wave) propagating parallel to the sloping bottom, would dissipate sufficient energy by turbulent mixing to cause sediment resuspension and transport along and off the slope. Furthermore, studies on cold water corals (Frederiksen et al., 1992) and large sponges (Klitgaard, 1995) around the Faeroes Islands have observed a link between internal waves and the cross-slope zonation of benthic fauna and proposed that internal waves impinging on the slope would increase the food availability by mean of redistribution of suspended particles in the bottom mixed layer. The relevance of the PROCS programme is further reinforced by the combination of the basin morphology and waves characteristics, which may lead to geometric focussing of internal waves and hence concentration of energy at particular depths (Maas et al., 1997).

This thesis is the sedimentology/geochemistry contribution to the PROCS programme. The objectives of this component are: 1) To determine the zonation of settling and erosion fluxes on the slope, as controlled by turbulent mixing in the bottom waters. 2) To establish the influence of short-term forcings (due to e.g., internal waves) on the generation of nepheloid layers and the resulting off and down-slope transport of resuspended material and 3) To assess the behavior of biogenic compounds (Corg, $BSiO_2$) on the slope, in relation to the cross-slope sediment (re)distribution. Such combined high frequency measurements have not been carried out on continental slopes of the Northwestern European margin before.

STUDY AREA

The PROCS programme was carried out in the Faeroe-Shetland Channel (FSC) in the North Atlantic Ocean. The FSC is located 60°N, 6°W to 63°N, 1°W and connects the Norwegian Sea with the North Atlantic and the Iceland Basin (Fig. 3). The shelf break is situated at about 200 m water depth and in the axis the channel is about 1200 m deep. The Shetlands margin slope is gentle (< 1% on average), about 50 km wide, and devoid of canyons.

The FSC has a complex hydrography that consists of five different water masses flowing in three layers on the eastern side of the channel (Turell et al., 1999; Hansen and Østerhus, 2000). The surface waters, whose main component is the North Atlantic Water (NAW), flow from south-west to north-east. The intermediate waters are made up of two components: MNAW (Modified North Atlantic Water) occupies a band across the channel at depths between 300 m and 700 m and flows from south-west to north-east, while AI/NIW (Arctic Intermediate/North Icelandic Water) flows from north-east to south-west at depths between 600 m and 800 m (Fig. 3, see Turell et al., 1999 for more details). Finally, bottom waters flow from north-east to south-west and consist of the NSAIW (Norwegian Sea Arctic Intermediate Water) and the FSCBW (Faeroe-Shetland Channel Bottom Water). The main thermocline is found between 400 and 600 m and shows its steepest gradient at ~550 m (Hansen and Østerhus, 2000; Van Raaphorst et al., 2001).

The sediment distribution roughly follows the isobaths. Hard coarse sands with many iceberg ploughmarks are found in a band between 300 and 450 m, while glacial gravel and pebbles are found between 450 and 600 m (Masson, 2001). Finer muddy sands cover the slope till the deepest part of the channel (Stoker et al., 1993) with ice rafted boulders (up to several meters in diameter) present at all depths (Masson, 2001). [210]Pb and [234]Th inventories of surface sediments showed that a zone of recent sediment deposition exists between 550 and 850 m water depth (Van Raaphorst et al., 2001; Grutters et al., 2001).

Previous work in this area provided evidence for the occurrence of internal waves (Sherwin, 1991; Van Raaphorst et al., 2001) which makes this basin a suitable place for the study of short-term processes and their impact on sediment resuspension and zonation across the continental slope.

INSTRUMENTATION AND SAMPLING STRATEGY

In 1999, two cruises were undertaken as part of the PROCS programme. Cruise PRO1 was conducted in spring 1999 (April 14th – May 5th) and PRO2 in fall 1999 (September 21st – October 13th). During each cruise a number of moorings, equipped with near-bottom sediment traps, turbidity sensors and current meters were deployed close to the seabed along a transect perpendicular to the slope between depths of 470 m and 1000 m (Fig. 3a). During the cruise PRO1, 4 moorings were deployed at 471, 700, 777 and 1000 m, while during PRO2, 5 moorings were deployed at 550, 700, 800, 900 and 1000 m, respectively. In between the two cruises, 3 moorings were deployed at 550, 800 and 1050 m, covering a longer time period of 5 months (PRO LT). Unfortunately, the shallowest mooring was trawled by fishing activity shortly after deployment so no data is available from that depth. A summary of the moorings and the deployed equipment is given in Table 1.
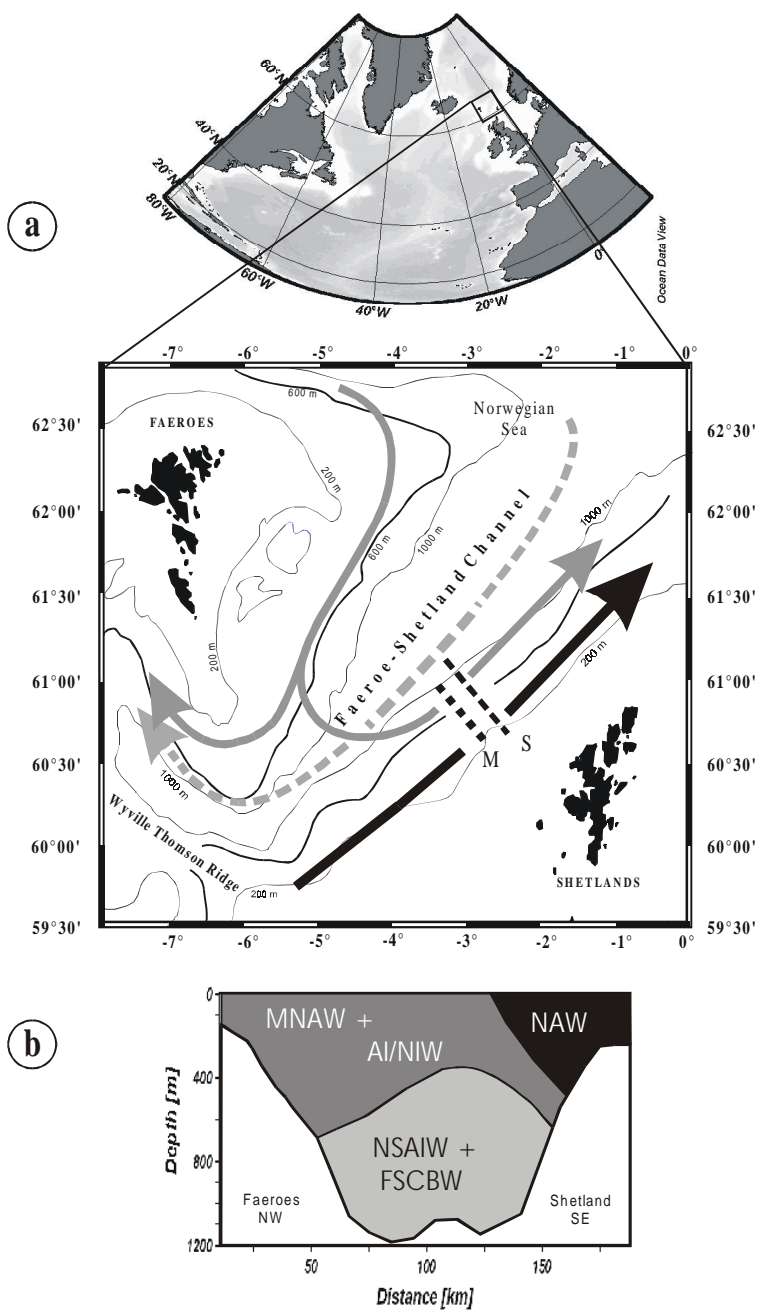
Fig. 3. *Map of the study area (**a**) with position of the mooring (M) and the transect along which surface sediment were sampled (S). The arrows represent the main flow of water masses as shown on vertical cross section (**b**). For signification of the acronyms, see text.*

The sediment traps were positioned with their apertures at 2 and 30 meters above the bottom (mab) (except for PRO LT where traps were deployed at 2 mab only). They are hereafter identified by the number of the mooring followed by the height above the bottom at which they stand, for instance C5-2 and C5-30 for traps from mooring C5 at 2 and 30 mab, respectively. Two types of sediment traps were used during PROCS: Technicap PPS 4 traps with 12 collecting cups (250 ml) and Kiel-type HDW traps with 20 collecting cups (250 ml). Sampling for cruise PRO1 started on April 19 (day 108) 0:00 and ended on April 30 (day 120) 24:00 hrs. For PRO2, sampling started on September 26 (day 268) 0:00 and ended on October 7 (day 279) 24:00 hrs and for PRO LT, sampling started on May 5 (day 125) 0:00 and ended on September 14 (day 257) 24:00. The HDW trap used during cruise PRO1 (C8-2) was programmed so that the initial 8 collecting intervals of 24 hrs could be covered by 16 intervals of 12 hrs, providing a more detailed record of the particle flux, followed by 4 intervals of 24 hrs and for PRO2, the HDW trap (C5-2) was programmed so that the cups 3 to 18 covered a period of 8 days with a sampling resolution of 12 hrs each. Cups 1, 2, 19 and 20 sampled for 24 hrs each as for PPS 4 traps. The sediment trap settings and sample processing are described in detail in Bonnin et al. (2002).

Table 1. *Summary of the position, sampling time and intervals of the instrumentation that equipped the moorings deployed during PROCS.*

Mooring	Instruments	Water depth (m)	Height above bottom, z (m)	Sampling interval
PRO1-C3	Current meters OBS, PPS 4 traps	471	8, 21, 34, 47 2, 30	60 (s) 240 (s), 24 hours
PRO1-C5	as PRO1-C3	700	as PRO1-C3	as PRO1-C3
PRO1-C6	as PRO1-C3	777	as PRO1-C3	as PRO1-C3
PRO1-C8	Current meters OBS, PPS 4 trap (30 mab), HDW trap (2 mab)	1000	as PRO1-C3	60 (s) 240 (s), 24 hours, 12 hours
PRO2-C1	as PRO1-C3	550	as PRO1-C3	as PRO1-C3
PRO2-C3	as PRO1-C3	700	as PRO1-C3	as PRO1-C3
PRO2-C5	as PRO1-C3	800	as PRO1-C3	as PRO1-C3
PRO2-C6	as PRO1-C8	900	as PRO1-C3	as PRO1-C8
PRO2-C8	as PRO1-C3	1000	as PRO1-C3	as PRO1-C3
PRO LT-D1	failed	550		
PRO LT-D3	Current meters OBS, PPS 4 traps	800	8 2	10 minutes 1 hour, 24 hours
PRO LT-D5	as PRO LT-D3	1050	8 2	10 minutes 1 hour, 24 hours
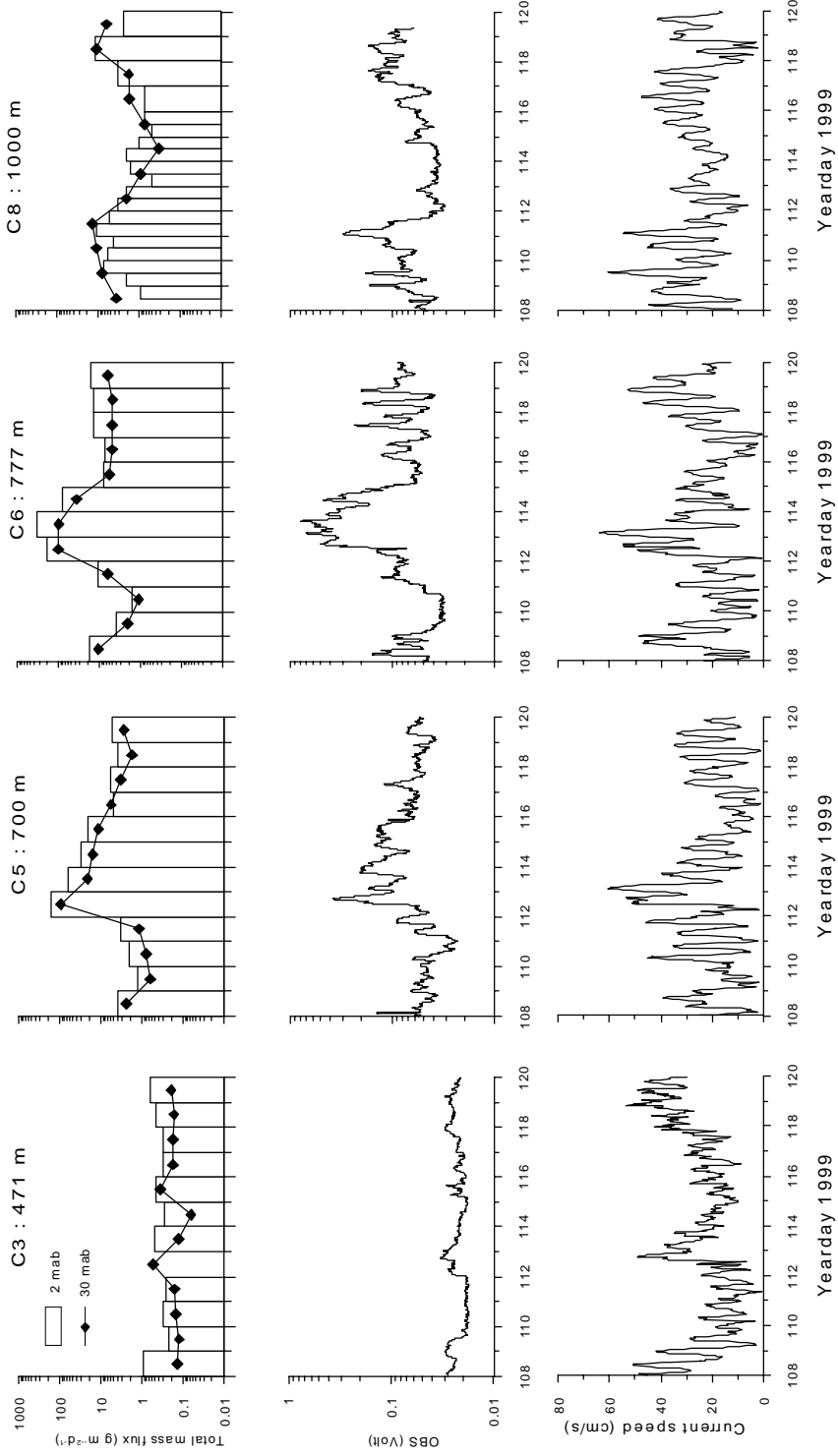
Fig. 4. *Total mass flux (TMF), near-bottom turbidity (8 mab) from Optical backscatter sensors (OBS) and near-bottom current velocity (21 mab) for PRO1.*

In order to measure the turbidity of the near-bottom water, Seapoint STM optical backscatter sensors (OBS) were mounted on the bottom sediment trap frames to measure infrared light (wave length 880 nm) scattered by particles at angles between 15 and 150 degrees. The data are given in the original unit (Volt) to avoid any bias due to uncertainties in calibration with suspended matter concentration in the water (Bonnin et al., 2002).

Furthermore, currents were measured by a number of current meters on these moorings, positioned at heights of 8, 21, 34 and 47 mab (Aanderaa RCM-8s and RCM-9s) sampling at the high rate of 1 minute^{-1}. A more detailed description of the instrumentation, current velocity and data interpretation is given is Hosegood and Van Haren (2003).

HIGH VARIABILITY OF BOTTOM CURRENT SPEEDS AND SEDIMENT RESUSPENSION FLUXES

Results of near-bottom sediment traps, turbidity and current meters are shown in figures 4, 5 and 6 for PRO1, PRO2 and PRO-LT, respectively. For all the stations current velocity at all depths above the bottom showed the importance of the semi-diurnal tide (M2). Although our short-term observation of near-bottom current speeds were of insufficient duration to resolve the spring neap-tide cycle, fluctuations with a period of 4 to 7 days were modulating the M2 signal (e.g., the period between maximum speeds at 900 and 1000 m depth during PRO2). A spectral analysis performed on current velocities recorded during a 5-month deployment (PRO-LT) showed a periodicity of 3 to 10 days (Fig. 7). Similar observations were made for this region on even longer current speed time series by Hosegood (1999) who observed a ~4-days periodicity for the current signal in the deeper part of the FSC.

Current velocity was high at all depths, reaching up to 75 cm s^{-1} (Fig. 6) at 21 mab on day 159 at 1050 m (PRO-LT). High mean bottom current velocities were observed at the lower (1000 m) and the upper slope (471 and 550 m) while lower velocities were found at mid-slope (700-800 m). Details on the averaged current speeds at all depths are given in Bonnin et al. (2002) for PRO1 and in Hosegood and Van Haren (2003) for PRO2.

Near-bottom sediment trap and OBS data indicated considerable spatial and temporal variability across the slope, both in the flux of intercepted material and in the intensity of turbidity close to the seabed during the deployment periods (Fig. 4 to 6). The total mass flux (TMF) at 2 and 30 mab was higher at mid-slope (550-777 m) than on the lower and upper slopes. TMF at 700 and 777 m on days 112 and 113 were one to two orders of magnitude higher than during the rest of the deployment period suggesting occurrence of abrupt and intense events. Several results indicate that the TMF recorded by the sediment traps deployed deeper than 471 m mainly reflect resuspension of seabed material: 1) Maximum fluxes were observed during peak bottom current velocity, 2) intercepted fluxes reached extremely high values (as high as 350 g m^{-2} d^{-1}), which cannot be
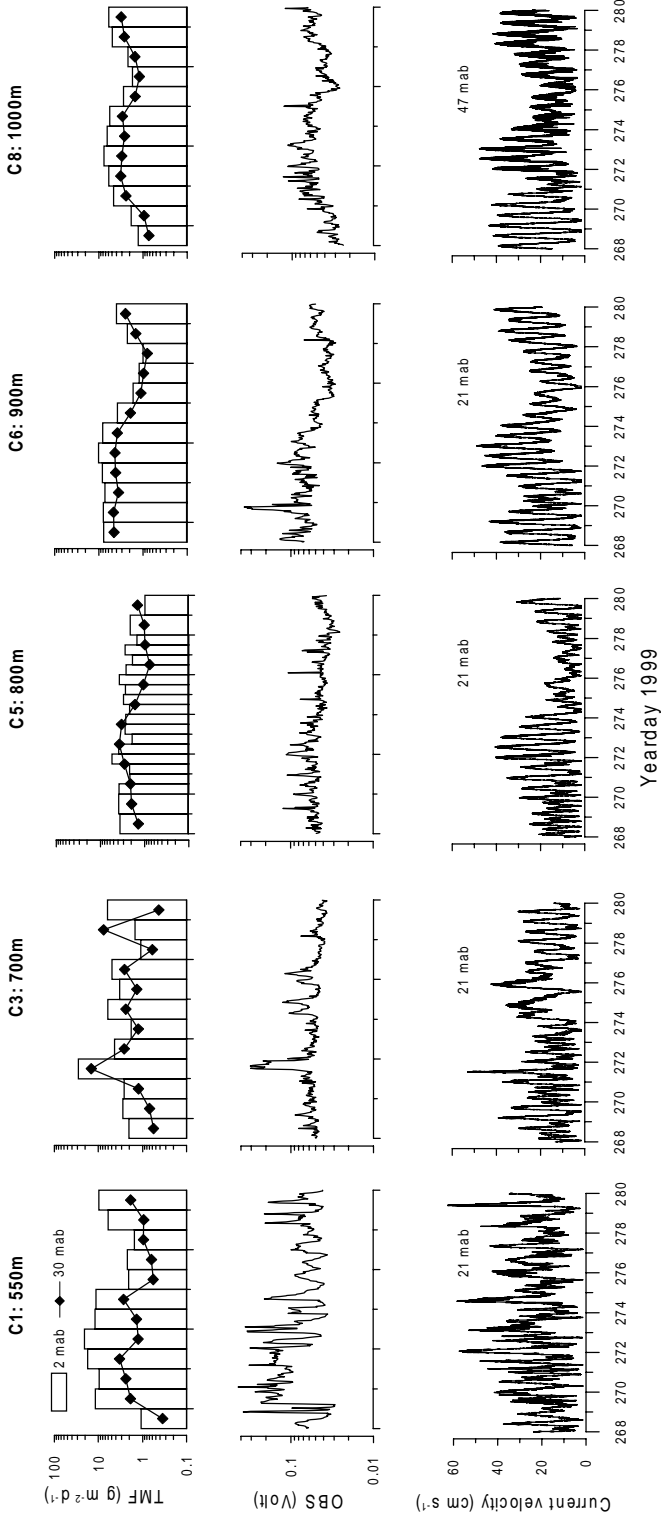
Fig. 5. *Total mass flux (TMF), near-bottom turbidity (8 mab) from Optical backscatter sensors (OBS) and near-bottom current velocity (21 mab except for mooring C8 at 47 mab) for PRO2.*

explained by vertical settling alone and with magnitudes that have only been observed in submarine canyons (e.g., Baker and Hickey, 1986; Schmidt et al., 2001) which, due to their geometry and direct connection with continent and terrigenous input, favor high sediment flux, and 3) particle fluxes were higher at 2 mab than at 30 mab (by a factor of 2 on average) even during periods of moderate particle flux indicating that resuspension does not coincides with high flux events only but took place at any time at depths greater than 471m. The most interresting feature is that cross-slope variability of the particle flux does not match with the cross-slope zonation of the averaged current velocity, as the highest resuspension flux is observed where the mean current velocity is lowest. This suggests that the material eroded locally during intense resuspension events is not exclusively due to the intensity of the long-term currents. Short-term mechanisms, independent from the intensity of the bottom current speed, are involved in the observed massive sediment resuspension.
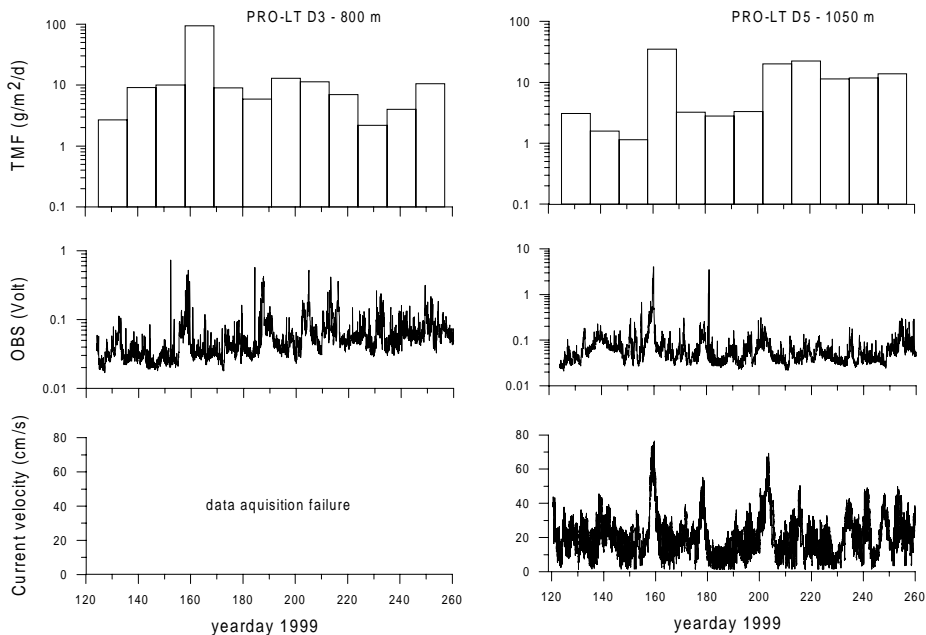

Fig. 6. *Total mass flux (TMF), near-bottom turbidity (8 mab) from Optical backscatter sensors (OBS) and near-bottom current velocity (21 mab) for PRO LT.*

The total mass flux obtained from near-bottom traps closely follow the OBS signal with high values corresponding to high OBS values and vice versa, suggesting that the total mass flux recorded in the traps is directly related to the concentration of particles in the near-bottom water column (Fig. 8). It is, however, difficult to establish the particle concentration in the water from OBS data, as optical sensors are more sensitive to fine

particles (Conner and De Visser, 1992; Bunt et al., 1999). The total resuspension flux was lowest on the upper slope (< 500 m), as was observed at 471 m during PRO1 with an intercepted flux in the near-bottom traps < 1 g m^{-2} d^{-1} (Fig. 4). The highest resuspension fluxes were observed at depth greater than 500 m but were limited in time and associated with a single event that occurred only once during the 12 days of each of the short-term deployments. Nevertheless, the 12 day-averaged resuspension flux measured during short-term deployment (e.g., 25.5 g m^{-2} d^{-1} at 700 m, PRO1) is of the same order as the TMF measured during sampling intervals in the long-term deployment (e.g., 12.9 g m^{-2} d^{-1} at 800 m, days 191-202 and 20.1 g m^{-2} d^{-1} at 1050 m, days 202-213). This demonstrates that a massive resuspension event as observed during PRO1 may have occurred repeatedly during the long-term deployment but does not appear as clearly as during the short-time deployment due to integration of the mass flux over a longer period of time (11 days vs. 1 day). Furthermore, from the long-term observation it is apparent that resuspension fluxes may exceed the highest TMF observed at 777 m during PRO1, as is the case for cup 4 (days 158 to 169) at 800 m during PRO LT, with an averaged TMF of 94 g m^{-2} d^{-1}, nearly twice as large as the integrated TMF over the 12 day period for trap C6-2 (~60 g m^{-2} d^{-1} including a TMF of 350 g m^{-2} d^{-1} on day 112). This suggests that during this time interval, resuspension fluxes reached even larger daily TMF or that high total mass fluxes were sustained for a longer period of time.
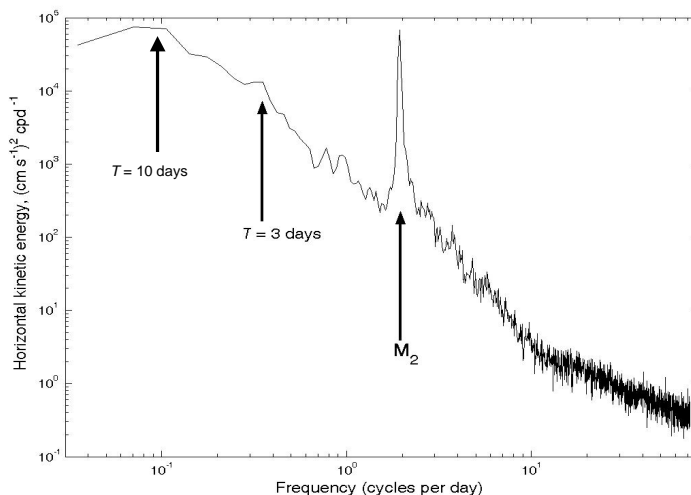

Fig. 7. *Spectra of kinetic energy from ADCP at 60 mab as observed from 800 m water depth during PRO-LT.*
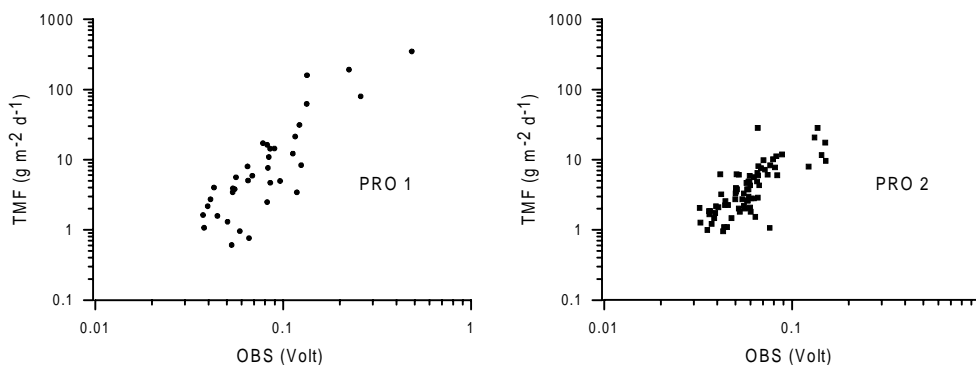
Fig. 8. *Total mass flux (TMF) measured from sediment traps vs. turbidity (OBS) for both spring (PRO 1) and fall (PRO 2) cruises. The OBS data has been averaged over a 24-hours period so that it can be compared with traps flux data.*

IMPORTANCE OF THE TIME-SCALE OF OBSERVATION

Our observations show that massive resuspension occurred during peak bottom currents. However, at a given depth, the relationship between the magnitude of the resuspension fluxes and bottom current speeds averaged over a period of one day show no correlation (Fig. 9) in contrast to the Middle Atlantic Bight (Biscaye et al., 1994) or the Iberian margin (Van Weering et al., 2002). Nevertheless, at low average current speeds little resuspension was observed, e.g., at 800 m during PRO2. The lower current speeds at this depth may explain why Van Raaphorst et al. (2001) observed a zone of enhanced sediment deposition at mid-slope. For some moorings however, where current speeds showed a clear semi-diurnal signal superimposed on a lower frequency modulation of the current (period of ~4 days, Fig. 4 to 6), the resuspension (made of fine particles) flux pattern seemed to follow the long-term current fluctuation (e.g., at 1000 m during PRO1 and 900 m during PRO2) and suggests the importance of such low frequency oscillations in the amount of material resuspended. It is important to note though that the maximum amplitude of the lower frequency fluctuation (~20 cm s^{-1}) is much lower than the maximum amplitude of the M2 signal (~50 cm s^{-1}) and it is likely that resuspension is due to the combination of the M2 oscillation and the lower frequency fluctuation of the current and that the latter acts as a modulator rather than a trigger mechanism.
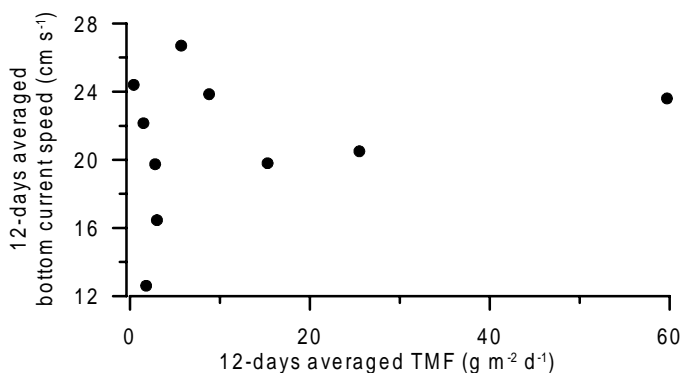
Fig. 9. *Bottom current speeds plotted vs. near-bottom TMF both averaged over a 12-days period. No correlation appears from this plot suggesting that high resuspension fluxes were not triggered by long-term variations in the current speeds.*

Resuspension fluxes observed on the lower slope that are associated with the M2 signal and the lower frequency fluctuation of the current were essentiaqlly composed of fine particles and never exceeded 10 g m^{-2} d^{-1} which is one to two orders of magnitude lower than the maximum resuspension fluxes observed e.g. on day 112 (700 and 777 m) during PRO1 or around day 160 (800 and 1050 m) during PRO LT. This points at an additional, short-term process occurring within the tidal period, that in combination with the lower frequency and M2 signal triggers the massive resuspension fluxes observed at mid-depth on the slope of the FSC.

Therefore, we believe that short-term deployments of moorings combining fast sampling near-bottom sediment traps, turbidity sensors and current meters are the best way to spatially and temporally study and resolve the processes facilitating massive resuspension of surface sediments on the continental slope and further influencing the residence time and fate of organic matter in the water column as well as in the surface sediments.

ORIGIN OF RESUSPENDED SEDIMENTS

Near-bottom sediment traps data showed evidence of massive sediment resuspension and transport on the SE slope of the Channel. However, these large sediment fluxes are somehow contradictory with the modern sedimentation conditions, which are characterized by a moderate primary productivity in the surface waters (Riegman and Kraay, 2001) and a low continental input. Given these conditions, it is difficult to explain how large amounts of material can be intercepted by the sediment traps. Van Raaphorst et

al. (2001) showed from ^{210}Pb analysis of surface sediment that preferential deposition was taking place at mid-slope depths on the west Shetland slope. This was confirmed by Grutters et al. (2001) who showed that accumulation of amino acid-rich organic matter was taking place at mid-slope depths indicating that cross-slope distribution of organic matter is also determined by near-bottom processes. Giving the morphology of the channel, with its funnel shape that makes it a large natural 'sediment trap', accumulation of sediments would be expected along the deepest part of the channel. The fact that the major sediment resuspension flux and deposition area are found at mid-slope and not in the axis of the channel suggests strong interactions with near-bottom currents. The question of the origin of the material caught by the traps, however, remains open and is one of the main issues of this thesis.

***

This thesis is structured around four manuscripts that have either been published or submitted for publication in peer-reviewed journals. All four manuscripts are based on data collected on samples from near-bottom sediment traps and surface sediments, as well as on measurements of near-bottom current velocity, turbidity and temperature. My contribution to the work described in these manuscripts included the onboard technical work during the PROCS cruise (preparation of traps, recovery of samples, coring, core slicing etc...), the processing of the suspended matter, sediment trap and surface sediment samples. I was also responsible for the reported sedimentological, geochemical and statistical analyses. As first-author of Chapters 2, 4 and 5, I wrote the first manuscript drafts and revised them based on the comments, suggestions and criticisms of the co-authors. Wim van Raaphorst worked closely with me during the realisation of Chapter 2 and provided the original impetus for Chapter 4. Phil Hosegood and Hans van Haren performed the analyses of the physical data presented in Chapter 3. All co-authors contributed to the writing of Chapter 3.

REFERENCES

Anderson, R.F., Rowe, G.T., Kemp, P.F., Trumbore, S. and Biscaye, P.E., 1994. Carbon budget for the mid-slope depocenter of the Middle Atlantic Bight. *Deep-Sea Research II* 41, 669-703.

Antia, A.N. and Peinert, R., 1999. Particle flux at the Iberian Margin, Ocean Margin Exchange II Report, pp. 249-254.

Atzetzu-Scott, K., Johnson, B.D. and Petrie, B., 1995. An intermittent, intermediate nepheloid layer in Emerald Basin, Scotian Shelf. *Continental Shelf Research* 15, 281-293.

Baker, E.T. and Hickey, B.M., 1986. Contemporary sedimentation processes in and around an active west coast submarine canyon. *Marine Geology*, 71, 15-34.

Biscaye, P.E., Anderson, R.F. and Deck, B.L., 1988. Fluxes of particles and constituents to the eastern United States continental slope and rise: SEEP-I. *Continental shelf Research* 8, 855-904.

Biscaye, P.E., Flagg, C.N. and Falkowski, P.G., 1994. The Shelf Edge Exchange Processes experiment, SEEP-II an introduction to hypotheses, results and conclusions. *Deep-Sea Research II* 41, 231-252.

Biscaye, P.E. and Anderson, R.F., 1994. Fluxes of particulate matter on the slope of the southern Middle Atlantic Bight: SEEP-II. Deep Sea Research II 41, 459-509.

Bogucki, D., T. Dickey and L.G. Redekopp, 1997. Sediment resuspension and mixing by resonantly generated internal solitary waves. *Journal of Physical Oceanography* 27, 1181-1196.

Bonnin, J., Van Raaphorst, W., Brummer, G.-J. A., Van Haren, H. and Malschaert, H., 2002. Intense mid-slope resuspension of particulate matter in the Faeroe-Shetland Channel: short-term deployment of near-bottom sediment traps. *Deep-Sea Research I* 49, 1485-1505.

Brunner, C.A. and Biscaye, P.E., 1997. Storm-driven transport of foraminifers from the shelf to the upper slope, southern Middle Atlantic Bight. *Continental Shelf Research* 17, 491-508.

Bunt, J.A.C., Larcombe, P. and Jago, C.F., 1999. Quantifying the response of optical backscatter devices and transmissometers to variations in suspended particulate matter. *Continental Shelf Research* 19, 1199-1220.

Cacchione, D.A. and D.E. Drake, 1986. Nepheloid Layers and Internal Waves Over Continental Shelves and Slopes. *Geo-Marine Letters* 6, 147-152.

Chang, G.C., Dickey, T.D. and Williams, A.J., 2001. Sediment resuspension over a continental shelf during Hurricane Edouard and Hortense. *Journal of Geophysical Research* 106, 9517-9531.

Churchill, J.H., Wirick, C.D., Flagg, C.N. and Pietrafesa, L.J., 1994. Sediment resuspension over the continental shelf east of the Delmarva Peninsula, *Deep-Sea Research I* 41, 341-363.

Conner, C.S. and De Visser, A.M., 1992. A laboratory investigation of particle size effects on an optical backscaterrance sensor. *Marine Geology* 108, 151-159.

Csanady, G.T. and Hamilton, P., 1988. Circulation of slope water. *Continental Shelf Research* 8, 457-484.

Dickson, R.R. and McCave, I.N., 1986. Nepheloid layers on the continental slope west of Porcupine Bank. Deep-Sea Research 33, 791-818.

Durrieu de Madron, X., Abassi, A., Heussner, S., Monaco, A., Aloisi, J.-C., Radakovitch, O., Giresse, P., Buscail, R. and Kerherve, P., 2000. Particulate matter and organic carbon budgets for the gulf of Lions (NW Mediterranean). *Oceanologica Acta* 23 (6), 717-730.

Durrieu de Madron, X., Castaing, P., Nyffeler, F. and Courp, T., 1999. Slope transport of suspended matter on the Aquitanian margin of the Bay of Biscay. *Deep-Sea Research II* 46, 2003-2027.

Epping, E., Van der Zee, C., Soetaert, K. and Helder, W., 2002. On the oxidation and burial of organic carbon in sediments of the Iberian Margin and Nazaré canyon (NE Atlantic). *Progress in Oceanography* 52, 399-431.

Frederiksen, R., Jensen, A., Westerberg, H., 1992. The distribution of the scleratinian coral Lophelia Pertusa around the Faeroe Island and the relation to internal mixing. *Sarsia* 77, 157-171.

Gardner, W.D., 1989a. Periodic resuspension in Baltimore Canyon by focusing of internal waves. Journal of Geophysical Research 94, 18185-18194.

Gardner, W.D., 1989b. Baltimore Canyon as a modern conduit of sediment to the deep sea. *Deep-Sea Research* 36, 323-358.

Grutters, M., Van Raaphorst, W., Boer, W., Malschaert, H. and Helder, W., 2001. Mid-slope accumulation of amino acid-rich organic matter across the Faeroe-Shetland Channel. Geologica Ultraeictina, 213, PhD Thesis, 96 pp.

Hansen, B. and Østerhus, S., 2000. North Atlantic-Nordic Seas exchanges. *Progress in Oceanography* 45, 109-208.

Herman, P.M.J., Soetaert, K., Middelburg, J.J., Heip, C., Lohse, L., Epping, E., Helder, W., Antia, A.N. and Peinert, R., 2001. The seafloor as the ultimate sediment trap-using sediment properties to constraint benthic-pelagic exchange processes at the Goban Spur. *Deep-Sea Research II* 48, 3245-3265.

Hosegood, P., 1999. Mesoscale variability on the continental slope of the Faeroe-Shetland Channel. MSc Applied Marine Science Dissertation.

Hosegood, P. and Van Haren, H., 2003. Ekman-induced turbulent mixing over the continental slope in the Faeroe-Shetland Channel. *Deep-Sea Research I* 50, 657-680.

Huthnance, J.M., 1981. Waves and currents near the continental shelf edge. *Progress in Oceanography* 10, 193-226.

Jahnke, R.A., Reimers, C.E. and Craven, D.B., 1990. Intensification of recycling of organic matter at the sea floor near ocean margins. *Nature* 348, 50-54.

Klitgaard, A.B., 1995. The fauna associated with outer shelf and upper slope sponges (Porifera, Desmospongiae) at the Faeroe Islands, Northern Atlantic. *Sarsia* 80, 1-22.

Lampitt, R.S., 1985. Evidence for the seasonal deposition of detritus to the deep-sea floor and its subsequent resuspension. *Deep-Sea Research* 32 (8), 885-897.

Maas, L.R.M., Benielli, D., Sommeria, F. and Lam, F.-P.A., 1997. Observation of an internal wave attractor in a confined, stable stratifies fluid. Nature 388, 557-561.

Masson, D., 2001. Sedimentary processes shaping the eastern slope of the Faeroe-Shetland Channel. *Continental Shelf Research* 21, 825-857.

McCave, I.N., 1986. Local and global aspects of the bottom nepheloid layers in the World Ocean. *Netherlands Journal of Sea Research* 20, 167-181.

McCave, I.N., Hall, I.R., Antia, A.N., Chou, L., Dehairs, F., Lampitt, R.S., Thomsen, L., Van Weering, T.C.E. and Wollast, R., 2001. Distribution, composition and flux of particulate material over the European margin at 47°-50°N. *Deep-Sea Research II* 48, 3107-3139.

Monaco, A., Biscaye, P.E., Soyer, J., Pocklington, R. and Heussner, S., 1990. Particle fluxes and ecosystem response on a continental margin: the 1985-1988 Mediterranean ECOMARGE experiment. Continental Shelf Research 10, 809-839.

Monaco, A., Durrieu de Madron, X., Radakovitch, O., Heussner, S., Carbonne, J. 1999. Origin and variability of downward biogeochemical fluxes on the Rhone continental margin (NW Mediterranean). *Deep-Sea Research I* 46, 1483-1511.

Moum, J.N., Caldwell, D.R., Nash, J.D. and Gunderson, G.D., 2002. Observations of boundary mixing over the continental slope. *Journal of Physical Oceanography* 32, 2113-2130.

Riegman, R. and Kraay, G.W., 2001. Phytoplankton community structure derived from HPLC analysis of pigments in the Faeroe-Shetland Channel during summer 1999: the distribution of taxonomical groups in relation to physical/chemical conditions in the photic zone. *Journal of Plankton Research* 23 (2), 191-206.

Schmidt, S., de Stigter, H.C. and van Weering, T.C.E., 2001. Enhanced short-term sediment deposition within the Nazaré Canyon, North-East Atlantic. *Marine Geology* 173, 55-67.

Sherwin, T.J., 1991. Evidence of a deep internal tide in the Faeroe-Shetland channel. In: B.P. Parker (Editor), Tidal Hydrodynamics. Wiley Interscience, Chichester, pp. 469-488.

Stoker, M.S., Hitchen, K. and Graham, C.C., 1993. The geology of the Hebrides and West Shetland shelves, and adjacent deep-water areas, United Kingdom Offshore Regional Report. British Geological Survey, London.

Thomsen, L. and Van Weering, T.C.E., 1998. Spatial and temporal variability of particulate matter in the benthic boundary layer at the N.W. European continental margin (Goban Spur). *Progress in Oceanography* 42, 61-76.

Thorpe, S.A. and White, M., 1988. A deep intermediate nepheloid layer. *Deep-Sea Research* 35 (9), 1665-1671.

Turell, W.R., Slesser, G., Adams, R.D., Payne, R. and Gillibrand, P.A., 1999. Decadal variability in the composition of Faeroe Shetland Channel bottom water. *Deep-Sea Research I* 46, 1-25.

Van Raaphorst, W., Malschaert, H., van Haren, H., Boer, W. and Brummer, G.-J., 2001. Cross-slope zonation of erosion and deposition in the Faeroe-Shetland Channel, North Atlantic Ocean. *Deep-Sea Research I* 48 (2), 567-591.

Van Weering, T.C.E., McCave, I.N., De Stigter, H.C., Hall, I. and Thomsen, L., 1998. Recent sediments, sediment accumulation and carbon burial at Goban Spur, N.W. European continental margin. *Progress in Oceanography* 42, 5-35.

Van Weering, T.C.E. and McCave, I.N., 2002. Benthic processes and dynamics at the NW Iberian margin: an introduction. *Progress in Oceanography* 52, 349-372.

Van Weering, T.C.E, de Stigter, H.C., Boer, W. and de Haas, H. 2002. Recent sediment transport and accumulation on the NW Iberian Margin. *Progress in Oceanography* 52, 349-372.

Vitorino, J., Oliveira, A., Jouanneau, J.M. and Drago, T. 2002. Winter dynamics on the northern Portuguese shelf. Part 1: physical processes. *Progress in Oceanography* 52, 129-153.

Walsh, I., Fisher, K., Murray, D. and Dymond, J., 1988. Evidence for resuspension of rebound particles from near-bottom sediment traps. *Deep-Sea Research* 35 (1), 59-70.

Walsh, J.P. and Nittrouer, C.A., 1999. Observations of sediment flux to the Eel continental slope, northern California. *Marine Geology* 154, 55-68.

Wang, B.J., Bogucki, D.J. and Redekopp, L.G., 2001. Internal solitary waves in a structured thermocline for resuspension and the formation of thin particle-laden layers. *Journal of Geophysical Research* 106, 9565-9585.

Wollast, R., 1991. The coastal organic carbon cycle: fluxes, sources and sinks. In: Mantoura, R.F.C., Martin, J.-M, Wollast R. (eds), Ocean margin processes and global change. Wiley Interscience, Chichester, 365-381.

Wollast, R. and Chou, Lei. 2001. Ocean Margin Exchange in the Northern Gulf of Biscay: OMEX I. An introduction. *Deep-Sea Research II* 48, 2971-2978.

Wollast, R. and Chou, Lei. 2001. The carbon cycle at the ocean margin in the northern Gulf of Biscay. *Deep-Sea Research II* 48, 3265-3293.

CHAPTER 2

Intense mid-slope resuspension of particulate matter in the Faeroe-Shetland Channel: short-term deployment of near-bottom sediment traps

ABSTRACT

An array of 4 moorings was deployed on a transect perpendicular to the south-eastern slope of the Faeroe-Shetland Channel to measure near-bottom fluxes during a 12-day period in spring 1999. Each mooring combined current meters and 2 sediment traps equipped with optical backscatter sensors (OBS) situated at 2 and 30 meters above the bottom, at water depths of 471, 700, 777 and 1000 m. During the deployment, near-bottom current velocities increased abruptly (within a few hours) to values as high as 55 cm s^{-1} at all stations except the deepest one. The sudden change in the cross-slope component of the current was immediately followed by a severe drop in temperature. Massive sediment fluxes were intercepted in the mid-slope traps on the same day and probably associated with the strengthening of the along-slope component. Organic carbon and nitrogen content of the trap samples were, except for the shallowest mooring, much lower than in particulate matter in the water column. During the high flux event, particles possessed lower organic carbon and nitrogen values than during lower flux periods. This indicates that sedimentary material entered the traps. A simple multi-component mixing model was applied to the trap samples to estimate the relative contribution to our total mass fluxes of material from different sources: primary settling from the water surface, rebound material, and the aged sediment proper. It shows that fluff is the main contributor to the resuspended flux but that coarse sediment proper is resuspended at mid-slope during the strong and abrupte increase in the current velocity.

INTRODUCTION

Although continental margins form only 11% of the world ocean surface area, more than 20 % of the global primary production takes place there (Wollast, 1991) making them a key study area for organic carbon budget investigations. Large multidisciplinary programmes conducted in the recent past have shown the importance of the continental slope, the boundary zone connecting the productive shelf to the deep ocean, to the global budget of particulate matter: SEEP I and II at the Middle Atlantic Bight (Walsh et al., 1988; Biscaye et al., 1994; Biscaye and Anderson, 1994), OMEX I at Goban Spur (Van Weering et al. 1998), OMEX II at the western Iberian margin (Van Weering and de Stigter, 1999; Antia and Peinert, 1999; Epping et al., 2001) and ECOMARGE in the Gulf of Lions (Monaco et al., 1990). These studies pointed out that particle flux to the slope sediment is mainly supplied by lateral transport from the shelf break rather than by pelagic settling. Nevertheless the final conclusion of the SEEP I and II programmes, i.e. the presence of a mid-slope organic carbon depocentre, was not validated by the observations during OMEX.

Erosion at the shelf edge and upper slope may be caused by strong boundary currents (Thomsen and van Weering, 1998; Durrieu de Madron et al., 1999a) or be related to tidal motions (Vangriesheim and Khripounoff, 1990). It was also argued that short-term processes, like the breaking of internal waves on the slope, can cause substantial resuspension of sea floor material and generate detachment from the bottom of intermediate nepheloid layers (INL), which spread offslope along isopycnal surfaces (Dickson and McCave, 1986; McCave, 1986; Thorpe and White, 1988; Durrieu de Madron et al., 1999b; Van Raaphorst et al., 2001). These INLs are dynamic and intermittent features (Dickson and McCave, 1986; Van Raaphorst et al., 2001), whose occurrence and geographical extent may vary on short time-scales.

Here we present results from the PROCS (PROcesses at the Continental Slope) programme, carried out in the Faeroe-Shetland Channel (FSC), where we deployed 4 sets of moorings on a transect across the Shetland side of the channel (Fig. 1). On the mooring, sediment traps were deployed as close to the bottom as possible and equipped with Optical Backscatter Sensors, current velocity meters and temperature sensors to determine hydrodynamical and sedimentological changes near the seabed. Resuspension on slopes has been related to long-term fluctuations of along-slope currents (e.g., Thomsen and Van Weering, 1998) as well as to breaking of internal waves (Gardner, 1989a) and impingement of mesoscale features such as atmospheric perturbations and eddies (Gardner and Sullivan, 1981; McCave, 1986). Previous work in this area showed that the narrowness, the gentle facing slopes and the strongly stratified water column are favourable for the creation and reflection of internal waves (Sherwin, 1991). Van Raaphorst et al. (2001) showed that episodic nepheloid layers occur on the Shetlands slope at around 600 m depth. Therefore we deployed our moorings close to one another on a transect across the slope with the sediment traps closely spaced above each other (30 meters) to carefully look at the cross-slope zonation of resuspension/erosion. Although many authors have considered internal waves to be a possible mechanism for triggering sediment resuspension (Dickson and McCave, 1986; Thorpe and White, 1988; Gardner, 1989a, b), very few have quantified their

impact in terms of particle resuspension and redistribution across the slope. Also, sediment traps have been intensively used to measure the vertical flux of sea surface derived particles to the bottom (Antia et al., 1999; Monaco et al., 1999) and to measure resuspension and rebound fluxes in the deep oceanic environment (Gardner et al., 1983; Walsh et al., 1988). To our knowledge, nobody has used sediment traps to determine the resuspension of seabed material with a high time-resolution in an area influenced by internal waves and strong currents. This near-bottom sediment trap study across the continental slope is a first step towards such quantification. A simple end-member mixing model, based on particulate organic carbon and nitrogen contents, will be applied to determine the relative contribution of particles from different sources to our trap fluxes.
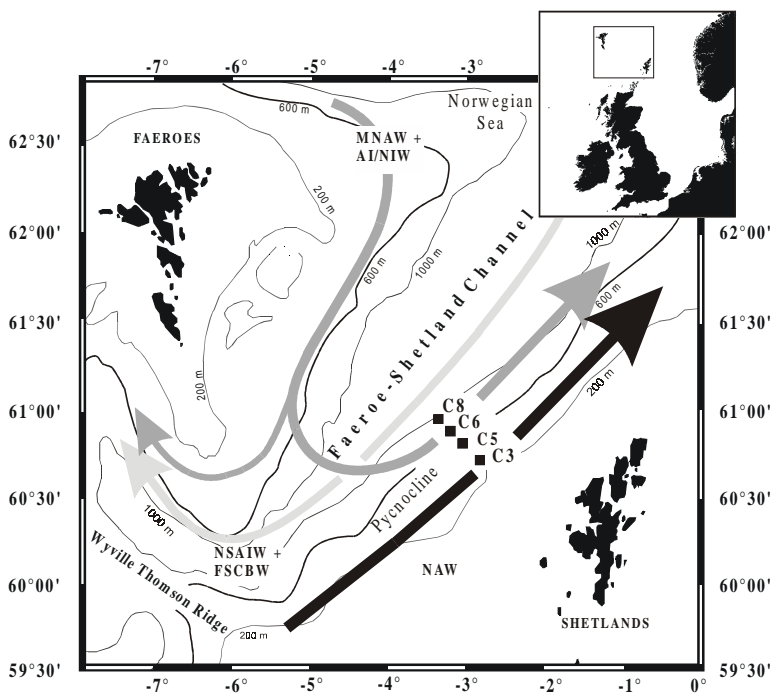
Fig. 1. *Map of the study area with position of the moorings and trajectories of the main water masses in the Faeroe-Shetland Channel. The 5 water masses described by Turrell et al. (1999) are grouped here into 3 according to direction of flow. Black arrow: NAW (North Atlantic Water), dark grey arrow: MNAW (Modified North Atlantic Water) and AI/NIW (Arctic Intermediate/North Icelandic Water), and light grey arrow: NSAIW (Norwegian Sea Arctic Intermediate Water) and FSCBW (Faeroe-Shetland Channel Bottom Water). The black line at 600 m represents the position of the major pycnocline where it intersects the bottom. For more details on the location of the moorings, see Table 1.*

CHARACTERISTICS OF THE STUDY AREA

The FSC is located 60°N, 6°W to 63°N, 1°W and connects the Norwegian Sea with the North Atlantic and the Iceland Basin (Fig. 1). The shelf break is situated at about 200 m depth and in the axis the channel is about 1200 m deep. The Shetlands margin slope is gentle (<1%), about 50 km wide, and devoid of canyons. The sediment distribution follows the isobaths, with hard sands in a band between 300 and 450 m, glacial gravel and pebbles (median grain size ~400 µm) in a band between 450 and 600 m, and finer muddy sands (median grain size ~150 µm) covering the slope to the deepest part of the channel (Stoker et al., 1993). The average particulate organic carbon (POC) and particulate nitrogen (PON) content (% dw) for surface sediment are 0.28 and 0.04% respectively (Table 1) with an average C/N ratio of 6.9. The POC and PON values for suspended particulate matter (TPM) are given in Table 2.

Table 1. *Position and water depth of the moorings, median grain size with % of particles < 10 µm (within brackets), POC and PON contents and POC/PON atomic ratio of surface sediments (0-2.5 mm depth interval)*

Moorings	Location of the moorings	Water depth (m)	Surface sediment median grain size (µm)	Surface sediment POC content (% dw)	Surface sediment PON content (% dw)	Surface sediment POC/PON
C3	60°48.48'N - 02°59.34'W	471	400 (8)	0.27	0.043	6.3
C5	60°55.36'N - 03°05.88'W	700	144 (17)	0.28	0.057	4.9
C6	60°56.91'N - 03°13.22'W	777	185 (15)	0.29	0.033	8.8
C8	61°00.09'N - 03°18.39'W	1000	149 (13)	0.27	0.036	7.5

The FSC has a complex hydrography comprising five different water masses flowing in three layers on the eastern side of the channel (Turell et al., 1999). The surface waters, whose main component is the North Atlantic Water (NAW), flow from south-west to north-east. The intermediate waters are made of two components: one occupies a band across the channel at a depth between 300 m and 700 m and flows from south-west to

north-east (MNAW), and the other one (AI/NIW) flows from north-east to south-west at a depth between 600 m and 800 m (Fig.1 or see Turell et al., 1999 for more details). Finally, the bottom waters flow from north-east to south-west and comprise the Norwegian Sea Arctic Intermediate Water (NSAIW) and the Faeroe-Shetland Channel Bottom Water (FSCBW). The main thermocline is found between 400 and 600 m (Van Raaphorst et al., 2001) and shows its steepest gradient at ~550 m (Fig. 2a and c). Vertical turbidity profiles (Fig. 2b and d) of the water column show rather low values in the upper photic zone, clear water below the thermocline and an increased turbidity in the vicinity of the seabed (the bottom nepheloid layer; BNL). The near bottom turbidity is minimum on the upper slope and maximum at mid-slope both on the Shetland and Faeroe side of the channel but with a clear maximum on the Shetland side. Figure 2 also gives us information on the dynamics of the BNL, which was thicker and denser on day 112 than on day 116, indicating the intermittence of the BNL.

Table 2. POC and PON content of the total particulate matter (TPM) in the water column and close to the bottom (~5 mab) for different depths of the overlying water column.

Water depth (m)	POC content (% dw) of TPM	Standard deviation (number of samples)	PON content (% dw) of TPM	Standard deviation (number of samples)
0-20	10.0	5.1 (27)	0.67	0.23 (27)
50-150	5.9	2.9 (28)	0.13	0.09 (28)
200-500	5.0	2.2 (54)	0.09	0.07 (52)
600-900	4.0	1.6 (15)	0.06	0.05 (13)
bottom < 500 m	3.9	2.2 (10)	0.07	0.05 (7)
bottom 500-700 m	3.3	1.2 (6)	0.07	0.06 (6)
bottom 700-900 m	4.7	2.2 (3)	0.05	0.03 (3)
bottom > 900 m	4.3	2.0 (10)	0.06	0.02 (9)

MATERIAL AND METHODS

Four moorings, C3, C5, C6 and C8, including 2 sediment traps and 4 current meters each were deployed on a transect perpendicular to the Shetland margin at bottom depths of 471, 700, 777 and 1000 m, respectively (see Table 1 for coordinates). Sediment traps were positioned with their apertures at 2 and 30 meters above the bottom (mab). They are hereafter identified by the number of the mooring followed by the height above the

bottom at which they stand, for instance C5-2 and C5-30 for mooring C5 at 2 and 30 mab, respectively.
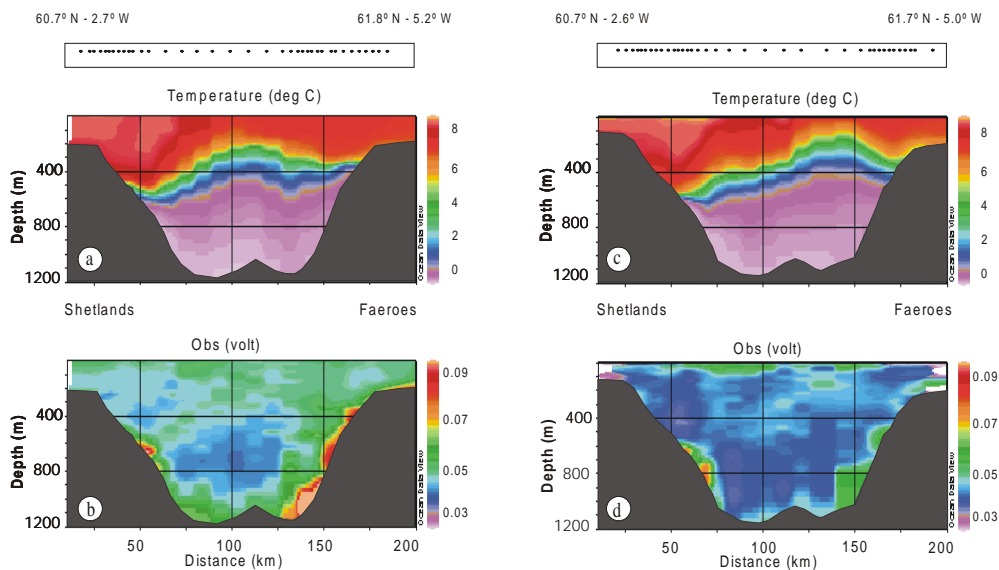
Fig. 2. *Temperature (plots a and c) and turbidity (OBS) (plots b and d) section across the Faeroe-Shetland Channel on days 111-112 (plots a and b) and days 117-118 (plots c and d) obtained from CTD casts. The dots in the rectangles on top of the plots indicate the position of the measuring stations. This cross-section shows the strong temperature gradient in the channel and the enhanced turbidity at mid-slope on the Shetland side. Note also that, to some extent, the turbidity follows the position of the pycnocline. A color version of b and d is shown on p. 98, plots a and b.*

Sediment traps and trap samples treatment

Two types of sediment traps were used in this study: Technicap PPS 4 traps with 12 collecting cups (250 ml) were used for moorings C3, C5, C6 and trap C8-30, and a Kiel-type HDW trap with 20 collecting cups (250 ml) was used for trap C8-2. All PPS traps collected for 12 synchronised intervals of 24 hours starting on April 19 0:00 hour (day108) and ending on April 30 24:00 hours UTC (day 120). The HDW trap was programmed so that the initial 8 collecting intervals could be covered by 16 intervals of 12 hours, providing a more detailed record of the particle flux, followed by 4 intervals of 24 hours. For each mooring the trap at 2 mab was mounted on a NIOZ-designed anchor frame, which allowed the sediment traps to be as close as possible to the seabed. This frame, including weight and acoustic release system with a total weight under the water of 800 kg, effectively reduced the motion of the line. However considerable tilt was still observed in the bottom trap at

700 and 777 m (see section *5.2*) indicating movement of the anchor frame at very high current speed. To allow sampling in the high-energy regime of the FSC, all traps were modified from their conventional conical shape to cylindrical shape by adding a 1.5-m long PVC cylinder with baffled aperture (10 mm hexagons). The resulting total length of the effectively cylindrical traps is 2 m and the collecting area on the top of the trap is 0.042 m^2 (aspect ratio 8). Thus, all sediment traps have a similar collection area and a uniform shape. Cylindrical traps with high aspect ratio are appropriate to moderate energy conditions (Gardner, 1985) but still may give biased results in high-energy fields (Butman, 1986; Butman et al., 1986; Gust, 1994) and we are aware of these problems. The additional PVC cylinder mounted on trap C3-30 was lost at some unknown time during deployment, making it difficult to compare its fluxes with those of the other traps.

Prior to deployment, all collecting cups were filled with a mixture of seawater taken from the deployment site and depth, $HgCl_2$ (0.50 g l^{-1}) as biocide to prevent organic matter degradation and a pH-buffer ($Na_2B_4O_7.10H_2O$; 2.00 g l^{-1}) to minimise carbonate dissolution. All programmed samples were recovered except cup number 5 of trap C3-2, which was filled but lost during recovery. After retrieval of the moorings, the trap samples were stored at 4°C until further processing at the NIOZ. The first sample of trap C8-2 was not processed as it was heavily contaminated with numerous badly preserved amphipod swimmers.

All samples were inspected with a binocular microscope, and swimmers, when present, were handpicked. Total suspended matter was determined after filtration of the residue in the collecting cups through pre-weighted Poretics® polycarbonate filters (47 mm ∅, 0.4 µm pore size). When the amount of material was too large to be processed directly, the samples were split (up to 1/16th for the 5th sample of trap C6-2) before filtration with a manual roto splitter. The loaded filters were rinsed with 2 ml milli-Q water to remove the salts and frozen at -20ºC, then freeze-dried and finally weighed after being exposed for at least 24 hours in a humidity-controlled chamber of 30% relative humidity (Van Raaphorst et al. 2001).

Particulate organic carbon and nitrogen measurements

POC and PON content of the sediment trap samples was determined with a Carlo Erba NA 1500 Analyser according to the procedure described by Verardo et al. (1990) modified by Lohse et al. (2000). The samples were carefully scraped from the filters and crushed in an agate mortar. Inorganic carbon was removed from the samples by progressive and controlled acidification with sulphurous acid. The precision is ± 0.3% for organic carbon and ± 1.6% for nitrogen. Only the samples from moorings C5, C6 and C8 were fully analysed. The amounts of material collected in traps C3-30 and C3-2 were too small to allow C and N measurements for each sample. No samples were analysed for trap C3-30, and the 12 samples from trap C3-2 were pooled into 5 larger samples.

Current meters, tilt meters and optical backscatter sensors

Aanderaa RCM-8 current meters, including temperature sensors, were sampling once every 60 seconds and were moored at 8, 21, 34 and 47 mab on each mooring line, but here we will report only those closest to the sediment traps, at 8 and 34 mab. Accuracy of the current data based on 10-min ensembles is $\pm$ 1 cm s^{-1} and $\pm$ 5° for speed and direction, respectively. Currents are positive to the north-east for the along slope component and positive to the north-west (downslope) for the cross-slope component. To provide indication of the motion of the sediment traps, they were all equipped with NIOZ-designed tilt meters with an accuracy of 0.2° that sampled every 4 minutes.

Seapoint STM optical backscatter sensors (OBS) were mounted on the sediment traps to measure infrared light (wave length 880 nm) scattered by particles at angles between 15 and 150 degrees. Calibration was performed by comparison with the total suspended matter concentration in the near-bottom water column sampled during CTD rosette (also equipped with OBS sensors) casts by filtration through Poretics® polycarbonate filters (47 mm $\varnothing$, 1.0 µm pore size). In addition we used sediment surface materials as well as sediment trap materials for calibration in the lab after the cruise. This showed that the OBS signal heavily depends on the particle size, in agreement with Bunt et al. (1999), who showed that optical devices are most sensitive to particles < 20 µm. Here, according to our estimates, it ranges from 1 mg l^{-1} for 0.1 Volt measured by the OBS for fine material, to 3.4 mg l^{-1} for 0.1 Volt for bulk surface sediment. On average, 1.8 mg l^{-1} corresponds roughly to 0.1 Volt. Hatcher et al. (2001) argued that OBS sensors are not depending on particles size (dependent on mass) but on particle projected area concentration which is independent of mass. Nevertheless our calibration data are provided to give an estimation only, but to avoid any bias due to calibration, turbidity in this paper will be indicated in the original unit, i.e. Volt, as measured by the OBS.

RESULTS

Physical properties of the near-bottom water

The 2-week average near-bottom (8 mab) resultant current speed was 24.4, 20.5, 23.6 and 26.7 cm s^{-1} at 471, 700, 777 and 1000 m, respectively (Fig. 3). The larger variability and the higher current speed both occurred at 777 m water depth. The averaged along-slope velocity was directed north-east with values of 19, 9 and 8 cm s^{-1} at 471, 700 and 777 m, respectively and southwest at 1000 m with speed of 8 cm s^{-1} (Fig. 4). Currents showed a high variability, with standard deviation ranging from 16 to 24 cm s^{-1}. Mean cross-slope currents were slightly directed upslope at mid-slope stations at velocities of 3 cm s^{-1} at 700 m and 777 m, and downslope at 471 m and 1000 m with flow velocities of 2.8 and 0.2 cm s^{-1}, respectively. Standard deviations were 8-13 cm s^{-1}, less than for the along-slope direction. Current speed at stations C3, C5 and C6 (at 8 and 34 mab) decreased

slightly from yearday 108 to 112, with a minimum on day 110, and then increased abruptly to reach a maximum value on day 112, showing high frequency current fluctuations close to the bottom. The velocity then diminished gradually to day 116 and strengthened again to the end of the record. At station C8, the velocity increased from day 108 to a maximum on day 109 then dropped gently to a minimum on day 117 and increased again with maxima on day 119. The oscillation signal was essentially semi-diurnal tidal (M2) for both the along-slope and cross-slope components at all the stations. Although our deployment time was too short to resolve the spring neap-tide cycle, we nevertheless observed variation with a period of 5 to 7 days during the deployment (Fig. 3 and 4).
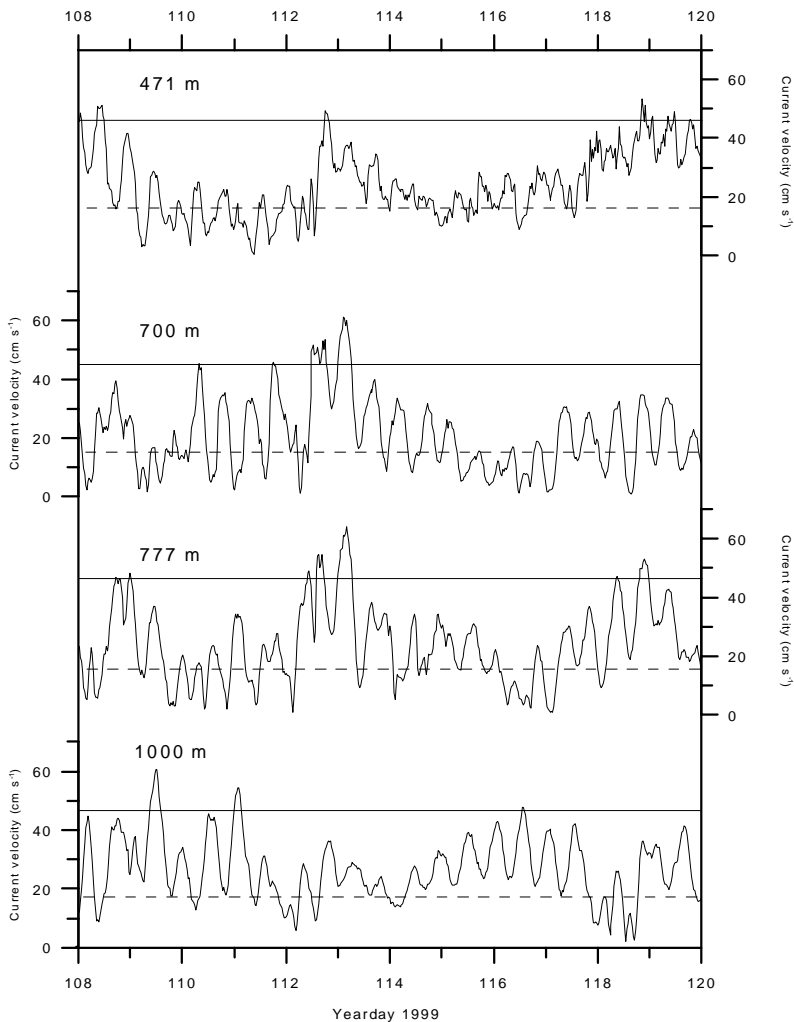
Fig. 3. *Current speeds at 8 mab for the four moorings. The dashed line represents the threshold speed at which aggregates might be resuspended and the solid line the threshold erosion current speed for sediment proper according to Thomsen and Gust (2000).*
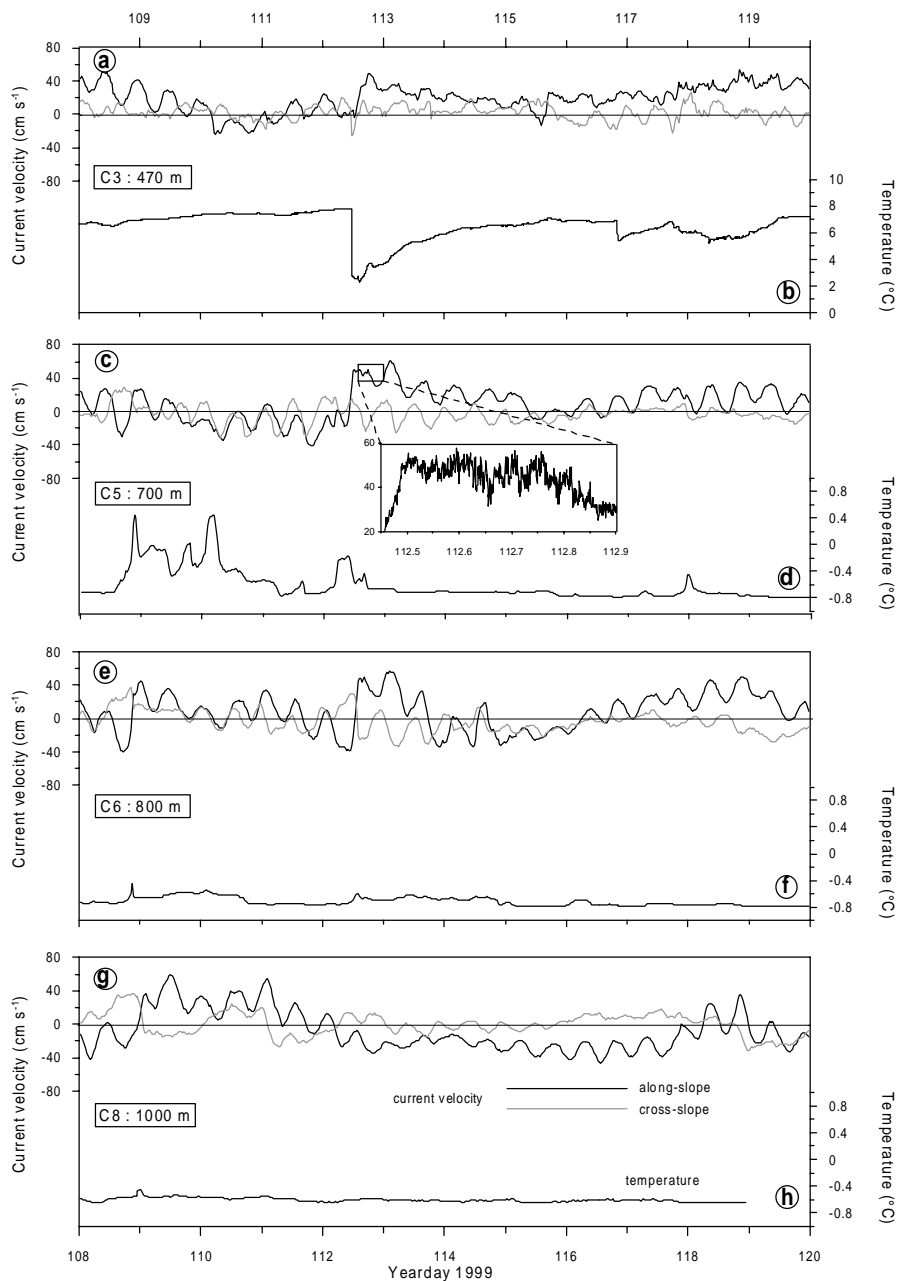
Fig. 4. *Currents (a, c, e, g) and temperature (b, d, f, h) at 8 mab for the different stations. In plot a, c, e, g, the grey line represents the cross-slope component of the current (positive values orientated downslope) and the black line the along-slope component of the current (positive values to the north-east). The data shown here are 30-minutes averages. The blow up for station C5 shows the high frequency variations observed for the along-slope component (1-minute averages) for 12h during day 112.*

High frequency variations appeared immediately after the current reversal of the along-slope component at day 112, reflecting enhanced high frequency activity of the near-bottom water mass (see blow-up Fig. 4c). An abrupt temperature drop at 471 m water depth (Fig. 4b) is associated with this major current reversal. At station C5, the temperature variation in the first part of the record showed that the isotherms were moving up and down the slope. The peak on day 112 appeared to be related to the abrupt drop in temperature higher up the slope (station C3, 471 m). This peak was accompanied by an increase in the turbidity (Fig. 5 f and g), as revealed by the optical backscatter sensors on the traps.

Total mass flux and turbidity

Microscopic observations revealed that the material found in all the traps during periods with relatively low mass fluxes consisted essentially of fluffy material composed of filaments, mucus and aggregates (reaching several mm in size), shells of planktonic forams (some still having their spines) and faecal pellets. However, during the high flux event (moorings C5 and C6) the material collected in the traps was composed mainly of lithogenic grains and planktonic and benthic forams embedded in a fluffy matrix suggesting a benthic origin of the particles.
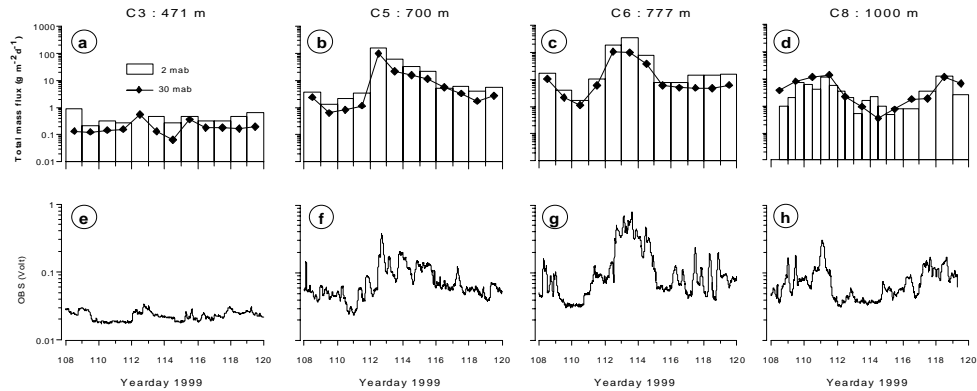
Fig. 5. *Total mass fluxes in the sediment traps of the moorings C3, C5, C6 and C8 (plots a to d) for traps at 30 mab (diamonds) and 2 mab (bars), and the turbidity (plots e to h) measured with the OBS sensors (2 mab) for each mooring.*

The total mass flux (TMF) for every trap is given in figure 5 (a-d). The intercepted fluxes closely follow the time series of the OBS (Fig. 5e-h). High TMF values correspond to high OBS values and vice versa, suggesting that the TMF recorded in the traps are directly related to the concentration of particles in the near-bottom water column. For moorings C3 (471 m), C5 (700 m) and C6 (777 m) TMF differed by a factor 2 between the

upper trap (30 mab) and the lower trap (2 mab) suggesting input from resuspension of seafloor material at 2 mab. At the shallowest station, the TMF was very low both at 2 mab and at 30 mab (Fig. 5a). Even though the cylinder of trap C3-30 was lost during deployment, its TMF matches well with those of trap C3-2. Traps of moorings C5 and C6 show comparable results with relatively low TMF during the first 4 days (day 108 to 111) followed by an abrupt increase at day 112 (Fig. 5b, c). Following this maximum on day 112, the TMF decreased gradually for mooring C5 (upper and lower traps) to reach background values again on day 116 (Fig. 5b). Further downslope, trap C6-30 showed the same pattern as traps C5-2 and C5-30 while trap C6-2 showed a maximum on day 113 rather than on day 112 (Fig. 5c). At the deepest station (Fig. 5d), the TMF pattern was completely different, as both upper and lower traps showed minimum fluxes during days 112 and 113 and maximum fluxes during days 111 and 118. Also in contrast to the other moorings higher on the slope, both traps of this mooring showed similar averaged TMF.

Organic carbon and nitrogen

High POC and PON contents were observed when TMF in the traps was low and vice versa (Fig. 6a-f), suggesting that high TMF may be due to resuspension of organic-poor sediments (Table 1). For C5, C6 and C8, the POC content ranged from 0.36 to 3.89 % and PON from 0.04 to 0.61%. For mooring C5 (700 m), maxima in POC and PON in bottom trap samples led those in the upper trap by one day. At mooring C6, the 2 traps displayed a synchronous signal of POC and PON. The POC and PON content are very similar to those in traps C5-2 and C5-30 situated 100 m higher on the slope. For mooring C8 we observed a lag of 2 days for the bottom trap for the maximum in both POC and PON (occurs on day 114 for trap C8-30 and on day 116 for trap C8-2).

DISCUSSION

Given the distance of the sediment traps to the seabed and the energetic conditions in the near-bottom water column, we cannot assume that the trap fluxes indicate net vertical settling. Our main goal is to assess the relative intensity of resuspension of particulate matter across a high-energy continental slope and to investigate the quality of the intercepted material rather than to establish net sedimentation rates. During the last 2 decades, sediment traps have been used intensively to study long-term (seasonal) fluxes of particles onto the continental slope like the Gulf of Lions in the Mediterranean (Monaco et al., 1990a, b), the Middle-Atlantic Bight (Biscaye et al., 1994), the Goban Spur at the mid-European continental margin (Antia et al., 1999). They have also been used to study near-bottom resuspension fluxes in various environments such as the north equatorial Pacific (Walsh et al., 1988), the western North Atlantic (Gardner et al., 1983; Gardner and Richardson, 1992), the northeast Atlantic (Lampitt et al., 2000) and the Oyster Grounds in

the North Sea (Van Raaphorst et al., 1998). However sediment traps have not been used so far to study the short-term processes that determine the resuspension of bottom sediments and their redistribution across the continental slope.

Hydrodynamics and resuspension potential

Resuspension of bottom material is strongly linked with current velocity. Thomsen and Gust (2000) found that a flow speed of 45 cm s^{-1} at 1 mab is necessary to initiate transport of sediment proper at the mid-slope continental margin of Goban Spur. Thomsen and Van Weering (1998) argued that currents about 20 cm s^{-1} are sufficiently strong to resuspend periodically surface layer aggregates and Lampitt (1985) suggests that currents > 7 cm s^{-1} should resuspend a loose phytodetritus layer deposited on the deep-sea floor. For the North Sea, Van Raaphorst et al. (1998) determined that the threshold speed for resuspension of fluff is about16 cm s^{-1}. In the Faeroe Shetland Channel current speeds exceeded 7 cm s^{-1} most of the time at all depths and currents >45 cm s^{-1} were also observed occasionally at all depths. Thus during most of the deployment time currents should be strong enough to erode a phytodetritus/aggregates layer when present and to keep it in suspension.
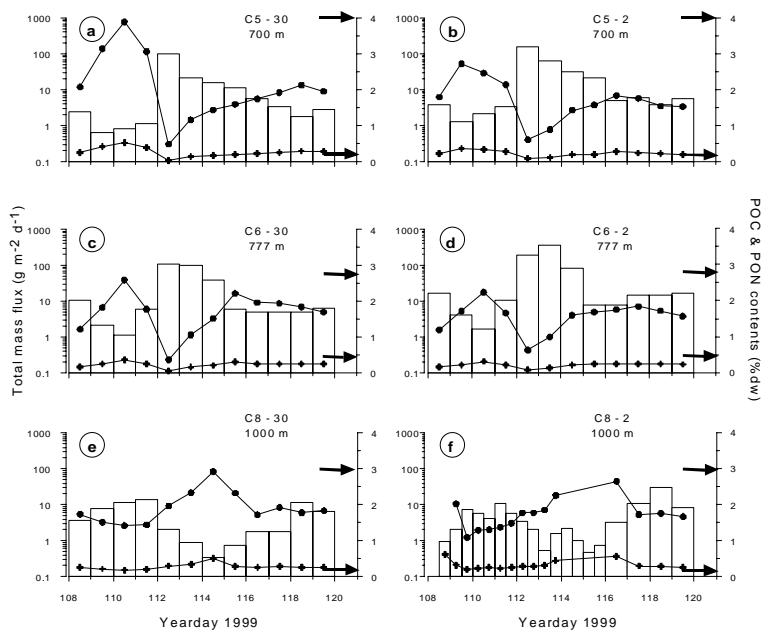
Fig. 6. *POC (circles) and PON (crosses) content in % of dry weight of the total dry mass in the trap samples. The bars represent the TMF as shown in Fig. 5. For comparison, on each plot on the right side, the upper arrow represents the POC content of suspended particles in the near-bottom water (~5 mab) and the lower one the POC content of the surface sediment (0-2.5 mm depth interval).*

Generally, higher turbidity was observed at higher current speeds and also the highest trap fluxes occurred on days with high current velocities. The deepest mooring, C8, which experienced, on average, slightly slower flow than on the upper slope, showed less turbidity and lower trap fluxes. The increase in turbidity and trap fluxes that took place on day 112 (moorings C5 and C6) appears to be due to resuspension generated by the strong reversal and intensification of the along-slope component. Van Raaphorst et al. (2001) observed a tidal shoaling of the major pycnocline in this area. The sequence on day 112 following the rapid upward motion of the pycnocline (observed down to 700 m) may be due to the passage of a tidal bore, or any other high-energy event. We conclude that resuspension of fine particles can occur at all depths across the slope during the entire study period. Currents sufficiently high to erode the sediment proper (>45 cm s^{-1}) also occurred at all depths but were restricted to a few hours only.

High trap fluxes and tilt effects

Tilt can bias the estimated budget of settling particles as it can result in either under or overestimation of the settling flux (Gardner, 1985; Gust et al., 1994). Tilt meters mounted on the traps revealed that the mid-slope traps had been tilted up to 36° (for trap C6-2) during the abrupt reversal in the current velocity on day 112 (Fig. 7), but that the average tilt was only 3.7°. Enhanced tilt was observed at current speeds over 30 cm s^{-1} whereas angles of more than 5° occurred at speeds above 50 cm s^{-1}. Strong flow may cause enhanced exchange between the trap and the water column but precautions to minimize this effect were taken by extending the aspect ratio of the sediment traps prior to deployment. It can nevertheless be questioned whether the trap data indicate genuine resuspension fluxes or mainly reflect tilt effects.

Following Gardner (1985), a first order correction for the effect of tilt on collection efficiency was made on our trap fluxes with the sine function:

$$F = F_T \int_0^{\Delta T} \frac{1}{1+1.4\sin 2\theta} dt \qquad \text{with } \Delta T = 1 \text{ day (trap interval)} \qquad (1)$$

where F is the corrected flux expected in a vertical cylinder, F_T is the observed flux in a tilted cylinder and θ is the degree of tilt from the vertical. Strong flow may also generate shear at the mouth of the trap that leads to break-up of aggregates and undersampling of fine material. Although this phenomena is difficult to quantify, equation (1), based on empirical observations, partially correct this effect. Correction for the tilt effect for trap C6-2 gives slightly lower flux values than those measured (by 0.2 to 12.8 % for the minimum and maximum tilt angle, respectively, Fig. 7c). Despite the relatively large tilt angles at some moments, the corrected fluxes show the same pattern as the uncorrected ones, and on day 113 the corrected flux of trap C6-2 remains very large (305 g m^{-2} d^{-1}). Tilt, since high

angles occurred during short periods only and their contribution to the integrated fluxes is therefore probably minor. Moreover, the correction is meant for sediment traps with an aspect ratio of ~5, and cylindrical traps with higher aspect ratio (8 in our case) are presumably less sensitive to tilt effects. This is also supported by the observation that during the times of strongest tilt, our sediment traps collected large amount of coarse and fast sinking particles (sand, foraminifera), which are much less affected by fluid motion in the traps (Gardner, 1985), thus limiting the bias due to tilt effects. Another argument in favour of a minor tilt effect on our flux estimates is the low TMF (~5 g m^{-2} d^{-1}) observed for example in trap C6-2 on days 118 and 119 for a tilt angle up to 10º, whereas with a similar tilt on day 112, a flux as high as 180 g m^{-2} d^{-1} was intercepted. We conclude that the high fluxes in our traps are not due to tilt effects.
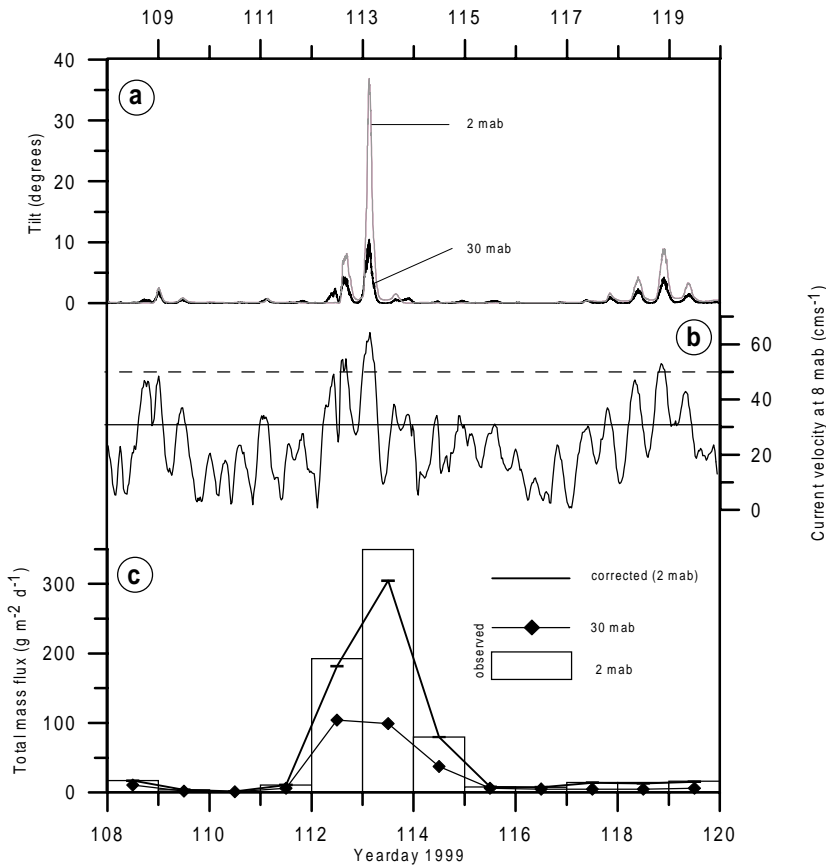
Fig. 7. *Tilt of the traps from the vertical (a), current velocities (b) (along-slope in dark line and cross-slope in grey line) and total mass flux (c) for trap C6-2. For total mass flux, the bar chart represents the intercepted flux by the trap at 2 mab, the line and diamonds the intercepted flux at 30 mab, and the solid line the corrected flux for trap C6-2 according to equation (1) from Gardner (1985).*

Temporal and spatial variability in the trap fluxes

High temporal variability of TMF was observed in almost all the traps. Small fluxes correspond to relatively low current velocities (~20 cm s^{-1} in average) and high fluxes to stronger currents (up to 61 cm s^{-1} 8 mab at 700 m water depth). At moorings C3, C5 and C6, the 2-fold higher TMF in the lower traps, relative to the upper ones, correspond to higher turbidity at 2 mab than at 30 mab, thereby confirming resuspension as a major source (Biscaye and Eittreim, 1977).

The average TMF of the mid-slope traps (C5 and C6) of 30.7 g m^{-2} d^{-1} during the 12-day deployment is higher than what has been observed elsewhere in open continental slopes at similar depth. On the Eel continental slope, Walsh and Nittrouer (1999) found values of 11.8 g m^{-2} d^{-1} at 15 mab (but with an important river discharge nearby), whereas Biscaye and Anderson (1994) found fluxes not higher than 10 g m^{-2} d^{-1} at 10 mab during the SEEP I and II experiments in the Middle Atlantic Bight. Our values are close to those observed in submarine canyons where Baker and Hickey (1986) found fluxes up to 200 g m^{-2} d^{-1} a few meters above the bottom with an average of 60 g m^{-2} d^{-1} at 450 m water depth. However, our deployment time is shorter than that of the studies cited above, which, considering that we caught an extremely high flux event, makes direct comparison difficult.

The cross-slope differences in TMF are considerable, as on average only 0.3 g m^{-2} d^{-1} was captured at the shallowest station (C3), 5 g m^{-2} d^{-1} at the deepest station (C8), and up to 160 g m^{-2} d^{-1} (C5-2) and 350 g m^{-2} d^{-1} (C6-2) at the mid-slope stations. This suggests that the mid-slope is far more active in terms of resuspension/deposition than the rest of the slope. Amin and Huthnance (1999) showed that a mid-slope source of resuspendable sediments is necessary to explain maximum concentration of particles in the BNL generally observed at this depth. The increase of the flux in the 700 and 777-m traps is intense and abrupt, with, according to the OBS sensors mounted on the traps, only a few hours between the minimum and maximum turbidity, suggesting a relatively nearby source for this short-term resuspension event. The hypothesis of a nearby source for the resuspended material is also supported by the presence of coarse particles in the traps.

Origin of the resuspended material

The sediments on the slope of the FSC are of glacial origin and composed mainly of coarse sands and gravel (Stoker et al., 1993), likely because the high bottom current speed in this region does not allow for a large sedimentary reservoir of fine and easily resuspendable particles. Moreover, The FSC is a mesotrophic area with a primary production ranging from 1.2 to 3.8 gC m^{-2} d^{-1}, with the lowest values in the northern channel and the highest in the southern and middle channel (Riegman and Kraay, 2001). Although these primary production values are relatively high, primary settling associated with export fluxes from the euphotic zone can not explain the largest fluxes of particles in our traps, although it may explain part of our background fluxes. According to Suess (1980) the above primary production may, on average, give deposition fluxes between 0.06 and 0.2

gC m^{-2} d^{-1} at the seabed at 700 m. This estimate is in good agreement with our background fluxes (0.07 gC m^{-2} d^{-1} at 700 m water depth) but certainly cannot explain fluxes orders of magnitude higher.

On the long term, local source for the fluxes intercepted in our near-bottom traps seems unlikely. A more likely explanation is that it is fuelled from lateral advection from further up-stream, possibly from the Wyville-Thomson Ridge, being transported by strong contour currents. The particle-loaded water may migrate vertically on the slope from below the pycnocline to the bottom of the channel depending on the cross-slope velocity (Oey, 1998). The processes are thus not limited to a 2D cross section view but 3D interactions between along-slope and cross-slope mechanisms must be considered (Dickson and McCave, 1986; Biscaye and Anderson, 1994). Nevertheless, during periods of lower current speeds particles may preferentially accumulate temporarily on the mid-slope as indicated by increased ^{210}Pb (Van Raaphorst et al., 2001) and ^{234}Th inventories (Grutters et al., submitted) at 700-800 m depth until an event of higher flow velocity occurs, as observed on day 112. We saw earlier that flow conditions at any depth on the slope are capable of bottom material erosion. Therefore, the absence of resuspension at mooring C3 (471 m) could be due to lack of material available for resuspension. Indeed, sediments at 471 m consist of coarse, hard sands with very little fine grains (less than 7% < 63 µm in the upper 2.5 mm, Grutters et al., submitted). The coarser fraction of the resuspended particles probably settles out close to the point of erosion while the finer particles probably settle further along-slope. OBS transects across the FSC (Fig. 2b) show a distinct turbidity maximum on the Shetland slope between 550 and 900 m (just below the major pycnocline), suggesting that resuspension occurred within this depth interval on the slope. The reason why no resuspension of sediment proper was found at the deepest station is probably that the major source of material is situated at shallower depth (above 850 m) and that the upslope flow does not allow particles to reach the deepest part of the channel.

Composition of resuspended flux

As suggested by Thomsen and Van Weering (1998), BNLs are partially sustained by refractory resuspended particles and partially by fresh labile aggregates, the so-called "rebound" flux (Walsh et al., 1988). Elemental analysis performed on our trap material yielded a negative correlation between TMF and their POC and PON contents. If we assume that the small amount of material collected in traps C3 reflects the primary flux reaching the seabed (which is probably already an overestimation, as a small amount of resuspension may take place here as well), the traps deeper down the slope, which intercepted much higher TMF, would mainly reflect resuspension. The time lag in the POC and PON signature between the upper and bottom trap of mooring C5 also indicates that the material caught by the traps originated mainly from the seabed. At mooring C6, the 2 traps display a synchronous signal of POC and PON although a lag one day with respect to the bottom trap is observed for the TMF. This suggests that the 2 traps of this mooring received material with a similar geochemical signature and may originate from the same place.

Moreover, the POC and PON contents are very similar to those obtained in traps C5-2 and C5-30 situated 100 m higher up on the slope, indicating that material in the traps of these two moorings also has a similar source. For mooring C8 we observed a lag of 2 days for the bottom trap for both POC and PON maxima (occurring on day 114 for trap C8-30 and on day 116 for trap C8-2), which suggests, on the contrary, settling from an INL entrained higher up-slope.
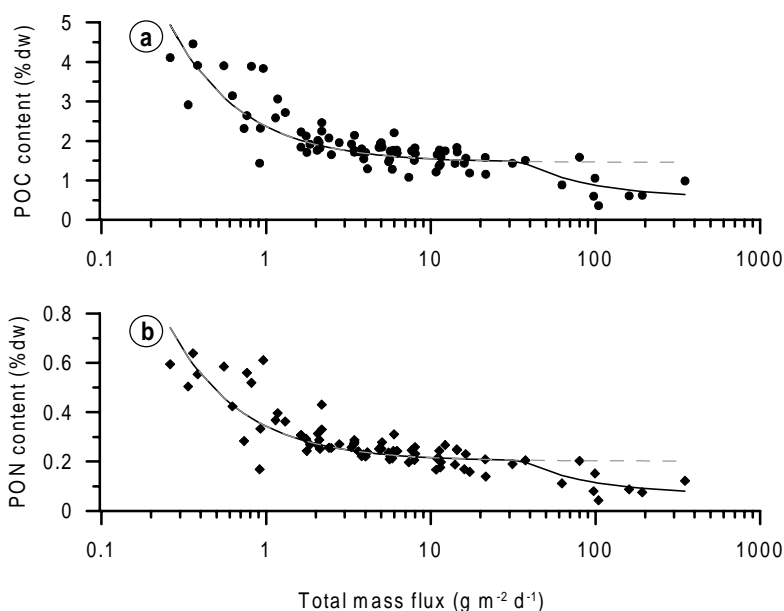

Fig. 8. *POC (a) and PON (b) content versus total mass flux for the entire sediment trap data set. The dashed regression line represents equation (3) with values of $(C_0-C_r).S_0 = 0.90$ g m^{-2} d^{-1} and $C_r = 1.52\%$ for (a) and $(C_0-C_r).S_0 = 0.14$ g m^{-2} d^{-1} and $C_r = 0.20\%$ for (b). The solid line represents equation (6) with additional parameters $\alpha = 0.21$ for (a) and 0.04 for (b) and $C_b = 0.31\%$ for (a) and 0.06% for (b).*

To determine whether the resuspended particles collected in our traps have similar properties as the top layer of the surface sediments or the suspended particles in the water column we follow the approach of Jago et al. (1993) and apply the two-component mixing model of Morris et al. (1987). In this model it is assumed that the TMF consists of a constant background (primary flux) S_0 with carbon content C_0, and a variable rebound flux S_r having a carbon content C_r:

$$TMF \times POC = S_0 \cdot C_0 + S_r \cdot C_r \tag{2}$$

Taking into account that the total mass flux $TMF = S_0 + S_r$, we can substitute for S_r in (2) and the POC content of the flux is then given by:

$$POC = (C_0 - C_r)\frac{S_0}{TMF} + C_r \qquad (3)$$
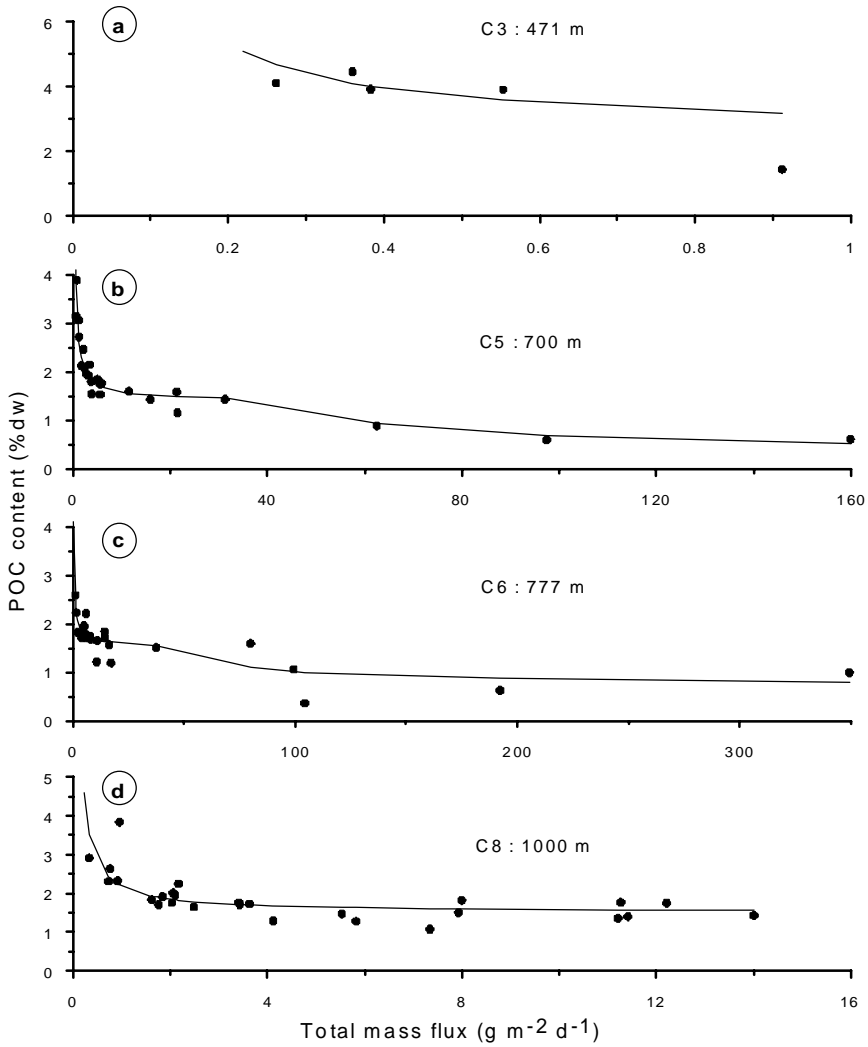
Fig. 9. *POC content versus total mass flux for separate stations. For stations C3 and C8 the solid line represents regression line obtained from equation (3) with $(C_0\text{-}C_r).S_0 = 0.5\ g\ m^{-2}\ d^{-1}$ and $C_r = 2.5\%$ for C3 and $(C_0\text{-}C_r).S_0 = 0.66\ g\ m^{-2}\ d^{-1}$ and $C_r = 1.52\%$ for C8. For stations C5 and C6, the regression line represents the results of equation (6) with $(C_0\text{-}C_r).S_0 = 1.53\ g\ m^{-2}\ d^{-1}$, $C_r = 1.42\%$, $\alpha = 0.07$, $C_b = 0.17\%$ for C5 and $(C_0\text{-}C_r).S_0 = 1.10\ g\ m^{-2}\ d^{-1}$, $C_r = 1.55\%$, $\alpha = 0.25$, $C_b = 0.42\%$ for C6.*

From the regression of POC against TMF using the entire sediment trap data set, C_r is calculated at 1.52 % (Fig. 7). This is approximately 2.5 times lower than the average value of POC in particles in the near-bottom water column (~4 %, see Table 2) and ~5 times higher than the average content in the upper 2.5 mm of the sediments (~0.28 %), and is in good agreement with Van Raaphorst et al. (1998) for the North Sea and with Lampitt et al. (2000) for abyssal conditions. They both found that particles that are resuspended during normal flow conditions are carbon-enriched compared to the bulk sediment suggesting that they are made up of aggregates that recently arrived at the seafloor or in the benthic boundary layer (BBL). However, the model cannot explain the low POC content at high TMF ($> \sim 35$ g m^{-2} d^{-1}), indicating that 2 end members are not sufficient to explain the variability of our trap contents.

We incorporated a third component in the model to check whether the material present in our traps during high TMF events (> 35 g m^{-2} d^{-1}) corresponds to bed material. We assume that trap samples for TMF > 35 g m^{-2} d^{-1} consist of the same rebound material found at fluxes up to 35 g m^{-2} d^{-1}, to which the material of the extra flux (assumed to be from sediment) is added. This is expressed by:

$$TMF \times POC = 35 \cdot POC_{35} + S_b \cdot C'_b \qquad \text{for } TMF > 35 \qquad (4)$$

and

$$C'_b = \alpha \cdot C_r + (1 - \alpha) \cdot C_b \qquad (5)$$

where POC_{35} corresponds to the modelled POC content, from (3), at TMF = 35 g m^{-2} d^{-1}, S_b is the additional flux of resuspended sediments, C'_b the POC content of the total resuspended particles at TMF > 35 g m^{-2} d^{-1}, C_b the POC content of surface sediments, α the percentage of rebound material of the resuspension pool in the trap samples at TMF > 35 and C_r the POC content of this rebound fraction (as in eq. (2) and (3)). Knowing that $TMF = 35 + S_b$, we arrive at the equation for the POC content at TMF > 35:

$$POC = \left[(C_0 - C_r)\frac{S_0}{35} + C_r \right] \times \left(\frac{35}{TMF} \right)$$
$$+ \left(1 - \frac{35}{TMF} \right) \times [\alpha \cdot C_r + (1 - \alpha) \cdot C_b] \qquad (6)$$

in which α and C_b are the only additional unknown parameters. We obtained a POC content C_b for the sediment end member of ~0.31 %, which is very close to the surface sediment carbon content value (0.28 % on average) and a mean value for $\alpha = 0.21$.

Although the model is more robust when applied to the entire data set (Fig. 8), we applied it to the individual stations as well. Figure 9 shows that for the shallowest station (C3, 471 m) and the deepest station (C8, 1000 m) the 2-end-member model (eq. 3) fits well with the POC data. It reflects mainly the small primary flux for C3 and shows that rebound material is the main component of the flux at station C8. The 2 mid-slope stations show that the 3-component mixing model fits the POC data best (especially at 700 m).
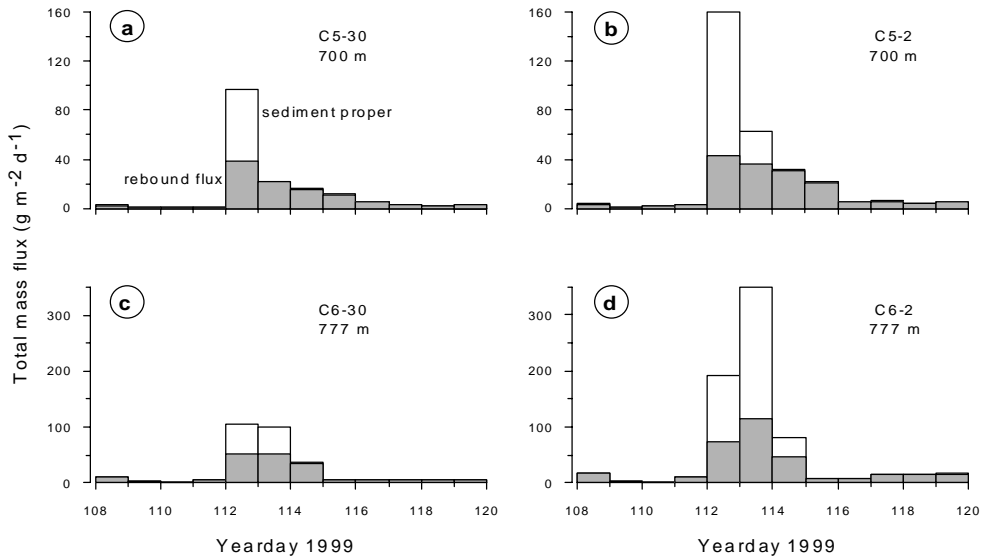
Fig. 10. *Relative contribution of rebound particles (grey) and sediment proper (white) to the total resuspension flux for the two mid-slope moorings. When TMF exceeded 35 g m^{-2} d^{-1}, the relative contribution of rebound to the total mass flux is given by α (α = 0.07 for C5 and 0.25 for C6). The primary flux remains within the thickness of the line of the x-axis.*

Conclusions

The fluxes intercepted in our traps were much higher than fluxes observed in other open slopes and mainly reflect resuspension of recently settled aggregates. During the 12-day deployment TMF were the highest at mid-slope composed of an admixture of material of sedimentary origin. Figure 10 shows the relative distribution of sediment proper relative

to the TMF in the mid-slope traps as given by α obtained from equation 6: it represents up to 70% of the TMF during the periods of strong increase of the near-bottom current speed. The material in our traps constitutes then a mixture between: 1) the primary settling particles that represents the majority of the flux on the upper slope down to at least 471 m water depth and which we assumed to be constant (~0.3 g m^{-2} d^{-1}), 2) the rebound particles that have been already in contact with the top layer of the sediment or the BBL, less rich in Corg than the primary settling particles with which they constitute the background flux on the slope deeper than 471 m during normal current speed; and 3) sediments that are resuspended under the extremely high current velocities (above ~50 cm s^{-1}) at 700 and 777 m on days 112-114 and which represents up to 70% of the TMF during day 112 in trap C5-2 and during day 113 in trap C6-2.

ACKNOWLEDGEMENTS

REFERENCES

Amin, M. and Huthnance, J.M., 1999. The pattern of cross-slope depositional fluxes. *Deep-Sea Research I* 46 (9), 1565-1591.

Antia, A.N., von Bodungen, B. and Peinert, R., 1999. Particle flux across the mid-European continental margin. *Deep-Sea Research I* 46, 1999-2024.

Antia, A.N. and Peinert, R., 1999. Particle flux at the Iberian Margin, Ocean Margin Exchange II Report, pp. 249-254.

Baker, E.T. and Hickey, B.M., 1986. Contemporary sedimentation processes in and around an active west coast submarine canyon. *Marine Geology* 71, 15-34.

Biscaye, P.E. and Eittreim, S.L., 1977. Suspended particulate loads and transport in the nepheloid layer of the abyssal Atlantic Ocean. *Marine Geology* 23, 155-172.

Biscaye, P.E., Flagg, C.N. and Falkowski, P.G., 1994. The Shelf Edge Exchange Processes experiment, SEEP-II an introduction to hypotheses, results and conclusions. *Deep-Sea Research II* 41, 231-252.

Biscaye, P.E. and Anderson, R.F., 1994. Fluxes of particulate matter on the slope of the southern Middle Atlantic Bight: SEEP-II. *Deep-Sea Research II* 41, 459-509.

Bunt, J.A.C., Larcombe, P. and Jago, C.F., 1999. Quantifying the response of optical backscatter devices and transmissometers to variations in suspended particulate matter. *Continental Shelf Research* 19, 1199-1220.

Butman, C.A., 1986. Sediment trap biases in turbulent flows: Results from a laboratory flume study. *Journal of Marine Research* 44 (3), 645-693.

Butman, C.A., Grant, W.D. and Stolzenbach, K.D., 1986. Predictions of sediment trap biases in turbulent flows: A theoretical analysis based on observation from the literature. *Journal of Marine Research* 44 (3), 601-644.

Dickson, R.R. and McCave, I.N., 1986. Nepheloid layers on the continental slope west of Porcupine Bank. *Deep-Sea Research* 33, 791-818.

Durrieu de Madron, X., Radakovitch, O., Heussner, S., Loye-Pilot, M.D. and Monaco, A., 1999a. Role of the climatological and current variability on shelf-slope exanges of particulate matter: Evidence from the Rhone continental margin (NW Mediterranean). *Deep-Sea Research I* 46 (9), 1513-1538.

Durrieu de Madron, X., Castaing, P., Nyffeler, F. and Courp, T., 1999b. Slope transport of suspended matter on the Aquitanian margin of the Bay of Biscay. *Deep-Sea Research II* 46, 2003-2027.

Durrieu de Madron, X., Abassi, A., Heussner, S., Monaco, A., Aloisi, J.-C., Radakovitch, O., Giresse, P., Buscail, R. and Kerherve, P., 2000. Particulate matter and organic carbon budgets for the gulf of Lions (NW Mediterranean). *Oceanologica Acta* 23 (6), 717-730.

Epping, E., Van der Zee, C., Soetaert, K. and Helder, W., 2002. On the oxidation and burial of organic carbon in sediments of the Iberian Margin and Nazaré canyon (NE Atlantic). *Progress in Oceanography* 52, 399-431.

Gardner, W.D., Richardson, M.J., Hinga, K.R. and Biscaye, P.E., 1983. Resuspension measured with sediment traps in a high-energy environment. *Earth and Planetary Science Letters* 66, 262-278.

Gardner, W.D., 1985. The effect of tilt on sediment trap efficiency. *Deep-Sea Research* 32 (3), 349-361.

Gardner, W.D., 1989a. Periodic resuspension in Baltimore Canyon by focusing of internal waves. *Journal of Geophysical Research* 94, 18185-18194.

Gardner, W.D., 1989b. Baltimore Canyon as a modern conduit of sediment to the deep sea. *Deep-Sea Research* 36, 323-358.

Gardner, W.D. and Richardson, M.J., 1992. Particle export and resuspension fluxes in the Western North Atlantic. In: Rowe, G.T. and. Pariente, V. (Eds), Deep-Sea Food Chains and the Global Carbon Cycle. Kluwer Academic Publishers, pp. 339-364.

Gardner, W. and Sullivan, L.G., 1981. Benthic storms: Temporal variability in a deep-ocean nepheloid layer. *Science* 213, 329-331.

Grutters, M., Van Raaphorst, W., Boer, W., Malschaert, H. and Helder, W. Labile organic matter accumulation due to resuspension and down slope transport on the Faeroe Shetland Channel. Submitted to *Deep-Sea Research I*.

Gust, G., Michaels, A.F., Johnson, R., Deuser, W.G. and Bowles, W., 1994. Mooring line motions and sediment trap hydromechanics: *in situ* intercomparison of three common deployment designs. *Deep-Sea Research I* 41, 831-857.

Hatcher, A., Hill, P. and Grant, J., 2001. Optical backscatter of marine flocs. *Journal of Sea Research* 46, 1-12.

Jago, C.F., Bale, A.J., Green, M.O., Howarth, M.J., Jones, S.E., McCave, I.N., Millward, G.E., Morris, A.W., Rowden, A.A. and Williams, J.J., 1993. Resuspension processes and seston dynamics, southern North Sea. Phil. Trans. R. Soc. Lond., *A343*, pp. 475-491.

Lampitt, R.S., 1985. Evidence for the seasonal deposition of detritus to the deep-sea floor and its subsequent resuspension. *Deep-Sea Research* 32 (8), 885-897.

Lampitt, R.S., Newton, P.P., Jickells, T.D., Thompson, J. and King, P., 2000. Near-bottom particles flux in the abyssal northeast Atlantic. *Deep-Sea Research II* 47, 2051-2071.

Lohse, L., Kloosterhuis, R.T., de Stigter, H.C., Helder, W., Van Raaphorst, W. and Van Weering, T.C.E., 2000. Carbonate removal by acidification causes loss of nitrogenous compounds in continental margin sediments. *Marine Chemistry* 69, 193-201.

McCave, I.N., 1986. Local and global aspects of the bottom nepheloid layers in the world ocean. *Netherlands Journal of Sea Research* 20, 167-181.

Monaco, A. Heussner, S., Courp, T., Buscail, R., Fowler, S.W., Millot, C. and Nyfeller, F., 1987. Particle supply by nepheloid layers on the Northwestern Mediterranean Margin. In:. Degens, E.T. Izdar, E. and Honjo, S. (Eds), Particle Flux in the Ocean. Mitteilungen aus dem Geologisch-Paleontologischen Institut der Universität Hamburg, pp. 109-125.

Monaco, A., Biscaye, P., Soyer, J., Pocklington, R. and Heussner, S., 1990a. Particle fluxes and ecosystem response on a continental margin: the 1985-1988 Mediterranean ECOMARGE experiment. *Continental Shelf Research* 10, 809-839.

Monaco, A., Courp, T., Heussner, S., Carbonne, J., Fowler, S.W. and Deniaux, B., 1990b. Seasonality and composition of particulate fluxes during ECOMARGE-I, western Gulf of Lions. *Continental Shelf Research* 10 (9/10/11), 959-987.

Morris, A.W., Bale, A.J., Howland, R.J.M., Mantoura, R.F.C. and Woodward, E.M.S., 1987. Controls of the chemical composition of particles populations in a macrotidal estuary (Tamar estuary, UK). *Continental Shelf Research* 7, 1351-1355.

Riegman, R. and Kraay, G.W., 2001. Phytoplankton community structure derived from HPLC analysis of pigments in the Faeroe-Shetland Channel during summer 1999: the distribution of taxonomical groups in relation to physical/chemical conditions in the photic zone. *Journal of Plankton Research* 23 (2), 191-206.

Sherwin, T.J., 1991. Evidence of a deep internal tide in the Faeroe-Shetland channel. In: B.P. Parker (Editor), Tidal Hydrodynamics. Wiley Interscience, Chichester, pp. 469-488.

Southard, J.B., Young, R.A. and Hollister, C.D., 1971.Experiemental erosion of calcareous ooze. *Journal of Geophysical Research* 76 (24), 5903-5909.

Stoker, M.S., Hitchen, K. and Graham, C.C., 1993. The geology of the Hebrides and West Shetland shelves, and adjacent deep-water areas, United Kingdom Offshore Regional Report. British Geological Survey, London.

Suess, E., 1980. Particulate organic carbon flux in the oceans–surface productivity and oxygen utilization. *Nature* 288, 260-263.

Thomsen, L. and Van Weering, T.C.E., 1998. Spatial and temporal variability of particulate matter in the benthic boundary layer at the N.W. European continental margin (Goban Spur). *Progress in Oceanography* 42, 61-76.

Thomsen, L. and Gust, G., 2000. Sediment erosion thresholds and characteristics of resuspended aggregates on the western European continental margin. *Deep-Sea Research I* 47 (10), 1881-1897.

Thorpe, S.A. and White, M., 1988. A deep intermediate nepheloid layer. *Deep-Sea Research* 35 (9), 1665-1671.

Turell, W.R., Slesser, G., Adams, R.D., Payne, R. and Gillibrand, P.A., 1999. Decadal variability in the composition of Faeroe Shetland Channel bottom water. *Deep-Sea Research I* 46, 1-25.

Vangriesheim, A. and Khripounoff, A., 1990. Near-bottom particle concentration and flux: temporal variations observed with sediment traps and nephelometer on the Meriadzek Terrace, Bay of Biscay. *Progress in Oceanography* 24, 103-116.

Van Raaphorst, W., Malschaert, H. and Van Haren, H., 1998. Tidal resuspension and deposition of particulate matter in the Oyster Grounds, North Sea. *Journal of Marine Research* 56, 257-291.

Van Raaphorst, W., Malschaert, H., van Haren, H., Boer, W. and Brummer, G.-J., 2001. Cross-slope zonation of erosion and deposition in the Faeroe-Shetland Channel, North Atlantic Ocean. *Deep-Sea Research I* 48 (2), 567-591.

Van Weering, T.C.E., McCave, I.N., De Stigter, H.C., Hall, I. and Thomsen, L., 1998. Recent sediments, sediment accumulation and carbon burial at Goban Spur, N.W. European continental margin. *Progress in Oceanography* 42, 5-35.

Van Weering, T.C.E. and de Stigter, H.C., 1999. Recent sediment transport and accumulation on the western Iberian Margin, Ocean Margin EXchange II Report, pp. 83-92.

Verardo, D.J., Froelich, P.N. and McIntyre, A., 1990. Determination of organic carbon and nitrogen in marine sediments using the Carlo Erba NA-1500 analyzer. *Deep-Sea Research* 37 (1), 157-165.

Walsh, I., Fisher, K., Murray, D. and Dymond, J., 1988. Evidence for resuspension of rebound particles from near-bottom sediment traps. *Deep-Sea Research* 35 (1), 59-70.

Walsh, J.P. and Nittrouer, C.A., 1999. Observations of sediment flux to the Eel continental slope, northern California. *Marine Geology* 154, 55-68.

Wollast, R., 1991. The coastal organic carbon cycle: fluxes, sources and sinks. In: Mantoura, R.F.C., Martin, J.-M, Wollast R. (eds), Ocean margin processes and global change. Wiley Interscience, Chichester, 365-381.

CHAPTER 3

Solibore-induced sediment resuspension as a dominant transport mechanism on continental slopes

ABSTRACT

The hydrodynamics at continental slopes usually favours locally enhanced mixing, suspension, deposition and transport of particulate matter, and the supply of organic matter to the benthic community. At the slope, tidal flows and internal waves may enhance currents periodically beyond the threshold required to resuspend sediments, but, much shorter, particularly intense, events have the potential to erode the surface sediment layer altogether, exposing the underlying sediment and allowing the release of nutrients to the water column. Here, we present detailed measurements of such an event, characterized by an intense internal wave, which we refer to as a "solibore", previously proposed to occur but not as yet observed. We find, by mean near-bottom sediment traps deployed a few meters above the bottom, that the solibore generates massive sediment resuspension fluxes 2 orders of magnitude greater than background levels, whilst high resolution temperature and velocity measurments demonstrate a non-linear wave train behind the rotor. Furthermore, grain size analysis of material resuspended during the passage of the solibore indicated that coarse particles ~100 µm in diameter were eroded and illustrate the high energetic potential of the observed mechanism. The interaction of solibores with the seabed provides a potentially dominant mechanism for upward tranport of sediment over continental slopes that may counteract downward advection of material by gravity.

INTRODUCTION

Sediment resuspension at continental margins is generally considered to be caused by strong boundary currents, eddies, periodic tidal flow and internal waves (McCave, 1986; Cacchione and Drake, 1986; Dickson and McCave, 1986; Thorpe and White, 1988; Huthnance et al., 2001), whereby enhanced near-bed velocities increase the bed-shear stress above a critical threshold enabling the suspension of sediment. However, much shorter but particularly intense events have the potential to erode surface sediments. Among those short and energetic events, solibores propagating up the continental slope were proposed, from laboratory and numerical experiments (Helfrich, 1992; Vlasenko and Hutter, 2002), to be important for sediment resuspension. A 'solibore' refers to intense internal waves which display the characteristics of both internal turbulent bores, with strong turbulent dissipation and causing a net change of stratification and shear, and trains of solitons or internal solitary waves (ISW) (Henyey and Hoering, 1997).

The majority of observations that may be interpreted as solibores have been made in shelf seas where they result from the nonlinear steepening of the leading edge of the shoreward propagating internal tide (e.g., Sandstrom and Elliot, 1984; Holloway, 1987; Heathershaw et al. 1987; Johnson et al., 2001) which forms hydraulic jump or baroclinic bores propagating up a slope. Solibores, and specifically ISW's, generally appear to have little impact on sediment resuspension due to their dynamic influence being constrained in the vicinity of the near surface density interface along which they propagate as waves of depression. When the situation is reversed however so that the thinner layer lies beneath a thicker, lighter layer, ISWs become waves of elevation and may interact with the sloping bottom to promote near-bed mixing and resuspension (Bogucki et al., 1997). However, up to now, near-bottom solibore-like features have only been observed in laboratory experiments (Helfrich, 1992) and numerical simulations (Lamb, 2002; Vlasenko and Hutter, 2002) on the shoaling of ISW. These form baroclinic bores of high density water propagating up the slope just as nonlinear effects during the near-critical reflection of internal gravity waves from sloping bottom may generate upslope propagating thermal fronts, associated with upslope currents and temperature drops. As the wave shoals, its rear face steepens to the point where kinematic instabilities lead to wave breaking and the eventual formation of soliton-like waves of elevation that propagate up the slope (Vlasenko and Hutter, 2002) or "turbulent boluses" (Helfrich, 1992). Such boluses or solitary waves with trapped cores (Lamb, 2002), also are potentially very effective mechanism for on-slope sediment transport. In this paper we show how a solibore propagating up the continental slope, resulting from nonlinear evolution of a hydraulic jump, is responsible for disproportionately large sediment fluxes and as such represents an alternative mechanism for sediment transport on the continental slope regions. This represents the first observation of such a feature in oceanographic setting and provide important insight into their potential in influencing mixing processes, which are of major concern for the fate of particulate and dissolved matter and the distribution of biological communities.

OBSERVATIONS

In spring 1999, an oceanographic survey was made along a transect across the south-eastern continental slope of the Faeroe-Shetland Channel, north of Scotland as part of the PROCS (Processes at the Continental Slope) programme. During this survey, a set of 6 moorings was deployed at different positions. 3 types of moorings were used: a-type mooring combining an upward looking Acoustic Doppler Current Profiler (ADCP) with a thermistor string, b-type mooring equipped with an upward looking ADCP and c-type mooring on which was mounted 4 near-bottom current meters and 2 sediment traps equipped with turbidity sensors (Optical Backscatter Sensor, OBS). The events and features described here were observed during the period of Julian day 108 to 120. A summary of the instrumentation employed during this study as well as the sampling resolution is presented in Table 1.

Table 1. *Summary of instrumentation employed during PROCS 99-1 between days 108 and 120, 1999. All Aanderaa RCM-8s and RCM-9s were equipped with temperature sensors.*

Moorings and position	Instruments	Depth (m)	Height above bottom, z (m)	Sampling interval
PRO1C3 60°49'N, 2°59'W	RCM-9, -8, -8, -8	471	8, 21, 34, 47	60 (s)
	OBS, Sediment trap		2, 30	240 (s), 24 (hrs)
PRO1A2 60°49'N, 3°00'W	RDI 600 kHz ADCP	494	3.26 – 30.26 0.5m bins	30 (s)
	NIOZ thermistor string*		2 – 33 1 m intervals	30 (s)
PRO1B4 60°53'N, 3°06'W	RDI 75 kHz ADCP	605	17 – 357 4m bins	300 (s)

As PRO1C3**:** PRO1C5, 700 m, 60°55'N, 3°11'W; PRO1C6, 777 m, 60°57'N, 3°13'W; PRO1C8, 1000 m, 61°00'N, 3°18'W
Sediment trap: PPS 4 (12 cups) for PRO1 C3, C5 and C6. Kiel type-HDW trap (20 cups) for C8.
OBS: Seapoint STM Optical Backscatter Sensor (wave length 880 nm)
* - van Haren et al. (2001)

The most striking feature, for the present study was the sharp increase in the sediment flux at mid-slope. On day 112 near-bottom sediment fluxes at 700 m increased abruptly from ~1 g m^{-2} d^{-1} to 160 g m^{-2} d^{-1} (Fig. 1) and remained high for 2-3 days. At 777 m, maximum resuspension flux reached 350 g m^{-2} d^{-1} and occurred on day 113. Strong turbidity peaks were observed on the same day at both depth (Fig. 1) indicating that particle fluxes measured from near-bottom traps were genuine and not a trapping artefact. Furthermore, particle fluxes measured from traps situated at 30 meters above the bottom (mab) display identical pattern during the whole trapping period but with on average a

factor of 2 lower. The fluxes at 471 m and 1000 m were considerably smaller, with mean values of 0.2 g m^{-2} d^{-1} and 5 g m^{-2} d^{-1} respectively over the whole deployment period. Because of the scouring of the bed by the slope current, the bed material at depths of < 500 m is composed of hard coarse sand (Van Raaphorst et al., 2001) which is considerably more difficult to resuspend than the finer unconsolidated sediments lower down the slope. Local resuspension was thus unlikely at this depth, with the observed flux being mainly the result of primary settling. Resuspension fluxes obtained from all the near-bottom sediment traps are described in more detail in Bonnin et al. (2002).
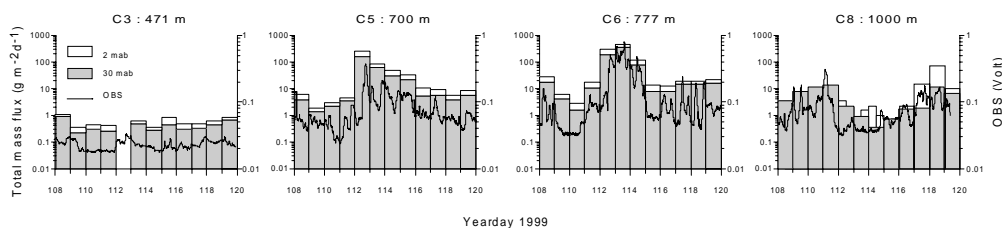
Fig. 1. *Sediment fluxes from traps positioned with their aperture at 2 and 30 mab (white and grey bars, respectively) and optical backscatter sensor (OBS) data (black lines) at 2 mab throughout deployment period. Sediment fluxes at mid-slope (700 and 777 m) were O(10^2) larger than at 471 and 1000 m after an intense and abrupt increase on day 112. In contrast to 700 m and 777 m, resuspension at 1000 m was low during days 112 and 113 and proportional to current velocity suggesting that the bed shear stress mechanism associated to strong boundary current is the dominant sediment erosion mechanism and that the dynamic influence of the solibore does not extend to this depth. The OBS signal shows a good correlation with trap data and indicates that the large sediment fluxes are genuine and not due to trapping artefact.*

On the same day massive resuspension was observed, turbulent intrusion of the thermocline up the slope was observed during a CTD and microstructure profile transect on day 112 (Fig. 2). The enhanced turbulence below the thermocline extended from a depth in excess of 700 m to 450 m, with the rate of dissipation of turbulent kinetic energy, $\varepsilon > 5 \times 10^{-7}$ W kg^{-1}. Vertical eddy diffusivities, estimated as $K_z = 0.2\varepsilon/N^2$ (Osborn, 1980) where the buoyancy frequency N is;

$$N = \left(-\frac{g}{\rho_o} \frac{\Delta\rho}{\Delta z} \right)^{\frac{1}{2}}$$

where g is the acceleration due to gravity, ρ_0 is a reference density and $\Delta\rho/\Delta z$ is the density gradient calculated over 25 m vertical intervals. K_z is in excess of 10^{-4} m^2 s^{-1} at all time within the bottom 30 m, with the maximum value at 620 m where $K_z = 10^{-1}$ m^2 s^{-1} at 10 mab. Data from OBS attached to the CTD illustrated a region of increased turbidity corresponding to the spatial extent of the density intrusion (Fig. 2 in Bonnin et al., 2002).
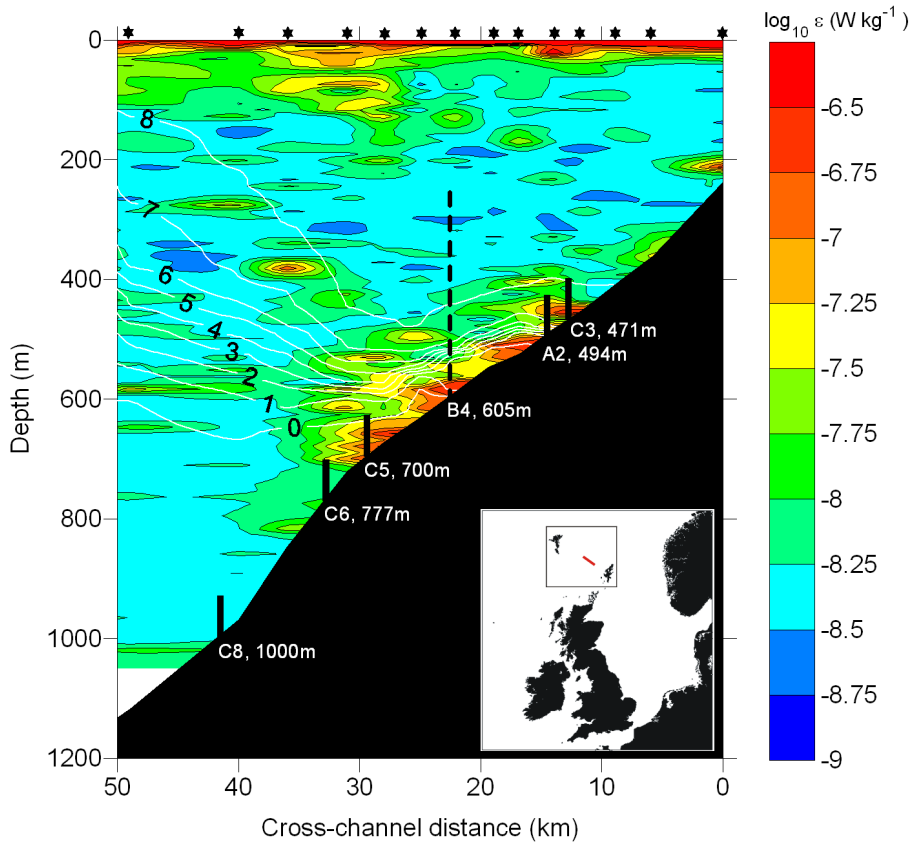
Fig. 2. *Temperature (white lines) and dissipation rate of turbulent kinetic energy, ε (color scale), over the slope during the passage of the solibore on day 112. Temperature was measured by a Conductivity-Temperature-Depth (CTD) probe whilst turbulent velocity fluctuations were measured by the FLY II free falling microstructure probe (Dewey et al., 1987). The noise level of the FLY is 10^{-9} W kg^{-1}. Rates of dissipation of turbulent kinetic energy are calculated as $\varepsilon = 7.5\nu\{(\partial u/\partial z)^2\}$, where ν is the kinematic viscosity of seawater and u is the turbulent horizontal velocity component. The black lines indicate the vertical extent of the moorings and the stars on top the position of the casts. The figure shows clearly the up-slope surge of the thermocline that is associated with the massive resuspension.*

A distinct drop in temperature observed at 471 m of 4.6°C over one minute on day 112 (Fig. 3a), and a reversal of the cross-slope current velocity from a down-slope to an up-slope orientation with a maximum amplitude of 52 cm s^{-1} (Fig. 3b) indicate strong and short-term perturbations of the hydrodynamic conditions. Similar reversals were observed at 700 m and 777 m depth, but the temperature drops were not evident due to their location far beneath the thermocline. A distinct period of warming at 471 m (and at 700 m to a lesser extent) over 4 days prior to the event on day 112 implied the depression of the thermocline down the slope, whilst a smaller temperature drop (~2°C) occurred 4 days later on day 116 and displayed the same dynamic features albeit with a lesser intensity. A surge in poleward
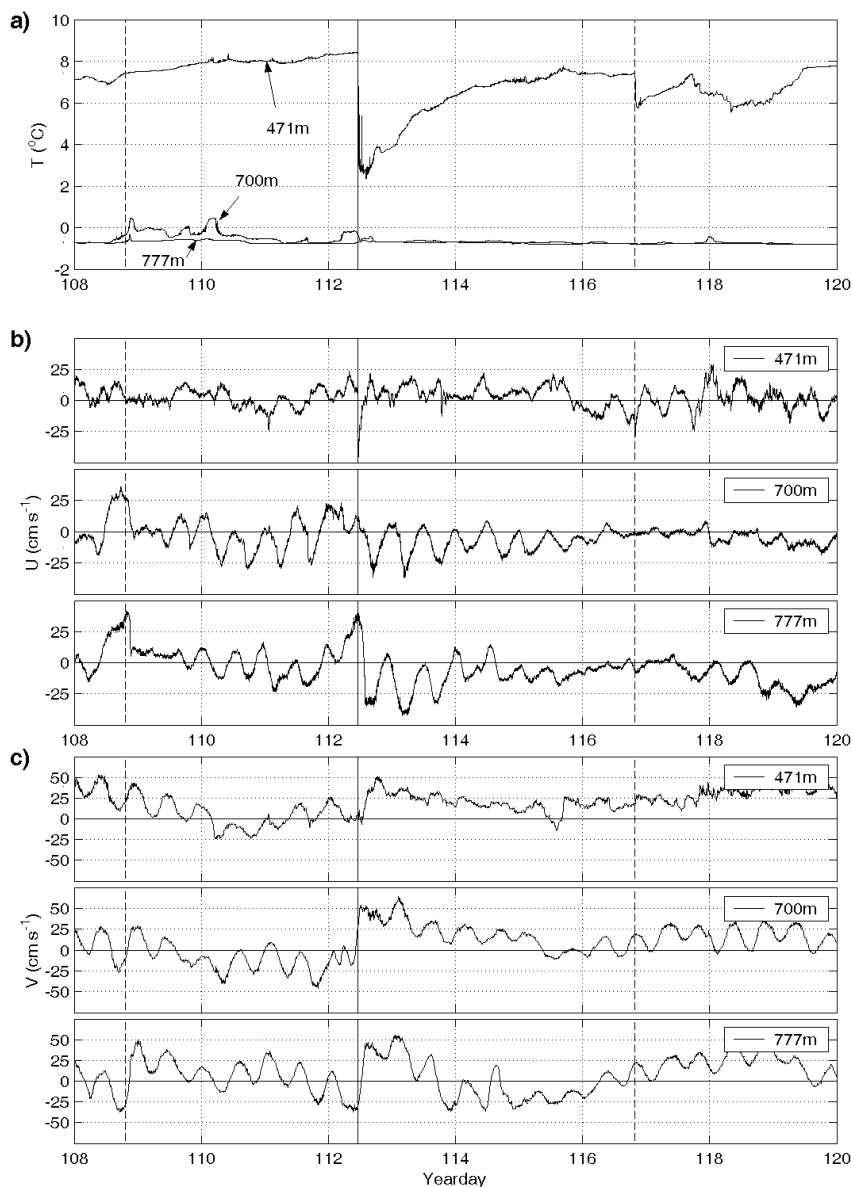
Fig. 3. *a) Temperature, b) cross-slope and c) long-slope velocities at a 8 m above the seabed, at depths of 471, 700 and 777 m. The vertical line on day 112 corresponds to the time of arrival of the temperature front at 471 m. A second, smaller but distinct drop in temperature is also observed at 471 m on day 116, although with a less pronounced signal in the current velocity except for a consistent and steady increase in poleward velocity. In contrast, 4 days earlier the current at 777 m exhibits the same strong gradients that were observed during day 112 despite the lack of a distinct signal in the temperature. Velocity components have been smoothed with a 5-point running filter.*

long-slope velocity was observed at all depths immediately following the hydrodynamic event, which at 700 m and 777 m represented a distinct reversal from the equatorward orientation prior to its passage (Fig. 3c). The surge was maintained over several semidiurnal tidal cycles and was observed both 4 days before and after.

DISCUSSION

High resolution measurements over the bottom 30 m of the water column at 494 m depth were enabled in the current study by the use of NIOZ thermistor string measuring temperature (Van Haren et al., 2001) and ADCP measuring all three velocity components, each sampling every minute and with a vertical resolution of 1 m and 0.5 m respectively. The features' resemblance to a solibore is clear as a bore-like face (at $t = 15$ minutes, Fig. 4) is followed by a wave train consisting of approximately 5 asymmetric waves extending into the thicker overlying layer (Fig. 4a). The linear long wave phase speed, is defined as:

$$c_{linear} = \left[\frac{g'H_1 H_2}{(H_1 + H_2)} \right]^{\frac{1}{2}}$$

where $g' = g(\rho_2 - \rho_1)/\rho_2$, and ρ_1, ρ_2 and H_1, H_2 are the upper and lower layer densities (calculated by establishing a temperature-salinity relationship from a CTD profile) and thicknesses, respectively. The speed c_{linear} behind the bore is 64 ± 18 cm s^{-1}, exceeding the speed of the bore itself which is 24 cm s^{-1}, determined by the time of arrival of the temperature front at 494 m and 471 m. Such a property, i.e. speed of the bore exceeded by the speed of the wave behind the bore, characterises bores (Henyey and Hoering, 1997). Furthermore, the temperature and velocity fields are consistent with the results of numerical models on the overturning of a hydraulic jump (Vlasenko and Hutter, 2002). Here, up-slope velocities easily exceeded 24 cm s^{-1} at the front of the wave train (Fig. 4b), satisfying the kinematic instability mechanism required for the overturning of the bore (Kao et al., 1985; Grue et al., 2000; Vlasenko and Hutter, 2002). Superimposed on the large scale shape of the solibore are small-scale horizontal particle velocities relative to upslope propagating internal solitary. Vertical velocities are directed upwards at the leading edges and downwards on the trailing edges of the individual waves, as expected for ISWs of elevation. However, the profiles of the waves are not of the sech^2 shape expected for ISWs; thus we propose that, the waves are in fact turbulent boluses resulting from an overturned hydraulic jump, resembling the solitary waves of elevation as observed in laboratory and numerical experiments. At the leading edge of the solibore a rotor, proposed to occur when internal waves break on a slope (Thorpe, 1998), is formed, indicated in figure 4c by the white arrows. Flow is contrary to the forward overturning of surface waves, with upwards velocities, of maximum amplitude 16.2 cm s^{-1} leading the downward flow, of maximum amplitude 14 cm s^{-1}.
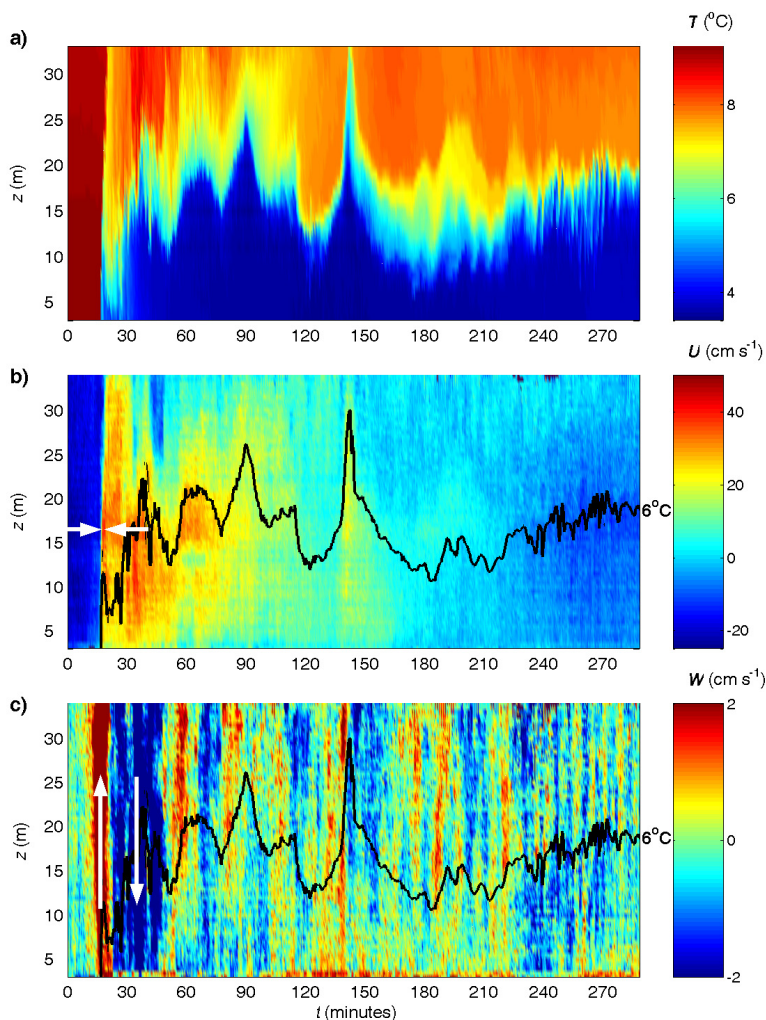
Fig. 4. *High resolution a) temperature, b) cross-slope and c) vertical velocities during the passage of the solibore. The time axis is redefined in minutes and referenced arbitrarily to an origin of t = 0 at approximately 15 minutes before the arrival of the leading edge of the solibore. The long-slope velocity component is negligible and thus omitted. The black line in b) and c) represents the position of the 6ºC isotherm. The initial temperature front at t = 15 minutes is followed by a train of 5 'soliton-like waves of elevation' with amplitudes, η, and wavelengths, L (calculated at 0.42η according to convention for solitary waves), of O(10m) and O(200m) respectively, and a packet of high frequency waves at t = 240 – 270 minutes with periods of the order of the local period of buoyancy oscillation ~5 minutes. A core of up-slope velocity is observed at the head of the solibore, with a maximum of 52 cm s⁻¹ at 16 mab. White arrows indicate the horizontally convergent currents at the leading edge and, in c), the rotor formed where upwards vertical velocities reaching 16.2 cm s⁻¹ are followed by a downwards flow reaching 14 cm s⁻¹. Vertical oscillations are observed with the passing of each subsequent wave, upwards on the leading faces and downwards on the trailing edges. The color scale in c) is compressed to visualise the vertical oscillations trailing the rotor.*

Figure 5 shows that coarse material was found at 30 mab at both 700 and 777 m water depth, indicating that sediment were not only advected horizontally but vertically as well. ISWs propagating up-stream near the seabed have the potential to facilitate resuspension during periods of low shear stress by creating an adverse pressure gradient that enables the vertical transport of the sediment against the vertical density gradient (Bogucki et al., 1997). This 'bottom pump' mechanism is, however, not consistent with our results because the resuspension we observe occurs during a period of strong currents and thus high shear stress. Enhanced turbulent dissipation may be caused in the present observations by both kinematic instabilities, when the large horizontal velocities in the solibore (> 40 cm s^{-1}) exceeded its phase speed (24 cm s^{-1}) (Vlasenko and Hutter, 2002), and by shear instabilities.
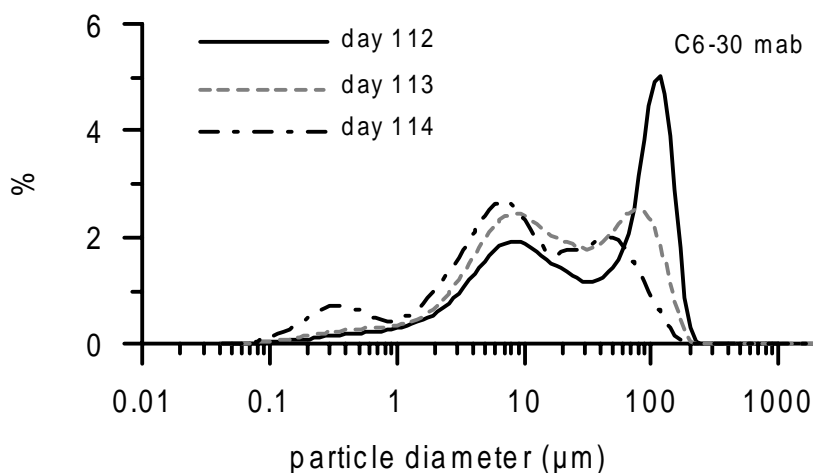
Fig. 5. *Particle diameter of material collected in sediment trap at 30 mab, 777 m depth on days 112, 113 and 114 measured with a Coulter LS 230 laser particle sizer. The energy associated with the solibore on day 112 was able to resuspend particles as large as 200 μm during day 112. Samples were ultra-sonicated prior to analysis implying that the largest fraction does not correspond to aggregates but to sediment proper, which show the intensity of the energy involved in the resuspension mechanism. Shift from the dominant particle size of ~100 μm on day 112 to ~8 μm on day 114 illustrates that the coarse particles settle out immediately after the event while finer particles remained longer in suspension in the water column. Particle as large as 100 μm were also observed at 2 mab (see Bonnin et al., Submitted).*

Shear stress due to strong long-slope boundary currents appears to be the major forcing mechanism of sediment resuspension at 1000 m and before and after the major event at mid-slope but not of the abrupt and high sediment fluxes observed at 700 and 777m on days 112 and 113. This suggests that an additional mechanism is required to explain

those particularly large and sudden fluxes. Given the data shown in figures 2 and 5 and the characteristics of the observed feature, we attribute the sediment resuspension to the rotor formed at the front of the solibore, the upward vertical velocity being particularly active in bringing the sediment several dozens of meters up in the water column. Such mechanism was also proposed by Johnson et al. (2001) to explain enhanced particle concentration near the bottom on the Californian shelf. However, their observations were made in shallower environment and no sediment fluxes were measured. Furthermore, the waves they observed were of depression while in our case they are of elevation. The 'soliton-like wave of elevation' following the temperature front is likely to entrain sediment in the water column, up to 30 meters above the bottom at least (Fig. 1), and hence facilitate transport of particle up the slope, as proposed by the experiments of Helfrich (1992) and Lamb (2002). As the waves subsequently decay, the material remaining in suspension appears to be advected by the down-slope currents following the solibore. This down-slope transport following the event, is also shown by the time lag between the maximum flux recorded at 700 m and 777 m and by the slightly higher flux recorded at 30 mab than at 2 mab at the deepest station (Fig. 1). Bonnin et al. (2002) showed that material collected in the trap during the major resuspension event was a mixture of fine and fluffy particles and coarse sediment proper. The data presented here suggest that the observed phenomenon produced sufficient energy to resuspend and transport not only the relatively loose material recently deposited at the surface of the seabed but also fairly coarse and heavy particles of sand (mainly quartz, feldspar and calcite particles, Van der Gaast, personal communication) > 100 µm in diameter for more than a day (Fig. 5).

The sudden reversal of the cross-slope velocity associated with the up-slope surge of the pycnocline points at a source for the resuspended material deeper than 470 m. Sediment is probably resuspended around 700 - 800 m and entrained up the slope to a depth where the stratification is strong enough to prevent particles to move further up and leading to sediment focusing below the main pycnocline between 550 and 850 m water depth, as shown by Van Raaphorst et al. (2001). The upslope transport of sediment is contrary to the usually assumed downslope sediment pathways from shelf seas to the deep ocean (Biscaye et al., 1994; Van Weering et al., 1998; McCave et al., 2001; McPhee Shaw et al., Submitted).

Observations from the present study illustrate the importance of short-term processes for the transport and zonation of sediments on the continental slope. The results presented here come from a single experimental period conducted for a period of 2 weeks and it might be questioned however, whether the event described in this paper is occurring on a periodic basis. Similar investigations conducted in the same area a few months later (September-October 1999) also showed abrupt sediment resuspension at mid-slope accompanied with a sudden drop in the temperature (Fig. 6) and suggest that the solibore observation is not a "lucky shot" but that such a phenomenon occurs recurrently on the Shetland slope. Although the event shown in figure 6 on days 271-272 is of smaller intensity as the feature detailed throughout this paper.

Furthermore, the 12 day-averaged resuspension flux at mid-slope reach 60 g m^{-2} d^{-1} and is of the same order as those observed in submarine canyons (e.g., Baker and Hickey, 1986), which, because they directly indent into the more biologically productive and continentally influenced shelf and because of focusing of internal waves Gardner (1989a, b) are places of enhanced sediment resuspension. The eastern slope of the Faeroe-Shetland Channel however, is remote from significant continental input such as estuary and devoid of canyons susceptible to favour sediment resuspension. The resuspension mechanism described in this paper suggests thus that short-term mechanisms are of utmost importance in the transport and cross-slope distribution of sediment on the slope.
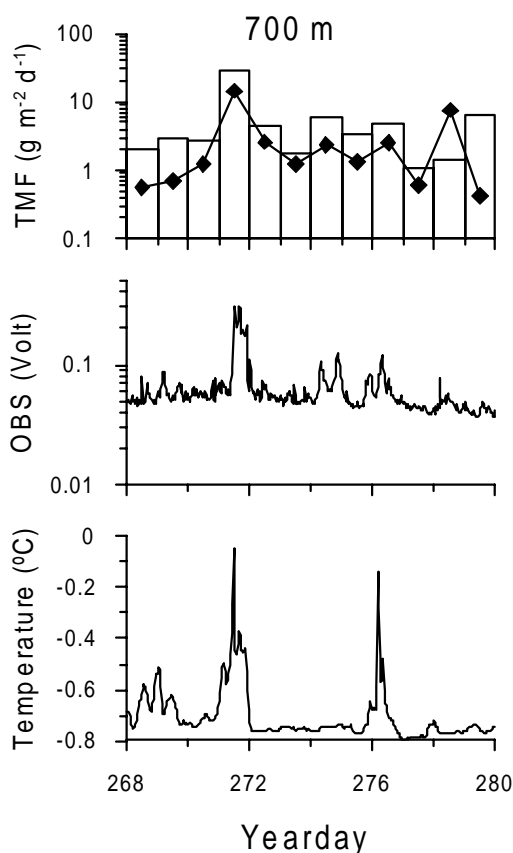
Fig. 6. *Near-bottom total mass flux (TMF) at 2 (bars) and 30 mab (diamonds), turbidity (OBS) and temperature obtained in autumn 1999 in the Faeroe-Shetland Channel at 700 m water depth. The plots show the abrupt sediment resuspension on day 271 accompanied by a sudden increase in the turbidity and abrupt drop in temperature similar to that observed at 700 m at the same location during the spring deployment.*

Such energetic mechanism would play a significant role on the fate of the organic matter in the ocean, as the particles, which are probably entrained in several erosion-resuspension-deposition loops, will undergo enhanced remineralisation due to increased exposure in the turbulent benthic boundary layer. Figure 5 shows that the finest particles (in the order of 0.1 µm) were intercepted at 30 mab 2 days after the major resuspension event. This was shown to be the case on the Iberian margin (Thomsen et al., 2002) or at the Goban Spur slope (Thomsen and van Weering, 1998) where resuspension loops within the benthic boundary layer resulted in long-term horizontal fluxes of aggregated particles and release of dissolved organic carbon (Otto and Balzer, 1998). This seems to be true for Faeroe-Shetland Channel where fine and coarse particles were resuspended 30 mab at least.

Furthermore, high abundances of sponges were observed on the slope between 500 – 800 m (Rob Witbaard, pers. communication, 2003), indicating conditions conducive for biological growth. Fom data in the near-bottom water column and surface sediments, Bonnin and Van Raaphorst (Submitted) observed dissolved silica enrichment at mid-slope and emphasized the role of surface sediment and resuspended material in this enrichment. The size of particles resuspended by the solibore indicates the erosion of the upper centimeters of the seabed, enabling the exposure of deeper sediments to the overlying water and the diffusion of dissolved substances. Thus the degree of resuspension and the intensity of the solibore are important for the observed zonation of the benthic biological community.

The temperature and velocity signals observed at 471 and 777 m water depth, both prior to and after day 112 indicate an approximately 4-day periodicity associated with the forcing of the solibores (Fig. 3). A subinertial variability is further suggested by data from instruments deployed for 4 months following the current deployment period. Such a periodicity is not consistent with tidal forcing, for which a periodicity of 12.42 hours is expected (the M_2 principal lunar component), nor is the abrupt reversal in the long-slope current component at the beginning of the 4-day period and the ensuing sustained surge in the poleward direction. The solibore also appeared during a barotropic neap tide when internal tidal forcing would be expected to be weakest. Instead, strong winds were recorded in the region two days prior to each of the three events on days 108, 112 and 116. At this time, the cause of the 4-day periodicity remains obscure. Either internal baroclinic topographic-Rossby or Kelvin waves, generated by the wind fields over the ocean during the passage of the low pressure cells are the most probabale generators.

CONCLUSIONS

We have shown that high-resolution measurements made near the seabed over the continental slope reveal the presence of solibore, propagating up the slope and facilitating massive sediment resuspension due to the formation of a rotor at its leading edge. Grain size analysis shows that the enhanced resuspension of large particles permits the exposure of the underlying sediments, promoting biological growth, whilst seismic evidence implies the

upslope transport of sediment is a continuous process on a geological timescale. Despite their limited impact of deep ocean mixing due to their relatively infrequent occurrence, our measurements indicate not only the importance of solibores as a means of sediment transport, but also their evolution from a hydraulic jump, representing the first observations in the field thus far. Our results may also be of interest to the oil community who are continuously expanding their regions of interest for drilling further offshore. Strong shear generated by the solibore in the near-bed region and the implications for seabed stability due to the continuous upslope transport of sediment and subsequent infilling of topographic irregularities will have direct consequences on drilling operations.

ACKNOWLEDGEMENTS

REFERENCES

Baker, E.T. and Hickey, B.M, 1986. Contemporary sedimentation processes in and around an active west coast submarine canyon. *Marine Geology* 71, 15-34.

Biscaye, P.E. and Anderson, R.F., 1994. Fluxes of particulate matter on the slope of the southern Middle Atlantic Bight: SEEP-II. *Deep Sea Research II* 41, 459-509.

Bogucki, D., T. Dickey and L. G. Redekopp, 1987. Sediment resuspension and mixing by resonantly generated internal solitary waves. *Journal of Physical Oceanography* 27, 1181-1196.

Bonnin, J., W. van Raaphorst, G-J. Brummer, H. van Haren and H. Malschaert, 2002. Intense mid-slope resuspension of particulate matter in the Faeroe-Shetland Channel: short-term deployment of near-bottom sediment traps. *Deep-Sea Research I* 49, 1485-1505.

Bonnin, J. and Van Raaphorst, W. Dissolved silica enrichment in the deep waters of the Faeroe-Shetland Channel. Submitted to *Deep-Sea Research I*.

Bonnin, J., Brummer, G.-J., Epping, H. G., Boer, W. and Grutters, M. Geochemical characterization of resuspended sediment on the SE slope of the Faeroe-Shetland Channel. Submitted to *Marine Geology*.

Butman, C.A., 1986. Sediment trap biases in turbulent flows: Results from a laboratory flume study. *Journal of Marine Research* 44 (3), 645-693.

Cacchione, D.A. and Drake, D.E., 1986. Nepheloid Layers and Internal Waves Over Continental Shelves and Slopes. *Geo Marine Letters* 6, 147-152.

Dewey, R.K., Crawford, W.R., Gargett, A.E. and Oakey, N.S., 1987. A microstructure instrument for profiling oceanographic turbulence in coastal bottom boundary layers. *Journal of Atmospheric and Oceanic Technology* 4, p 288-297.

Dickson, R.R. and McCave, I.N. 1986. Nepheloid layers on the continental slope West of Porcupine Bank. Deep-Sea Research 33(6), 791-818.

Gardner, W.D., 1985. The effect of tilt on sediment trap efficiency. *Deep-Sea Research* 32 (3), 349-361.

Gardner, W.D., 1989a. Periodic resuspension in Baltimore Canyon by focusing of internal waves. *Journal of Geophysical Research* 94, 18185-18194.

Gardner, W.D., 1989b. Baltimore Canyon as a modern conduit of sediment to the deep sea. Deep-Sea Research 36, 323-358.

Grue, J., Jensen, A., Rusas P.O., and Sveen, K.J. 2000. Breaking and broadening of internal solitary waves. *Journal of Fluid Mechanic* 413, 181-217.

Heathershaw, A.D., New, A.L. and Edwards, P.D., 1987. Internal tides and sediment transport at the shelf break in the Celtic Sea. *Continental Shelf Research*, 7 (5), 485-517.

Helfrich, K.R., 1992. Internal solitary wave breaking and run-up on a uniform slope. *Journal of Fluid Mechanic* 243, 133-154.

Henyey, F.S. and Hoering, A., 1997. Energetics of borelike internal waves. *Journal of Geophysical Research* 102 (C2), 3323-3330.

Holloway, P.E., 1987. Internal hydraulic jumps and solitons at the shelf break region on the Australian North West Shelf. *Journal of Geophysical Research* 92 (C5), 5405-5416.

Hosegood, P.J. and Van Haren, H., 2003. Ekman-induced turbulence over the continental slope in the Faeroe-Shetland Channel as inferred from spikes in current meter observations. *Deep-Sea Research* I 50 (5), 657-680.

Hosegood, P.J. and Van Haren, H. Near-bed solibores over the continental slope in the Faeroe-shetland channel. Submitted to *Deep-Sea Research II*.

Huthnance, J.M., Coelho, H., Griffiths, C.R., Knight, P.J., Rees, A.P., Sinha, B., Vangriesheim, A., White, M. and chatwin, P.G., 2001. Physical structures, advection and mixing in the region of Goban spur. *Deep-Sea Research II* 48, 2979-3021.

Johnson, D., Weidemann, A. and Scott Pegau, W., 2001. Internal tidal bores and bottom nepheloid layers. *Continental Shelf Research* 21, 1473-1484.

Kao, T.W., Pan, F.S., and Renouard, D., 1985. Internal solitons on the pycnocline: Generation, propagation and shoaling and breaking over a slope. *Journal of Fluid Mechanic* 159, 19-53.

Lamb, K.G., 2002. A numerical investigation of solitary internal waves with trapped cores formed via shoaling. *Journal of Fluid Mechanic* 451, 109-144.

McCave, I.N., 1986. Local and global aspects of the bottom nepheloid layers in the world ocean. *Netherlands Journal of Sea Research* 20, 167-181.

McCave, I.N., Hall, I.R., Antia, A.N., Chou, L., Dehairs, F., Lampitt, R.S., Thomsen, L., Van Weering, T.C.E. and Wollast, R., 2001. Distribution, composition and flux of particulate material over the European margin at 47°-50ºN. *Deep-Sea Research II* 48, 3107-3139.

McPhee-Shaw, E.E., Sternberg, R.W., Mullenbach, B. and Ogston, A.S., 2002. Observations of intermediate nepheloid layers on the northern California continental margin. Submitted to *Continental Shelf Research*.

New, A.L. and Pingree, R.D., 2000. An intercomparison of internal solitary waves in the Bay of Biscay and resulting from Kortewg-de Vries-Type theory. *Progress in Oceanography* 45, 1-38.

Osborn, T.R., 1980. Estimates of the local rate of vertical diffusion from dissipation measurements. *Journal of Physical Oceanography* 10, 83-89.

Otto, S. and Balzer, W., 1998. Release of dissolved organic carbon DOC from sediments of the NW European continental margin Goban Spur and its significance for benthic carbon cycling. *Progress in Oceanography* 42, 127-144.

Rhines, P., 1970. Edge-, bottom-, and Rossby waves in a rotating stratified fluid. *Geophysical Fluid Dynamic* 1, 273-302.

Sandstrom, H. and Elliot, J.A., 1984. Internal Tide and Solitons on the Scotion Shelf: A Nutrient Pump at Work. Journal of Geophysical Research 89 (C4), 6415-6426.

Thomsen, L. and van Weering, T.C.E., 1998. Spatial and temporal variability of particulate matter in the benthic boundary layer at the N.W. European Continental Margin (Goban Spur). *Progress in Oceanography* 42, 61-76.

Thomsen, L. and Gust, G., 2000. Sediment erosion thresholds and characteristics of resuspended aggregates on the western European continental margin. *Deep-Sea Research I* 47 (10), 1881-1897.

Thomsen, L., van Weering, T.C.E. and Gust, G., 2002. Processes in the benthic boundary layer at the Iberian continental margin and their implication for carbon mineralization. *Progress in Oceanography* 52, 315-330.

Thorpe, S.A and White, M., 1988. A deep intermediate nepheloid layer. *Deep-Sea Research* 35 (9), 1665-1671.

Thorpe, S.A., Keen, J.M., Jiang, R. and Lemmin, U., 1996. High-frequency internal waves in Lake Geneva. Phil. Trans. R. Soc. Lond., A354, 237-257.

Thorpe, S.A., 1998. Some dynamical effects of internal waves and the sloping sides of lakes. In: Physical Processes in Lakes and Oceans, Coastal and Estuarine Studies Volume 54, (Ed: Imberger, J.) 441-460, American Geophysical Union.

Van Haren, H., Groenewegen, R., Laan, M. and Koster, B., 2001. A fast and accurate thermistor string. *Journal of Atmospheric and Oceanic Technology* 18, 256-265

Van Raaphorst, W., Malschaert, H., van Haren, H., Boer, W. and Brummer, G.-J., 2001. Cross-slope zonation of erosion and deposition in the Faeroe-Shetland Channel, North Atlantic Ocean. *Deep-Sea Research I* 48 (2), 567-591.

Van Weering, T.C.E., McCave, I.N., De Stigter, H.C., Hall, I. and Thomsen, L., 1998. Recent sediments, sediment accumulation and carbon burial at Goban Spur, N.W. European continental margin. *Progress in Oceanography* 42, 5-35.

Vlasenko, V. and Hutter, K., 2002. Numerical experiments on the breaking of solitary internal waves over a slope-shelf topography. *Journal of Physical Oceanography* 32, 1779-1793.

CHAPTER 4

Silicic acid enrichment in the deep water of the Faeroe-Shetland Channel

ABSTRACT

To evaluate the relative contribution of continental slope sediments, resuspended particles and settling material to the refuelling of dissolved silica in a high-energy environment, a study was conducted in the Faeroe-Shetland Channel (FSC), one of the main pathways of the newly formed Atlantic Deep Water. Fluxes of silicic acid (DSi) to the water column determined by multiplying the DSi concentration gradient by the vertical eddy diffusion coefficient showed a maximum at mid-slope (600-800 m) with values reaching up to 1700 µmol m^{-2} d^{-1} near the seabed. The mere dissolution of settling biogenic silica, estimated at 30-120 µmol m^{-2} d^{-1}, cannot account for this refuelling of the deep-waters of the FSC with DSi. Benthic DSi effluxes on the slope, obtained from incubations and from modeling pore water DSi profiles, both indicated higher fluxes at mid-depth which corresponds to a zone of enhanced deposition and higher biogenic silica content. Contribution of DSi from benthic fluxes range from 370 to 740 µmol m^{-2} d^{-1} and can, to a large extent, sustain the enhanced calculated flux in the water column. Furthermore, the recurrent resuspension of bottom material, as observed at mid-slope being associated with turbulent flow, contributes to the increase in DSi concentrations in the deep water of the FSC with fluxes ranging from 60 to 800 µmol m^{-2} d^{-1}.

Our data illustrate the importance of the geomorphological setting of the basin which, with its shallow depth, funnel shape and turbulent conditions, favors the erosion and resuspension of surface sediment and the deposition of relatively fresh sediments at mid-slope, hence focusing the refuelling of passing waters with DSi.

INTRODUCTION

Silicon is a major element in the marine environment. It is utilized as silicic acid mainly by diatoms in the formation of their opal ($BSiO_2$) frustules. During the past decade many studies focused on the silica cycle because of the potential use of $BSiO_2$ in deep-sea sediments as a proxy for paleoproductivity reconstruction (e.g., Nelson et al., 1995; McManus et al., 1995; Tréguer et al., 1995). However, the applicability of this proxy is debated (e.g., Berger and Herguera, 1992; Nelson et al., 1995) mainly because of marked spatial and temporal variations in $BSiO_2$ preservation and a strong decoupling of the geochemical cycles of Si and C. Upon the cell death, diatoms frustules sink to the bottom of the ocean. Because the water column is undersaturated in silicic acid (DSi) with respect to biogenic silica, a major part of the biogenic silica produced in the euphotic zone dissolves during settling through the water column (Hurd, 1973). Nelson (1995) estimated that at a global scale at least 50% of the silica produced by diatoms in the euphotic zone dissolves in the upper 100 m of the water column. Diatom frustules that escape dissolution during settling reach the sea floor where the major fraction dissolves at the sediment-water interface or in surface sediments (e.g., Koning et al., 1997). Upon burial, dissolution continues, giving rise to pore water DSi concentrations well above those in the overlying water (e.g., Hurd, 1973; Schink et al., 1974; Rabouille et al., 1997). This concentration gradient drives an efflux of silicic acid across the sediment water interface, thereby returning dissolved silica to the water column. Although a major fraction of the $BSiO_2$ produced in the surface water dissolves, a non-negligible part of ~3% is finally buried in the sediment (Calvert, 1983; Tréguer et al., 1995).

Many areas with silica-rich bottom waters and $BSiO_2$-rich sediments such as the Southern Ocean (e.g., Rutgers van der Loeff and Van Bennekom, 1989, Rabouille et al., 1997) and the Pacific and Indian Oceans (e.g., Hurd, 1973, Koning et al., 1997) have been investigated with respect to their control on silica budgets.

In this study, we will focus on DSi regeneration in the low DSi concentration area of the Faeroe-Shetland Channel (FSC), one of the two major pathways of newly formed deep waters from the Nordic Seas to the North Atlantic. In this high-energy environment, bottom currents have been shown to create intense sediment resuspension on the continental slope. Our aim is to estimate the contribution of the sediment and resuspended matter in the enrichment of the bottom water of the FSC with silicic acid. Such investigation, combining water column, sediment trap and surface sediment data is essential to better understand the slope processes in the recycling of biogenic silica in a region of major significance for the global hydrography.

STUDY AREA

The FSC intrudes between the Faeroes and Shetland islands and connects the Norwegian Sea with the Iceland Basin and the North Atlantic Ocean (Fig. 1). The northern entrance is 1500-2000 m deep and progressively shoals southwards until it reaches a sill of about 1000 m deep southeast of the Faeroes. The channel turns west in front of the Wyville-
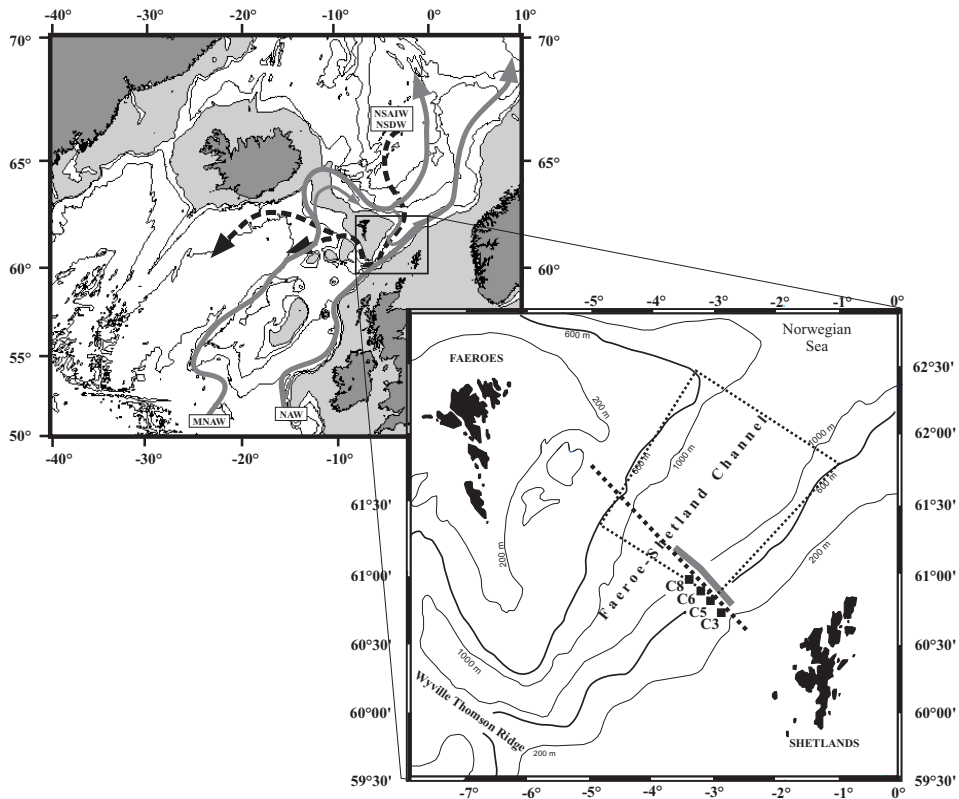

***Fig. 1.** Study area with hydrography simplified from Hansen and Østerhus (2000) mentioned by the arrows in the upper map. The grey arrows represent the inflow of surface warm water from the North Atlantic and the dashed black arrows the overflow cold bottom water flowing from the Norwegian Sea. NAW: North Atlantic Water, MNAW: Modified North Atlantic Water, NSAIW: Norwegian Sea/Arctic intermediate Water, NSDW: Norwegian Sea Deep Water. The lower map shows a blow up of the sampling area with positions of the multicore transect (solid line), the CTD rosette transect (dotted line) and sediment trap moorings (squares). The dotted trapezoid indicates the surface area (SA) used for calculation of balance DSi flux in the discussion.*

Thomson Ridge (WTR, with a sill depth at around 600 m). Subsequently, it deepens again to a depth of 1200 m between the WTR, the Faeroe Bank and the Faeroe Plateau, after which it prolongs into the Faeroe Bank Channel (FBC) orientated northwestward and opening into the north of the Iceland Basin. The hydrography of the FSC is rather complex with 4 water masses present (Hansen and Østerhus, 2000) that all play an active role in the thermohaline circulation. In a simplified view, one can consider two layers: the warm and saline surface waters (0-450 m) and the cold and less saline deep waters (450 m to the bottom). The surface waters consist of two components: the North Atlantic Water (NAW) and the Modified North Atlantic Water (MNAW). The NAW flows over the northern European continental slope and is restricted to the Shetland side of the channel. The MNAW skirts round the Faeroes on the west side, branches off into the FSC along the Faeroe plateau and turns back towards the northeast. The deep waters flow southwestward from the Norwegian Sea and consist also of two components (Turrell et al., 1999): the Norwegian Sea Arctic Intermediate Water (NSAIW) which flows between 450 and 800 m water depth and the Faeroe-Shetland Channel Bottom water (FSCBW originating from the Norwegian Sea Deep Water) which occupies the bottommost part of the channel. The deep water entering the Faeroe Shetland Channel and originating from the Norwegian Sea is a well mixed water mass.

The largest part of the FSC deep-waters is considered to flow to the North Atlantic via the FBC but there is also intermittent flow over the WTR that continues south of the FBC (Kuijpers et al., 1998). The FSC and the FBC form the main conduit for the deep-water flow from the Norwegian Sea to the North Atlantic with bottom currents flowing at speeds up to 1.0 m s^{-1} (Kuijpers et al., 2002). The water of the FSC is strongly stratified with the major pycnocline lying at ~600 m water depth across the Shetland slope. Temperature profiles of the FSC are shown in figure 2. Temperature decreases from > 8ºC near the surface on the Shetland side (NAW flowing north-eastwards) to –0.8ºC in the deepest part of the channel (FSCBW flowing south-westwards) with a steep gradient at ~600 m water depth as the temperature drops from 7 to 0ºC within 100 m.

MATERIAL AND METHODS

All samples were collected during 3 cruises of the PROCS (PROcesses at the Continental Slope) programme in the Faeroe-Shetland Channel: one cruise in spring 1997 from which only data from the surface sediment are presented, and 2 cruises in 1999 (spring and fall). Surface sediment as well as sediment trap and water samples (DSi and total particulate matter) data for the spring 99 cruise are shown in this study. From the fall cruise; only surface sediment and rosette bottles (DSi) are used here. During each survey, observations and sampling were made on a transect across the channel (Fig. 1) focusing particularly on the Shetland continental slope at the south-east of the channel.
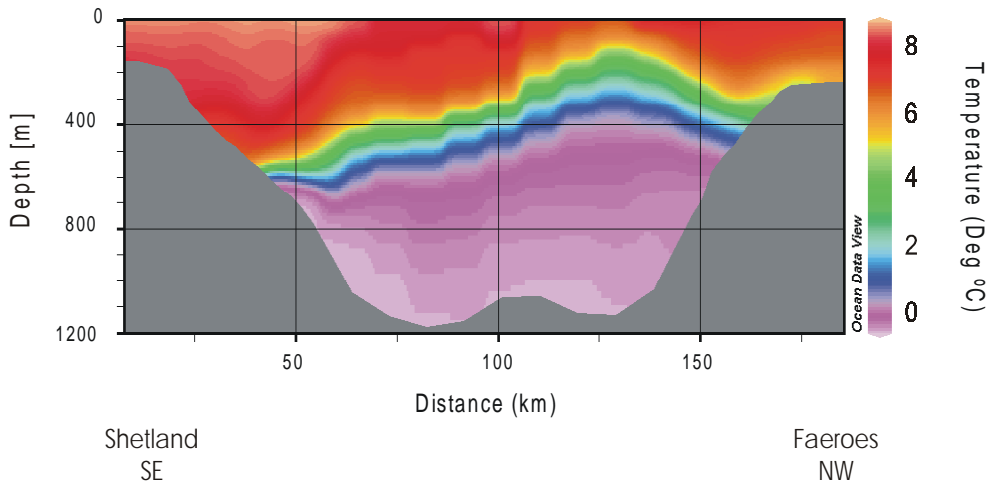
Fig. 2. *Temperature distribution across the Faeroe-Shetland Channel in spring 1999 on a transect made from the Shetland to the Faeroes during Julian days 116 to 118. Note that temperature show a very steep gradient at mid-depth on the Shetland side (~600 m water depth).*

Surface sediment cores and pore water collection

Sediment samples were collected using a multicorer (Barnett et al., 1984) at different stations on a section perpendicular to the Shetland slope from 300 to 1228 m water depth (Fig. 1). The corer was equipped with 12 polycarbonate tubes, which normally collected undisturbed cores of 20-35 cm long with clear overlying water: 8 tubes with inner diameter of 62 mm were used for sediment characterization and pore water collection, and 4 tubes with inner diameter of 95 mm were used for on-board incubation for measurement of DSi fluxes. Turbid cores indicating disturbance were discarded. Immediately after retrieval, the cores were transported into a cool container (~4ºC). For each core, the overlying water was sampled to measure DSi in the bottom water and was siphoned off with a syringe. The cores were sliced in intervals of 2.5 mm for the upper cm, 5 mm from 1 to 3 cm, 10 mm from 3 to 7 cm and 20 mm from 7 to 15 cm using the NIOZ high-resolution core slicer (Van der Zee et al., 2001). The slices of corresponding intervals of 3 to 4 cores were pooled and centrifuged for 9 minutes at 2500 rpm directly onboard and filtered through a 0.45 µm membrane filter. For a few stations no reliable pore water profiles could be collected because the sediments were too porous. The same slicing procedure was applied to the rest of the cores for sediment characterization and the sediment slices were frozen at -20ºC until further analysis on shore.

Sediment traps

Four moorings, C3, C5, C6 and C8, each including 2 sediment traps with their aperture positioned at 2 and 30 meters above the bottom (mab) respectively were deployed on a transect across the Shetland slope at water depths of 471, 700, 777 and 1000 m in April/May 1999 (Fig. 1). In addition, a long-term sediment trap was also deployed at 800 m water depth at 2 mab for a duration of 5 months following the spring deployment. To allow sampling in the high-energy regime of the FSC, all traps were modified from their conventional conical shapes to cylindrical shapes by mounting a 1.5-m long PVC cylinder on top with a baffled aperture (10 mm hexagons). The resulting total length of the traps is 2 m and the collecting area on the top of the trap is 0.042 m^2. Thus, all sediment traps have a similar collection area and a uniform cylindrical shape with an aspect ratio of 8 that was shown to be appropriate for relatively high-energy conditions (Gardner, 1985). The traps are hereafter identified by the number of the mooring followed by the height above the bottom at which they stand, i.e. C5-2, C5-30 etc. For more details on the sediment traps and trap samples treatment, see Bonnin et al. (2002).

Water column filtration and organic carbon analysis

Water samples were collected at 100 m intervals, from about 10 m above the bottom to 10 m below the sea surface during the upcast of CTD-rosette deployments. Water from 12 l NOEX bottles was transferred on-deck into 10 l Nalgene® bottles that were transported into the cool container (4ºC) for further processing. The bottles were shaken vigorously before a 2 l sub-sample was filtered through pre-weighted 1.0 µm Poretics® polycarbonate filters, using a low-vacuum system, to determine total particulate matter (TPM) and BSiO$_2$.

Sediment-water DSi effluxes

The sediment-water fluxes were determined by whole core incubation onboard and were predicted from DSi pore water profiles using a simple 1-D transport reaction model. Sediment cores were incubated onboard at in situ temperature directly after retrieval. For this, depending on the quality of the cores, two to four cores of 95 mm diameter were used. An electric stirrer was placed on top of the overlying water to reproduce the near-bottom turbulence prevailing at the seabed, resulting in an average effective diffusive boundary layer (DBL) of ~400 µm, as determined by oxygen microprofiling. For each core, a 10 ml water sample was taken every 30 minutes for 6 hours. The samples were stored at 4ºC until analysis. Dissolved silica was measured onboard using the colorimetrical method described by Grashoff et al. (1983) on a TRAACS 800+ auto-analyzer with an accuracy of 2% at full

scale of 5 to 20 μM. Fluxes were calculated from linear regression of the change in concentration during the incubations after correction for the effect of decreasing water volume due to sampling.

Alternatively, sediment-water fluxes were predicted from pore water profiles. The pore water profiles were described with a steady state diffusion-first order dissolution model (e.g., Aller and Benninger, 1981):

$$0 = D_s \frac{\partial^2 C}{\partial z^2} + k_d (C_a - C) \cdot$$ (1)

D_s is the whole sediment molecular diffusion coefficient for silicic acid corrected for tortuosity according to Andrews and Bennett (1981):

$$D_s = \phi^2 D_0,$$ (2)

where D_0 the free solution molecular coefficient (Wollast and Garrels, 1971), was corrected for temperature, using the Strokes-Einstein relation (Li and Gregory, 1974). ϕ is porosity; z denotes depth in meters, k_d is the apparent first order rate constant for dissolution (d^{-1}) and C_a is the apparent saturation silicic acid concentration reached at depth in mmol l^{-1}. The solution to equation (1) is:

$$C_{(z)} = (C_0 - C_a)e^{-\delta z} + C_a$$ (3)

where C_0 is the concentration of silicic acid at $z = 0$ in mmol l^{-1} and δ is $\sqrt{k_d/D_s}$ (m^{-1}). The diffusive exchange across the sediment-water interface was calculated according to Fick's first law of diffusion:

$$J_{(sed)} = -\phi \sqrt{k_d . D_s} \left(C_0 - C_a \right) \qquad \text{for } z = 0$$ (4)

Transport from the sediment to the overlying water maybe impeded by the DBL on the top of the sediment. The steady state diffusion-first order dissolution model was thus extended with a description of the DSi concentration in the diffusive boundary layer (Koning et al., 1997). The flux of silicic acid across the DBL can be described as:

$$J_{(dbl)} = -D_0 \frac{C_0 - C_w}{Z_{dbl}} \tag{5}$$

where C_w is the silicic acid concentration in the water overlying the sediment and Z_{dbl} the thickness of the DBL, usually < 0.5 mm. For calculation of the fluxes, we assumed a DBL of 0.4 mm (Koning et al., 1997). At $z = 0$, the flux across the DBL must equal the flux from the sediment. Thus, the concentration C_0 in eq. (3) to (5) can be expressed as:

$$C_0 = \frac{C_a \phi \sqrt{k_d D_s} + C_w \dfrac{D_0}{Z_{dbl}}}{\dfrac{D_0}{Z_{dbl}} + \phi \sqrt{k_d D_s}} \tag{6}$$

Solid phase biogenic silica

The $BSiO_2$ content in surface sediments, trap samples and total particulate matter was measured using the automated alkaline leaching technique described by Koning et al (2002) that in turn was adapted from the method of Müller and Schneider (1993). For trap samples and surface sediments, material was crushed with agate mortar and pestle. Sample size was between 0.3 mg and 1.9 mg for filters, 5 - 35 mg for trap samples and 25 - 95 mg for sediments.

The experimental details were described by Koning et al. (2002) and are recapped only briefly here. Samples were leached in 0.5M NaOH for 1.5 hour and a sample split was fed into a continuous flow analyzer and analyzed for silicic acid using the molybdate-blue spectrophotometric method (Strickland and Parsons, 1968). A second sample split was fed into a second auto-analyzer system for fluorimetric measurement of simultaneously dissolving aluminum. The analyzer output was recorded digitally every second and dissolution curves of silica and aluminum versus time were obtained. A standard calibration curve was measured for every batch of newly prepared leaching solution and showed little or no change in slope over time.

Following the procedure of Koning et al. (2002), a six-second average was used to reduce the number of data points and to dampen the influence of noise in the recorded dissolution curve. To determine the biogenic silica fraction in the sample, analytical model 2 described in Koning et al. (2002) was used for all our samples. This model describes the time courses of DSi and Al_{aq} during leaching assuming that the analysed samples are composed of a mixture of 2 reactive silica fractions and 1 linearly dissolving lithogenic fraction. Because no samples were available for replicate analysis it is not possible to produce any uncertainty values on our measured $BSiO_2$ content. Repeated run on surface sediment sample from the Iberian Margin showed an accuracy of 2% (Koning, pers. communication).
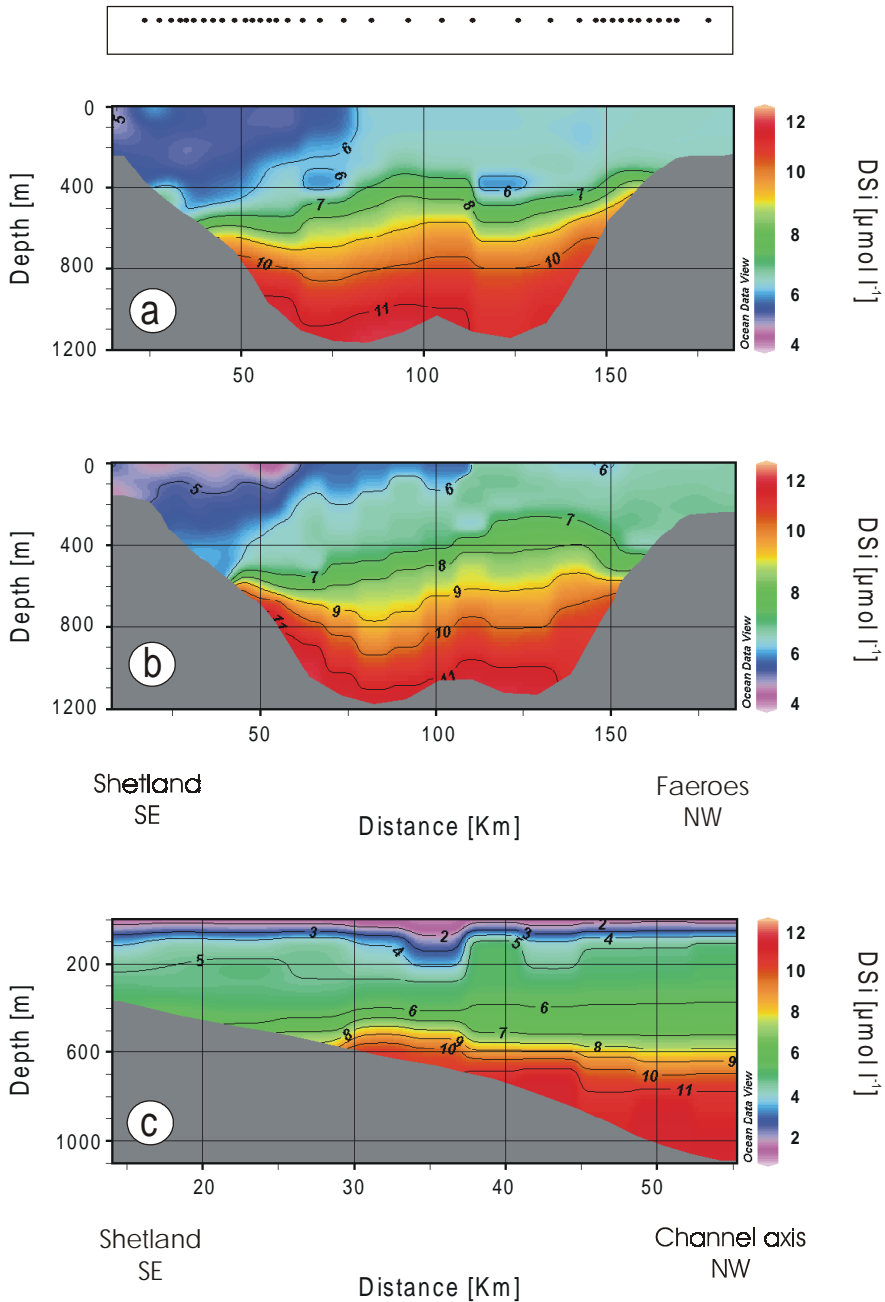
Fig. 3. *Distribution of the DSi concentration across the FSC. Plots a (days 109-112) and b (days 116-118) show the distribution for the spring cruise from the Shetland side (left) to the Faeroe side (right) while plot c shows the distribution for the fall cruise across the Shetland slope only (days 271-272). For all 3 sections, the concentration gradient is maximum at ~600 m water depth. The dots in the rectangles on top of the plots indicate the position of the measuring stations.*

RESULTS

DSi concentration in the FSC

DSi in the water column has been measured twice along one cross-channel transect during the April/May cruise, and once across the Shetland slope at the same location in September. For the two spring cross-sections the picture is fairly similar, the DSi concentration ranging between 4 µmol l^{-1} at the surface and 12 µmol l^{-1} at 5 m above the bottom (Fig. 3 a and b). For the September section, the general pattern is similar but with concentrations ranging from < 2 µmol l^{-1} at the surface to > 12 µmol l^{-1} at the foot of the slope (Fig. 3c). The lowest values were observed in the warm NAW flowing parallel to the Shetland shelf (Fig 1). For all transects, a steep gradient in DSi concentration was observed at mid-depth on the Shetlands slope at around 600 m water depth, where the major pycnocline meets the bottom.

Sediments

Solid phase- The top centimetres of the surface sediments on the upper slope, between 300 and 477 m, consisted of hard sand. From 477 to 600 m the sea floor was densely covered with gravel and cobbles deposited during the last glacial period. The median grain size was > 500 µm between 300 and 450 m, 400 µm at 477 m and decreased from 274 µm at 650 m to 158 µm at 800 m. The clay/silt fraction (< 63 µm) varied between 8% at 300 m to 24% at 850 m. For most of the stations a glacial clay layer was observed below 5 cm depth. Porosity in the upper cm's was between 0.48 at 375 m and 0.61 at 1228 m depth with a mean value of ~0.56 at mid-slope. Sediments were low in carbonates (inorganic C content between 1 and 1.5wt%) and organic matter (Corg content between 0.22 and 0.42wt%, Table 1).

BSiO$_2$ content of surface sediment across the Shetland slope ranged from 0.25% to 0.90% of dry weight at 477 and 1228 m water depth, respectively (Fig. 4a). BSiO$_2$ content shows a clear local maximum of 0.6-0.7% between 550 and 700 m water depth. Down-core profiles of BSiO$_2$ were made and, for selected stations, shown in figure 5. The profiles showed a clear difference between the shallowest and deepest stations with a very low content (0.13%) at 300 m and higher at 1100 m (0.8%). For the other stations, BSiO$_2$ content generally decreased with depth although the presence of the glacial clay layer at relatively shallow depth (2-4 cm) may complicate this interpretation, as it is the case at 550 m (Fig. 5). At mid-slope (e.g., 672 m), the glacial clay layer was found at much greater depth (10-12 cm), indicating enhanced deposition at this depth since the last glacial.
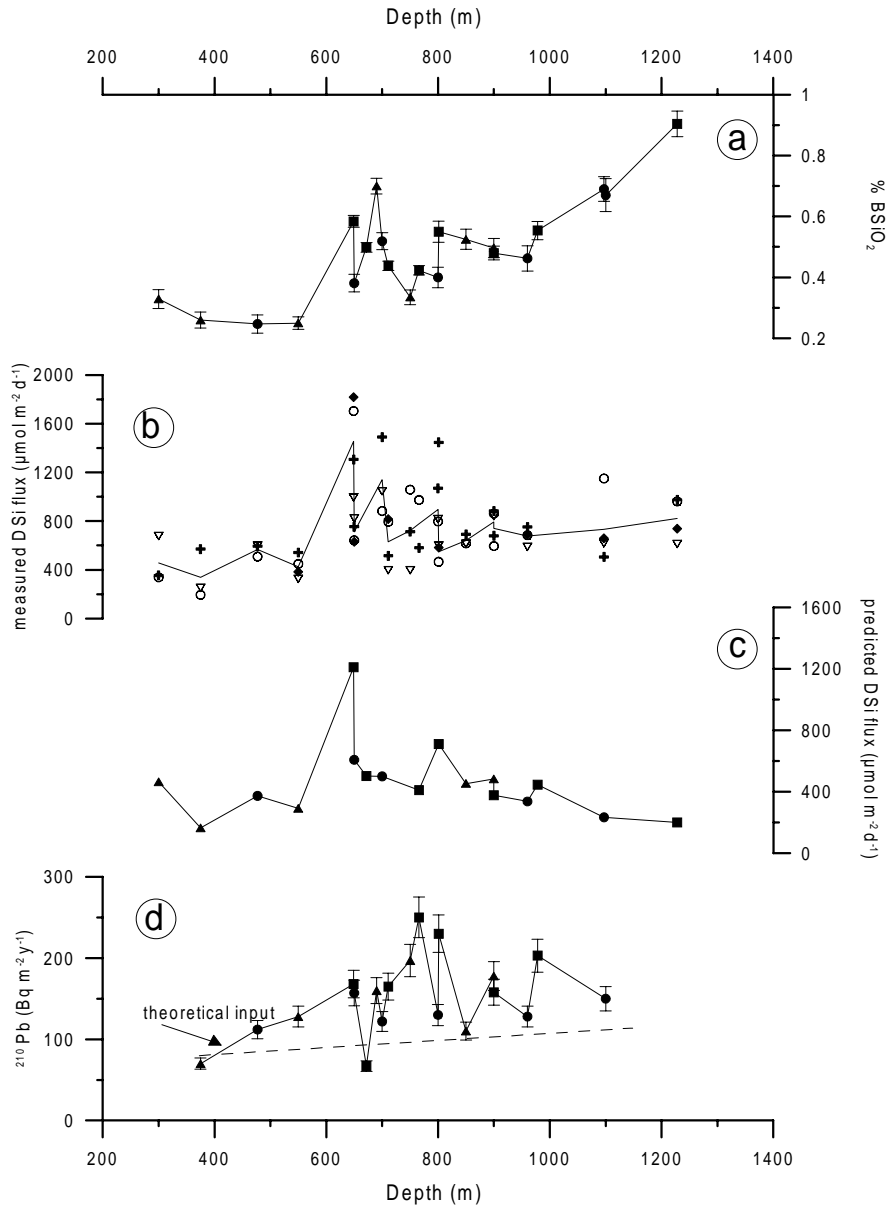
Fig. 4. *BSiO$_2$ content of the surface sediments (a), measured DSi efflux from on-board incubation (b), predicted DSi efflux from pore water profiles (c), ^{234}Th and ^{210}Pb input fluxes ((d) and (e), respectively) plotted versus depth. For plots a, c and e the squares represent the surface sediments sampled during cruise PROCS 97, the triangles the samples from PROCS 99-1 (spring) and the dots those from PROCS 99-2 (fall). For plot (b), for a given depth, the different symbols represent the flux value for every single core (between 2 and 4 depending on the stations) with which incubation experiments was carried on and the solid line represents the mean for each station. The theoretical ^{210}Pb input flux expected from atmospheric deposition and production from ^{226}Ra decay in the water column is indicated in (e). The error bars indicate 2xSD. The ^{210}Pb data were partly published in Van Raaphorst et al. (2001).*
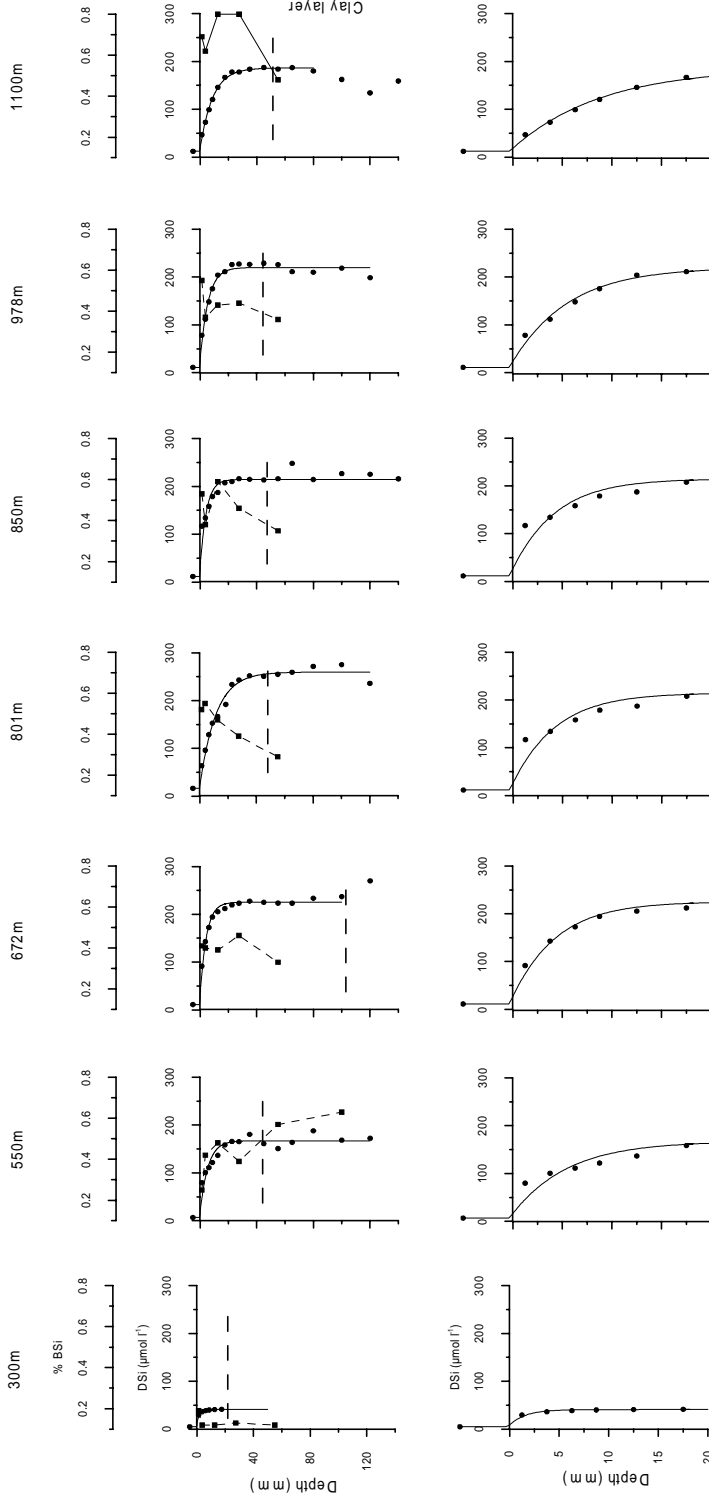
Fig. 5. *The upper plots show selected pore water profiles (dots) and BSiO$_2$ content in the sediments (squares). Pore water profiles are fit with the model described in the method part. For each station, the dashed line indicates the position of the glacial clay layer. It shows that deposition since the last glacial is higher at 672 m than anywhere else on the slope. The blow up of the top 20 mm of the pore water profiles (lower plots) shows that the pore water model do not fit the uppermost point, resulting in lower estimates of the DSi fluxes from this method.*

Table 1. *Location and depth of the surface sediment stations with Corg content.*

Depth (m)	Cruise	Long. (ºE)	Lat. (ºN)	Surface Corg (%dw)
300	Spring 99	-2.87	60.73	-
375	Spring 99	-2.91	60.76	0.29
477	Fall 99	-2.94	60.83	0.22
550	Spring 99	-3.05	60.85	0.25
649	Spring 97	-3.11	60.90	0.25
650	Fall 99	-3.08	60.93	0.29
672	Spring 97	-3.14	60.92	0.30
690	Spring 99	-3.14	60.91	0.27
700	Fall 99	-3.11	60.95	0.33
711	Spring 97	-3.17	60.93	0.22
750	Spring 99	-3.20	60.94	0.24
766	Spring 97	-3.21	60.95	0.23
800	Fall 99	-3.16	60.99	0.32
801	Spring 97	-3.23	60.96	0.23
850	Spring 99	-3.25	60.97	0.42
900	Spring 99	-3.80	60.76	0.29
900	Spring 97	-3.28	60.98	0.23
960	Fall 99	-3.23	61.02	0.26
978	Spring 97	-3.32	60.99	0.27
1097	Fall 99	-3.30	61.07	0.28
1100	Fall 99	-3.30	61.07	0.30
1228	Spring 97	-3.57	61.17	0.30

Pore water DSi concentrations and incubations- DSi concentrations in the overlying bottom water were between 5 and 15 µmol l⁻¹ from water overlying sediment cores. Concentrations reached an apparent equilibrium between 2 and 5 cm depth in the sediment at concentrations between 150 and 250 µmol l⁻¹ except for the shallowest stations (300 m) where the asymptotic concentration is < 100 µmol l⁻¹ (Fig. 5). The highest asymptotic concentrations in the sediment were found at 800 m water depth. The low concentration found at the upper slope where the sediment is essentially made up of coarse sand, are close to values found in the sandy North Sea sediments (Van Raaphorst et al., 1990; Gehlen et al. (1995).
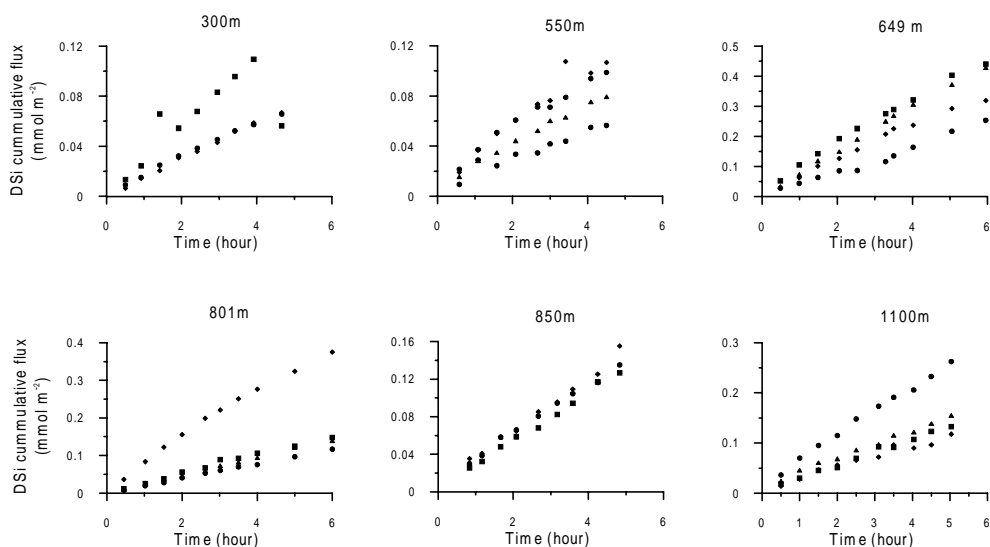
Fig. 6. *Examples of on-board incubation data from various depths across the Shetland slope with increasing DSi cumulative flux in the water overlaying the cores with time. The different symbols represent different cores incubated (3 or 4). The flux for each core was calculated by fitting a linear regression to the data points. The flux for each station was averaged from the different cores.*

Predicted and measured regenerated DSi fluxes

Results from on-board sediment cores incubations are shown for selected stations in figure 6. It shows the increase in DSi cumulative flux with time (variation of the DSi concentration corrected from the decrease the volume of overlying water due to sampling).

Mean DSi fluxes measured across the sediment water interface, varied from 339 µmol m^{-2} d^{-1} at 375 m water depth to 1455 µmol m^{-2} d^{-1} at 649 m (Fig. 4b). DSi fluxes were low on the upper and lower slope and showed a maximum at 649 m, which corresponds to the zone of maximum BSiO$_2$ content.

Regenerated fluxes predicted from the DSi pore water profiles (Fig. 5), were lower than the measured fluxes by a factor of 2 on average and ranged from 200 µmol m^{-2} d^{-1} at 1228 m to 809 µmol m^{-2} d^{-1} at 649 m (Fig. 4c). This may be explained by the fact that the model underestimates the DSi gradient in the pore water profiles at $z = 0$. Figure 5 shows a blow up of the upper 20 mm of the pore water DSi concentration and pore water fit and illustrates the poor fit of the model to data just below the sediment-water interface. Fluxes calculated between the first sediment interval and the overlying water are substantially higher than those obtained from the whole profile fit, with the highest value of 1500 µmol m^{-2} d^{-1} at 649 m. This is nearly twice as much as values predicted using the complete pore water profile (the same applies for the whole data set). Although DSi fluxes predicted from pore water fit and measured from incubations usually agree quite well for the deep sea (McManus et al., 1995, Dixit, 2001) these 2 methods may yield different fluxes for continental slope and shelf environments where pore water bioirrigation may play a non negligible role (Ragueneau et al., 1994, Tahey et al., 1994, Meile et al., 2001). Between 650 and 800 m higher abundance of deposit feeders and polychaetes are observed (Rogier Daan, NIOZ pers. communication). As our model did not include bioirrigation this may partly explain the discrepancies between predicted and measured values.

Sediment traps

Mid-slope resuspension of seabed material- Strong mid-slope resuspension (600-800 m) occurred on the Shetland side during the observartion periods. Total mass fluxes obtained by near-bottom sediment traps deployed in 1999 are shown in figure 7. Turbidity from Optical Backscatter Sensors (OBS) is shown in figure 8. Both data indicate that massive resuspension was observed at mid-slope both in spring and fall. Near-bottom sediment traps deployed in spring (Fig. 7a-d) show that resuspension at that time was particularly intense, reaching up to 350 g m^{-2} d^{-1} at 777 m. A longer-term near-bottom sediment trap was deployed in the same area at 800 m water depth (2 mab) between the spring and fall cruises (Fig. 7e). With TMF in excess of 2 g m^{-2} d^{-1} during the 5 months of deployment the long-term trap shows resuspension to be permanent at the time scale of the survey at least. Moreover, it illustrates that the intense resuspension event recorded at 800 meters in spring and discussed in Bonnin et al. (2002) with an average over the 12 days deployment of 60 g m^{-2} d^{-1} is not related to an exceptional and unique event, as events with even higher magnitude occurred between days 158 and 169 (94 g m^{-2} d^{-1}).

Table 2. *Sediment trap samples. Depth, Incubation time, BSiO₂ content, BSiO₂ (solid phase), BSiO₂ fraction that has dissolved in the cups (µM), particulate BSiO₂ flux (g m⁻² d⁻¹), dissolution rate and dissolution rate constant (k). The numbers into bracket next to the trap name correspond to the day (Julian) the corresponding cup was operating, as indicated in Fig. 7. When more than one day is mentioned indicate that several samples were pooled together because a very low amount of material was present in the cups.*

Traps	Depth (m)	Incuba-tion time (d)	$BSiO_2$ (dw%)	$BSiO_2$ (µM)	$BSiO_2$ settling flux (g m⁻² d⁻¹)	Dissolution rate (µmol l⁻¹ d⁻¹)	k (d⁻¹)
C3-30 (110)	441	10	9.50	5.22	0.014	1.03	0.0257
C3-30 (114)	441	6	7.30	1.77	0.005	1.13	0.0168
C5-30 (108-111)	670	10.5	3.61	16.87	0.045	0.78	0.0124
C5-30 (112)	670	8	0.52	356.9	0.955	1.70	0.0030
C5-30 (113)	670	7	1.93	155.4	0.416	2.43	0.0073
C5-30 (114)	670	6	2.42	144.1	0.386	3.01	0.0087
C5-30 (116-119)	670	2.5	3.46	43.5	0.117	3.28	0.0245
C5-2 (109-110)	700	10.5	3.79	37.9	0.102	0.81	0.0091
C5-2 (112)	700	8	0.65	675.5	1.807	0.33	0.0003
C5-2 (113)	700	7	1.24	289.7	0.775	2.85	0.0053
C5-2 (114)	700	6	2.39	279.6	0.748	4.24	0.0080
C5-2 (117-118)	700	2.5	3.32	63.5	0.170	4.75	0.0279
C6-30 (108-111)	747	10.5	3.34	63.1	0.169	0.37	0.0024
C6-30 (112)	747	8	0.54	335.2	0.897	1.34	0.0023
C6-30 (113)	747	7	1.61	597.1	1.597	0.31	0.0004
C6-30 (114)	747	6	2.66	372.7	0.997	3.20	0.0048
C6-30 (116-119)	747	2.5	3.73	68.6	0.184	0.94	0.0043
C6-2 (109-110)	777	10.5	3.85	121.4	0.325	0.82	0.0044
C6-2 (112)	777	8	1.07	768.7	2.057	0.33	0.0003
C6-2 (113)	777	7	1.61	2102.4	5.625	0.28	0.0002
C6-2 (114)	777	6	3.10	925.9	2.477	4.42	0.0035
C6-2 (117-118)	777	2.5	3.12	153.7	0.411	4.52	0.0121
C8-30 (118)	970	10	3.12	131.7	0.353	0.91	0.0028
C8-2 (111)	1000	9	2.55	106.7	0.286	1.27	0.0066
C8-2 (118)	1000	1.5	3.55	161.8	0.433	4.30	0.0130
C8-2 (112-116)	1000	6	2.60	14.5	0.039	0.17	0.0047

BSiO$_2$ content of the solid phase- The average BSiO$_2$ content in the trap samples was 8.4, 2.4 and 3.3 % on the upper, mid and lower Shetland slope, respectively. Detailed data are shown in Table 2. The BSiO$_2$ content was inversely related to TMF intercepted by the traps, with BSiO$_2$ values of 2.6-9.5% for the low TMF (< 5 g m^{-2} d^{-1}) and values of 0.5-3.1% for high TMF samples (> 5 g m^{-2} d^{-1}) which can be explained by dilution of BSiO$_2$ by resuspended aged seabed material.

The BSiO$_2$ content of the TSM varied with depth (Table 3). We distinguished 3 depth intervals: surface water (10-100 m), intermediate water (200-900 m depending on water depth) and near-bottom water (10 mab at total water depths ranging from 160 to 1180 m). The average BSiO$_2$ content of the total suspended matter was 8.4, 14.8 and 11.6% at the surface, intermediate and near-bottom water respectively.
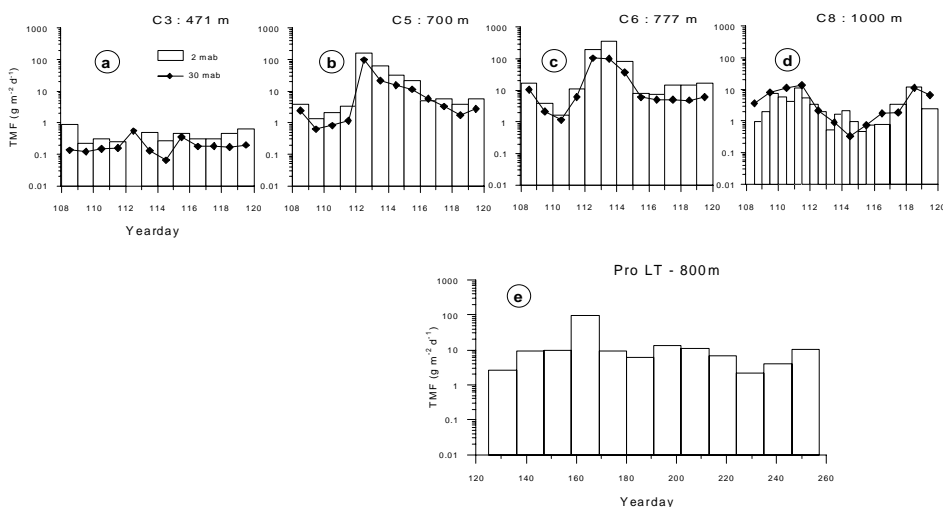
Fig. 7. *Total mass fluxes (TMF) from near-bottom sediment traps for short-term spring deployment (a to d) and long term deployment (spring to fall) in plot (e). The plots show that resuspension of sediment that was observed during a short period of time in spring do occur on a longer time scale.*

DSi concentration in trap bottles- Silicic acid in the trap bottles was analysed to provide information on the dissolution rate of the BSiO$_2$ in the near-bottom water column, based on the assumption that the solubility of non-biogenic silica is much lower than BSiO$_2$. The dissolution rate of BSiO$_2$ in the trap cups was obtained by dividing the DSi

concentration in the trap bottle by the number of days of incubation after correcting for the initial concentration of DSi in the water at the time of deployment. The rate constant of dissolution (k in d^{-1}) was calculated using the following formula:

$$k = \frac{DSi_{cup} - DSi_{sw}}{\Delta t} \cdot \frac{1}{BSi_{cup}} \qquad (7)$$

where DSi_{sw} and DSi_{cup} are the concentration (µM) of DSi in the seawater and trap cup at time of recovery, respectively. BSi_{cup} is the total amount of $BSiO_2$ trapped in the cups (= solid phase remaining plus the amount that has dissolved) and Δt the time of incubation (d).

We assume here a constant dissolution, resulting in a linear increase of DSi over time. However we are aware that the results obtained here may be biased as the dissolution rate of biogenic silica decreases with time (Van Cappellen and Qiu, 1997). Furthermore, the trap cups represent a small volume with increasing DSi concentration and with stagnant conditions and as such may not represent real water column conditions. Given uncertainties in the determination of the dissolution rate inherent to in situ investigation, the k values given below have to be taken as lower estimates.

The k values were inversely related to the TMF (Fig. 9), suggesting that old material with less reactive silica entered the traps during high resuspension events. The k value observed for the trap samples with very low total mass flux (C3-30, mainly reflecting the flux of primary material, Bonnin et al., 2002) varies between 0.017 and 0.026 d^{-1}. The high proportion of fecal pellets in those trap samples may explain the low k value. However, this value is in reasonable agreement with k found from trapped particles in the water column: 0.005 to 0.01 d^{-1} for the Norwegian Sea (Rickert, 2000), 0.072 ± 0.036 d^{-1} for the upper water column of the Sargasso Sea (Brzezinski and Nelson, 1995). For cups corresponding to high TMF (days 112 to 114 from moorings C5 and C6), k values ranging between 0.0002 and 0.028 were calculated (0.007 ± 0.006 d^{-1} on average) and mainly reflect the dissolution rate constant of reworked and older seabed material. This value is of the same order as values found by Rickert (2000) for surface sediments in the Norwegian Sea (0.001 d^{-1}) and calculated from laboratory resuspension experiments ($\sim 1 \times 10^{-7}$ s^{-1} = $\sim$ 0.008 d^{-1}, Gehlen and Van Raaphorst, 2002).

Table 3. *Total suspended matter, $BSiO_2$ concentration and $BSiO_2$ content of suspended mater collected from filters at various depth on the transect across the Faeroe-Shetland Channel. The depth intervals are detailed in section 3.4.*

Filter	Depth (m)	Depth interval	TSM (mg l^{-1})	BSiO$_2$ filter (μM)	BSiO$_2$ (%)
cdw 96	557	near-bottom	0.665	2.90	12.25
cdw 100	100	surface	0.835	2.81	9.46
cdw 102	602	near-bottom	0.55	3.59	18.36
cdw 104	400	intermediate	1.065	3.06	8.06
cdw 106	100	surface	0.74	3.14	11.92
cdw 108	10	surface	1.015	3.93	10.88
cdw 113	785	near-bottom	1.055	2.11	5.63
cdw 24	1087	near-bottom	1.7	3.69	6.09
cdw 25	900	intermediate	0.88	1.94	6.19
cdw 26	500	intermediate	0.62	4.10	18.59
cdw 27	300	intermediate	0.725	3.77	14.62
cdw 28	100	surface	1.485	3.63	6.87
cdw 41	1177	near-bottom	0.715	2.34	9.2
cdw 47	957	near-bottom	0.61	3.17	14.62
cdw 48	800	intermediate	0.49	2.86	16.4
cdw 53	713	near-bottom	0.54	2.85	14.8
cdw 54	600	intermediate	0.335	1.93	16.18
cdw 56	100	surface	0.525	1.37	7.34
cdw 58	632	near-bottom	0.535	2.46	12.89
cdw 61	100	surface	0.505	1.99	11.08
cdw 68	487	near-bottom	0.645	2.90	12.63
cdw 72	10	surface	0.58	1.45	7.02
cdw 78	154	near-bottom	0.61	3.02	9.27
cdw 80	10	surface	1.08	3.60	6.25
cdw 85	398	near-bottom	0.595	2.07	9.76
cdw 87	200	intermediate	0.38	1.96	14.51
cdw 88	100	surface	1.02	1.85	5.1
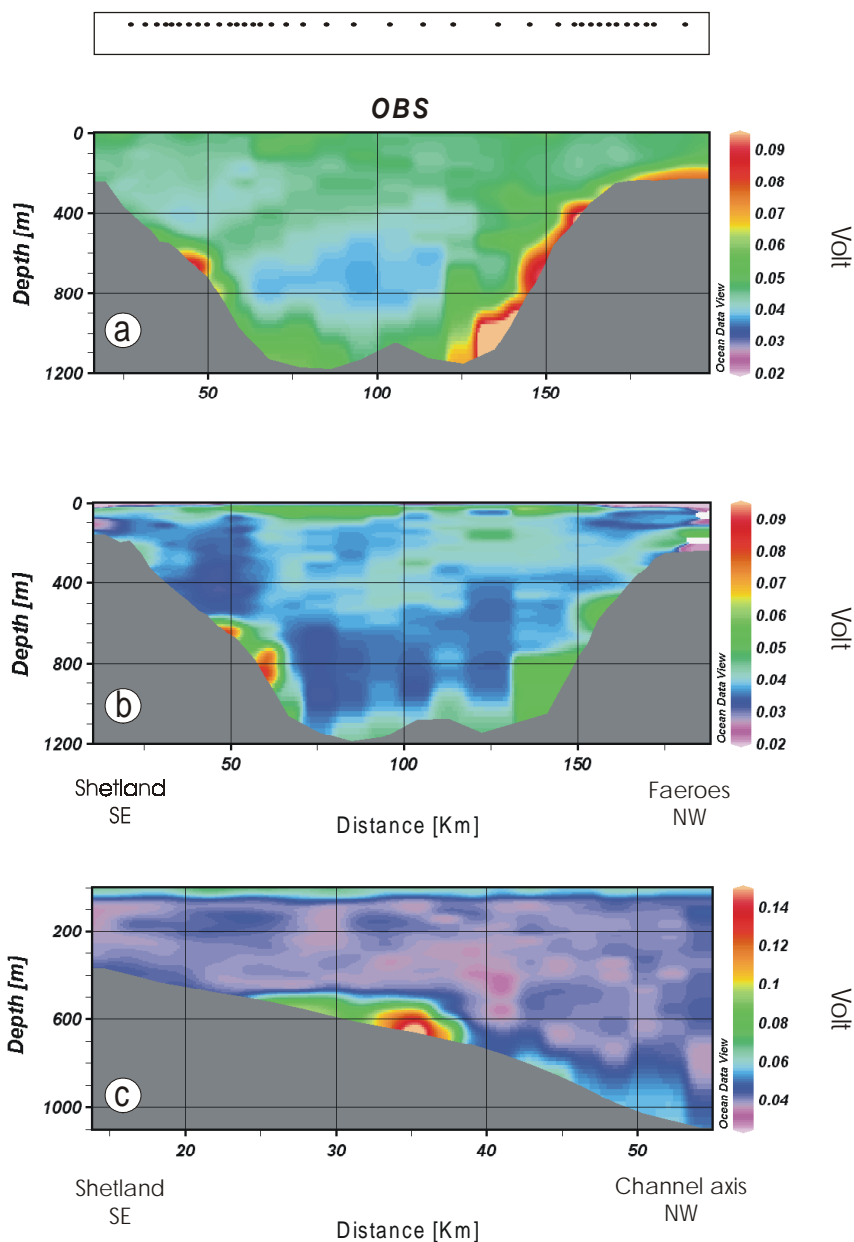
Fig. 8. *Turbidity distribution across the FSC as observed by Optical Backscatter Sensors (OBS) for the 3 sections already shown in Fig. 3 (spring 1999 plots (a) and (b), fall plot (c)). The data have been kept in their original units (Volt) to avoid any bias due to calibration. Higher voltage represents higher backscattering and hence higher turbidity. Note the recurrent intense resuspension spot at mid-slope on the Shetland side for both spring and fall.*
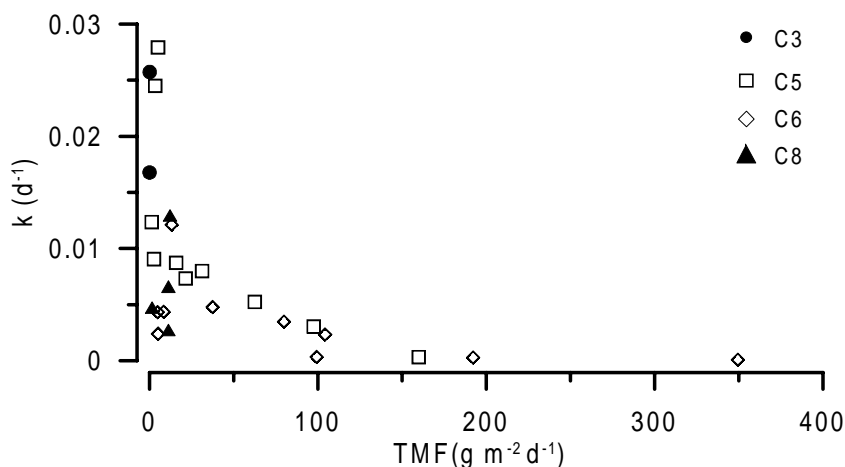
Fig. 9. *Dissolution rate constant (k) for sediment traps at 471 m (dots), 700 m (squares), 777 m (diamonds) and 1000 m (triangles) plotted versus total mass flux (TMF) observed in sediment traps. The plot shows that the k value decrease with increasing total mass flux, suggesting that material intercepted during higher fluxes corresponds to resuspended reworked material while material sampled during low flux have more reactive, i.e. fresh, material probably originating from settling particles (e.g., phytodetritus, faecal pellets).*

DISCUSSION

The content of silicic acid in the water masses along the conveyor belt increases substantially from the Arctic regions to the North Pacific (Broecker and Peng, 1982). Recent data from the World Ocean Atlas (1998) showed that DSi concentration at 1000 m water depth is ~10 μmol l^{-1} in the Norwegian basin, 40 μmol l^{-1} in the north Atlantic, rises to approximately 100 μmol l^{-1} in the south Atlantic to reach 170 μmol l^{-1} in the North Pacific. Thus, the deep water is progressively enriched in dissolved silica during aging along the conveyor belt. Dissolved silica data found in the deep water FSC fit into this picture, with values of 12 μmol l^{-1} at ~1300 m that are in good agreement with values reported by Van Bennekom (1985) for the same area. DSi concentrations in the deep waters are higher in the northern North Atlantic than in the Norwegian Sea suggesting that the deep water is being enriched in DSi during its transit from the Norwegian Sea to the northern North Atlantic via the FSC. The Faeroe-Shetland Channel deep water is admixed with Modified East Icelandic Water and Norwegian Sea Arctic Intermediate Water spilling over the Iceland-Faeroe Ridge to form the Iceland Scotland Overflow Water (e.g., Van Aken, 1988; Hansen and Østerhus, 2000) which limits the direct estimation of the input of DSi from the FSCBW to the deep water of the northern North Atlantic.
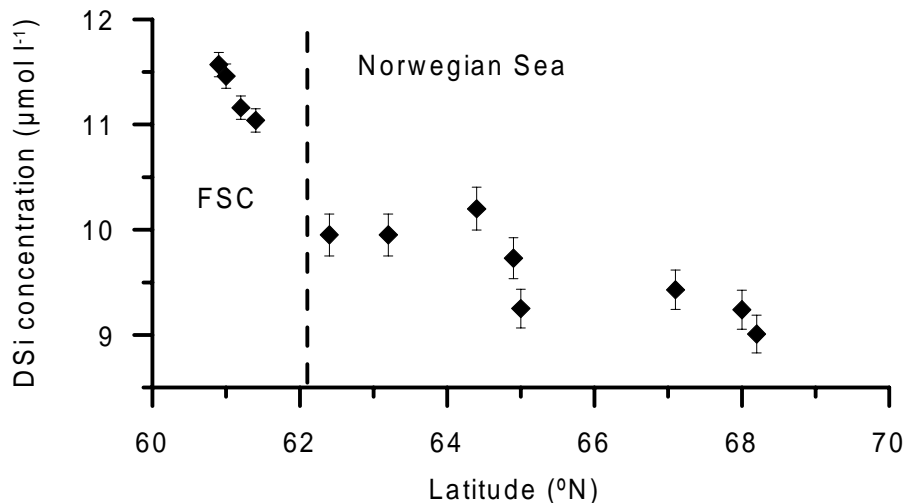
Fig. 10. *DSi concentration in deep water (~1000 m) in the Norwegian Sea and the Faeroe-Shetland Channel. Note the enrichment of ~1 to 1.5 µmol l^{-1} along the track of the overflow from the Norwegian Sea to the Faeroe-Shetland Channel. Data from the Norwegian Sea are partly coming from the ICES programme (1982) and partly from unpublished data from J. Van Bennekom. Error bars represent the standard deviation for data north of 62ºN and the accuracy of the silicic acid determination for data within the FSC.*

A comparison of DSi concentration along the FSC and in the water mass up-flow however, provides an indication of the potential significance of the FSC to recharge passing water. Water at ~1000 m in the southern NS and FSC and with a similar sigma $\sigma > 28.0$ kg m^{-3}, described as the upper limit of the Norwegian Sea Deep Water (Van Aken, 1988), reveals a significant and stepwise enrichment in DSi of ~1 µmol l^{-1} from the entrance of the FSC to the location where our cross-section observation were made (Fig. 10). The stepwise increase of the DSi concentration between the entrance (~62ºN) of the channel and our cross section (~61ºN) might be balanced by the input flux from the sediments. This can be written as follows:

$$Q \times \Delta C = SA \times J \tag{8}$$

Where Q is the mean volume flow (in Sv) of the deep water (> 600 m)in the channel, ΔC the difference in DSi concentration between the entrance of the channel and our cross-section for the deep water (~1000 m water depth), SA the surface area bathed by the bottom water from the entrance of the channel to our cross section and J the input DSi flux from the sediments. The input flux necessary to explain the DSi increase in the bottom water can then be expressed as:

$$J = \frac{Q\Delta C}{SA} \qquad (9)$$

Taking a flow out of the channel of 1 to 1.5 Sv (Van Aken, pers. com.) and a surface area bathed by the bottom water mass (deeper than 600 m) of 150,000 km^2 we obtained a flux from the sediment necessary to enrich the deep water mass by 1 to 1.5 µmol l^{-1} between 570 and 1300 µmol m^{-2} d^{-1}. The major goal of this study is to assess and, if possible, quantify the sources of the DSi enrichment observed at the time of sampling.

DSi fluxes in the water column

DSi fluxes in the water column were calculated using the vertical eddy diffusion coefficient K (in m^2 s^{-1}) as defined by Gargett (1984):

$$K = 1 \times 10^{-7} \times N^{-1} \qquad (10)$$

with the buoyancy frequency N (in s^{-1}) defined as:

$$N = \sqrt{\left(\frac{-g}{\rho}\right) \times \left(\frac{\Delta\rho}{\Delta z}\right)} \qquad (11)$$

where g is the mass acceleration, Δz the depth interval (10 m) and ρ the density of the water mass obtained from CTD casts. The vertical DSi flux in the water column is expressed as K×(ΔSi/Δz) with ΔSi/Δz being the gradient in DSi concentration at a given depth in the water column. Values for the vertical eddy diffusion coefficient ranges from 1.8 10^{-5} m^2 s^{-1} in the major thermocline zone to 1.4 10^{-3} m^2 s^{-1} near the seabed at mid-depth and are nearly all the time in excess of 10^{-4} m^2 s^{-1} in the bottom 30 meters (Fig. 11). The K estimates found in the water column are quite low compared to the values observed by others for the FSC and maybe due to different approach. Using a FLY II microstructure profiler, Hosegood et al. (Submitted) found that the vertical eddy diffusion coefficient was in excess of 10^{-4} m^2 s^{-1} in the bottom 30 meters but with higher maximum value at 10 meters above the bottom of 10^{-1} m^2 s^{-1} at 620 m water depth. Higher K values would result in higher flux in the water column particularly at mid-slope but would not change the pattern, i.e. with fluxes on the slope between 600 and 800 m than higher anywhere else in the channel.
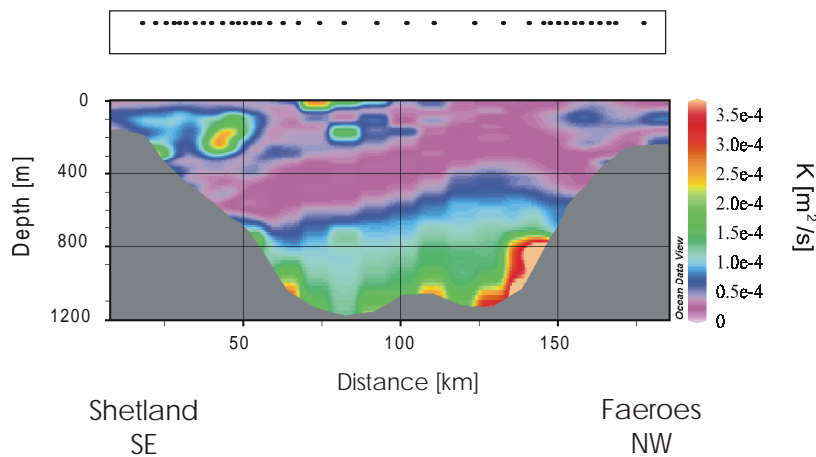
Fig. 11. *Plots of the distribution of the eddy diffusivity (K) in the water column (example of the second transect of the spring cruise).*

On the slope, in the vicinity of the seabed directly beneath the major pycnocline, calculated DSi fluxes are high and directed upwards while much lower fluxes were found for mid-depth water column and surface water (Fig. 12). The values at the seabed are ~100 µmol m^{-2} d^{-1} at the upper slope, but as high as 450 µmol m^{-2} d^{-1} at ~600-800 m water depth in April (Fig. 12a, b) and even > 1500 µmol m^{-2} d^{-1} in September (Fig. 12c).

Enhanced fluxes near the seabed particularly at mid-slope suggests that benthic dissolution processes are responsible for sustaining these fluxes. Dissolution of settling $BSiO_2$ is unlikely to explain alone the enhanced fluxes at mid-slope. We will nevertheless consider the dissolution of settling $BSiO_2$ in the water column in order to assess its contribution to the DSi concentration in the FSC.

Dissolution of silica in the water column

The TMF and mean $BSiO_2$ content in the sediment trap C3-30 are 0.18 g m^{-2} d^{-1} and 8.4%, respectively, which gives a mean total $BSiO_2$ flux at 440 m of 0.015 ± 005 g m^{-2} d^{-1} (300 to 600 µmol m^{-2} d^{-1}). We are aware that a trap deployed a few meters above the seabed can not provide unbiased particle settling flux. However, Bonnin et al. (2002) have shown using multi-component mixing model based on Corg content of surface sediment, trap material and suspended mater that the material present in the shallowest trap resulted mainly from primary particles. We therefore use the flux data obtained from this trap as the best estimation of the exported flux for this study. Riegman and Kraay (2001) determined a surface productivity in the late spring bloom of 1.6 to 3.8 gC m^{-2} d^{-1} in the FSC, to which diatoms contributed no more than 10%.
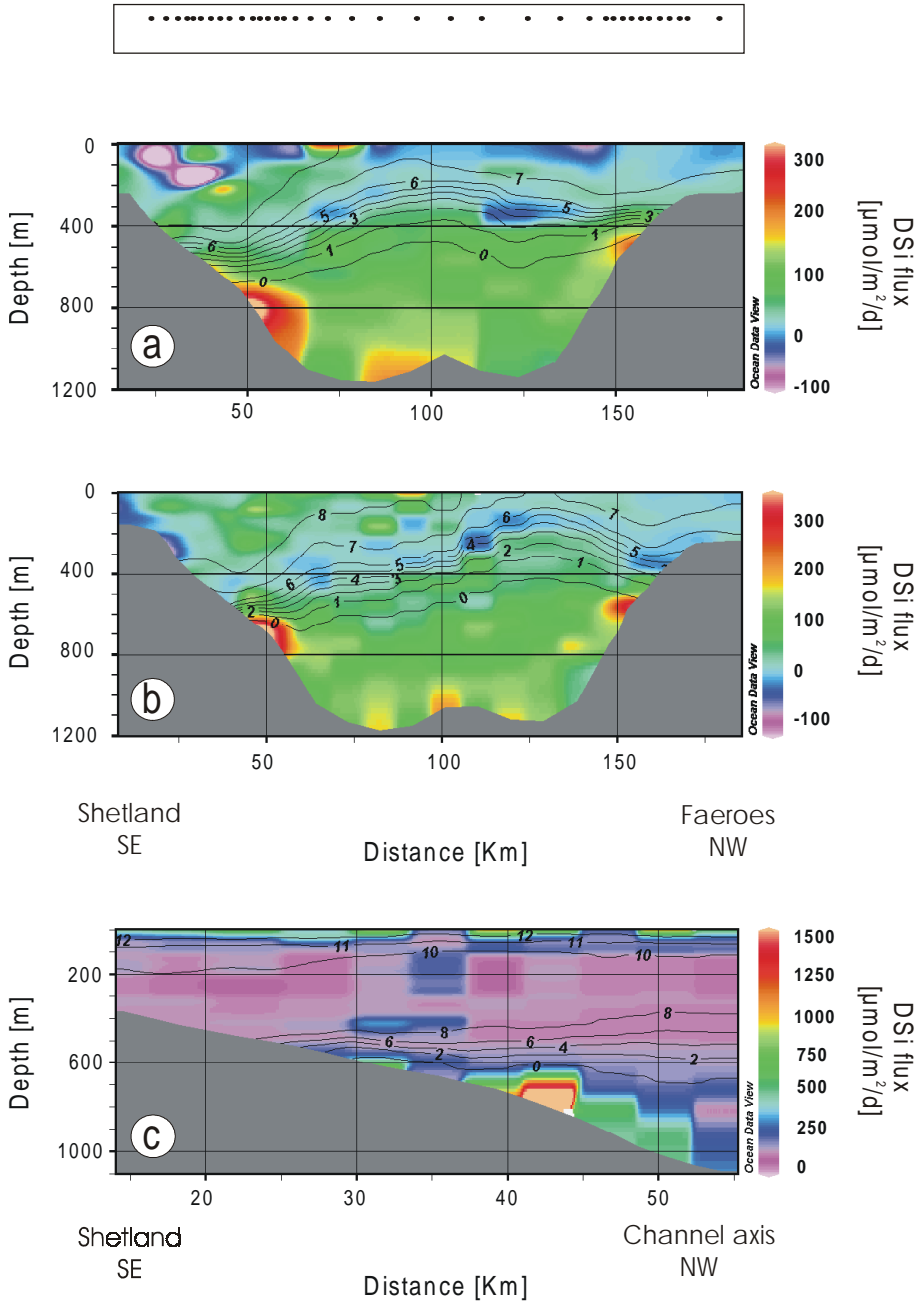
Fig. 12. *Dissolved silica fluxes in the water column for the 3 sections already shown in Fig. 3 (spring 1999 plots (a) and (b), fall plot (c)) calculated using the eddy diffusivity coefficient according to Gargett (1984), see text. The solid line on top of the plot shows the temperature distribution and indicates the density control on the flux distribution. Negative values indicate a net downward DSi flux.*

Assuming a Si:C ratio for diatoms of 0.13 (Brzezinski, 1985) we arrive at a $BSiO_2$ production in surface water of 0.021 to 0.049 $gSi\ m^{-2}\ d^{-1}$ or 750 to 1700 $\mu mol\ m^{-2}\ d^{-1}$ which is in good agreement with export flux calculated above. Considering that the $BSiO_2$ flux intercepted in the trap equals the export $BSiO_2$ flux minus the fraction that dissolved in the water column. This can be written as follows:

$$JBSi_{trap} = JBSi_{exp} - k.JBSi_{exp}.\ \Delta t \tag{12}$$

or

$$JBSi_{exp} = \frac{JBSi_{trap}}{1 - k\Delta t} \tag{13}$$

$JBSi_{trap}$ is the flux of biogenic silica in the trap, $JBSi_{exp}$ the export flux of $BSiO_2$, k is the dissolution constant and Δt the time of settling from the surface mixed layer to the trap depth. The amount that is dissolved in the water column is:

$$JBSi_{diss} = \frac{JBSi_{trap}}{1 - k\Delta t} \cdot k\Delta t \tag{14}$$

Accordingly, $BSiO_2$ dissolution in the trap C3-30 provides a mean dissolution rate constant (k) of 0.021 ± 0.006 d^{-1}. The settling velocity for particles in the ocean is very variable depending on the types of particles (Pilskaln et al., 1998) and the depth in the ocean (Berelson, 2002). Settling velocities of marine aggregates found in the literature range from 75 ± 40 $m\ d^{-1}$ in the waters off southern California (Alldredge and Gotschalk, 1988) and 140 ± 20 $m\ d^{-1}$ in the North Atlantic (Knappertsbush and Brummer, 1995). Taking these value, we arrive at a settling time of 3 to 10 days for the particles intercepted at 440 m (upper trap). The calculation yields a $BSiO_2$ dissolution flux of 30 ± 10 $\mu mol\ m^{-2}\ d^{-1}$ to 120 ± 40 $\mu mol\ m^{-2}\ d^{-1}$. Again, this calculation might be marred by uncertainties related to bias in the measurement of settling flux or the dissolution rate constant. The dissolution flux will also vary with the diatom production, which may vary throughout the year. DSi fluxes from the water column as well as from the sediments show higher values in early fall than in early spring (Fig. 4b, c, Fig. 12), which may be explained by the timing of the bloom in this area. According to Bett (2000), the spring bloom in the Faeroe-Shetland area occurs between late May and June and Riegman and Kraay (2001) found that in July 1999 the bloom was still at its initial phase suggesting that the spring bloom could not be traced in our traps. However, such value of the dissolution flux in the water column is in good agreement with the background dissolution flux estimated in the deep water mass (~100 $\mu mol\ m^{-2}\ d^{-1}$) but is clearly less than the estimated DSi flux at mid-slope (> 300 $\mu mol\ m^{-2}\ d^{-1}$, Fig. 11). Hence, the dissolution of settling particles cannot explain the high DSi flux at mid-slope and implies an input of DSi from the sediment.

Role of the sediment in DSi refuelling of the FSC

Higher $BSiO_2$ content at mid-slope corresponds to higher ^{210}Pb fluxes (Fig. 4a, d) which indicate a zone of enhanced deposition (Van Raaphorst et al., 2001) and thus could be due to deposition of material relatively rich in $BSiO_2$. DSi effluxes from sediments across the Shetland slope are lowest on the upper slope and increase substantially at mid-depth (Fig. 4b, c) which corresponds to the depth of higher $BSiO_2$ content of surface sediments. The ratio of $DSi_{asymp}/BSiO_{2\ surf.sed.}$, plotted versus water depth in figure 13 shows higher values at mid-slope indicating that the $BSiO_2$ that accumulates at mid-slope is more labile than on the upper or lower slope.
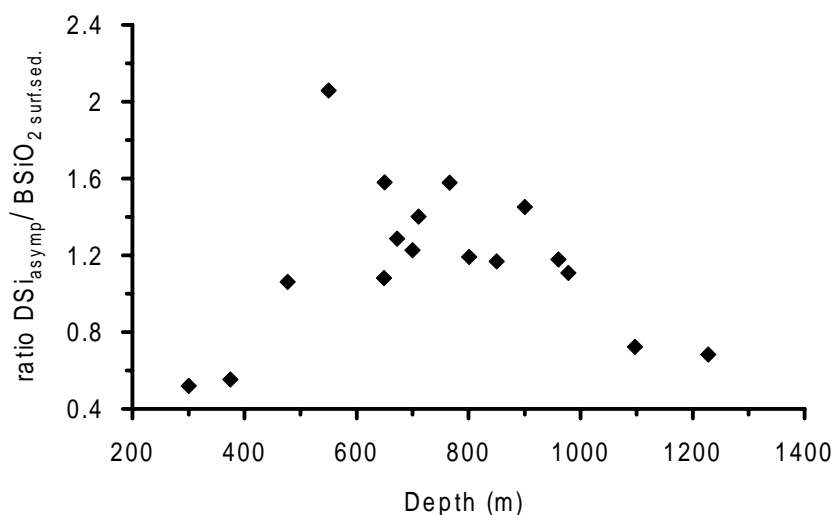
Fig. 13. *Ratio of asymptotic DSi concentration over $BSiO_2$ content in surface sediments plotted versus water depth across the Shetland slope. Higher ratio at mid-slope indicates that biogenic silica accumulated there was relatively labile compared to the upper or lower slope.*

Contribution of the sediment efflux to the DSi refuelling

Averaged DSi effluxes at the lower slope (> 800 m water depth) ranged between ~300 µmol m^{-2} d^{-1} (predicted) and 700 µmol m^{-2} d^{-1} (measured) and rise to ~500 µmol m^{-2} d^{-1} (predicted) and 800 µmol m^{-1} d^{-1} (measured) at mid-slope. Considering similar DSi fluxes on a band between 600 and 850 m water depth on the other side of the channel, the zone of enhanced DSi flux would represent ~1/3 of the considered area *SA* (Fig. 1, Eq. 8 and 9). Weighing the enhanced Dsi fluxes according to surface area they are representative of, provides input flux from the whole channel area deeper than 600 m between 400 and 800 µmol m^{-2} d^{-1}.

Thus, the dissolution flux from settling $BSiO_2$ of 30 to 120 µmol m^{-2} d^{-1} and the sediment DSi efflux weighed from their relative surface area coverage yield a maximum DSi flux to the deep water column from 430 to 920 µmol m^{-2} d^{-1}. This explains to a great extent the elevated flux in the water column observed at mid-slope but cannot fully account for fluxes as high as 1700 µmol m^{-2} d^{-1} observed in fall. Hence, another source of DSi is. Near-bottom sediment traps and turbidity profiles revealed that intense resuspension takes place between 600 and 850 m. The co-occurrence of such massive and recurrent particle resuspension at mid-slope with higher DSi fluxes in the water column, suggests that dissolution of resuspended $BSiO_2$ contribute substantially to refuel in DSi the deep water of the FSC.

Resuspension of bottom material as an additional source of DSi in the FSC

Resuspension of surface sediments has been reported as the origin of increased levels of DSi in near-bottom waters in shallow waters where storms have strong impact on sediments (Fanning et al., 1982). Recently, Gehlen and Van Raaphorst (2002) concluded after laboratory experiments that resuspension of bottom particles can enrich the DSi concentration of the bottom waters via desorption processes. Models of the effect of resuspension on the chemical exchange at the sediment-water interface (Rutgers Van Der Loeff and Boudreau, 1997) showed that particle resuspension in the benthic boundary layer (BBL) would not enhance silica dissolution (which mainly occurs at the sediment surface) unless near-bottom conditions are highly turbulent. In the FSC, strong bottom currents of up to 65 cm s^{-1} and non non-linear internal waves (Hosegood and Van Haren, 2003) were shown to trigger resuspension of phytodetritus and sediment (Fig. 8). Hosegood et al. (Submitted) showed, using a FLY-II microstructure profiler, that turbulence at mid-slope was high particularly when resuspension was observed. Therefore, resuspension of seabed material at mid-slope associated with turbulent flow may play a role in the refuelling of DSi in the deep water of the FSC.

The mean $BSiO_2$ content of near-bottom total suspended matter (10 mab) is 2.8 µmol l^{-1} which gives, using the k calculated from cups that collected mainly resuspended sediment (0.007 ± 0.005 d^{-1}), dissolution rate ranges between of 0.006 µmol l^{-1} d^{-1} and 0.03 µmol l^{-1} d^{-1} (6 to 30 µmol m^{-3} d^{-1}).

Sediment resuspension at mid-depth on the south-eastern slope of the FSC has been observe during all oceanographic surveys conducted in this area (see also Van Raaphorst et al., 2002 for a study conducted in 1997), which suggest that resuspension is a permanent feature at mid-slope. Therefore, the resuspension of bottom material at mid-slope is considered an ongoing process at time scales of half a year at least. Assuming continuous resuspension between 600 and 850 m and a BBL thickness varying between 30 and 80 m (Fig. 14) we arrive at a DSi flux in the mid-slope near-bottom water column of 180 to 2400 µmol m^{-2} d^{-1}. Similarly than what was done with efflux from surface sediment, weighting the input of DSi from resuspended material according to the surface area of the seafloor they are representative of yields fluxes of 60 to 800 µmol m^{-2} d^{-1}. Resuspension may not be

at steady state at time scale of a day and therefore this is to be considered as the upper limit. This approach gives, however, an indication that recurrent resuspension of seabed material over the slope associated with turbulent flow may be an additional source of DSi to the water column.

Beam attenuation Coef.
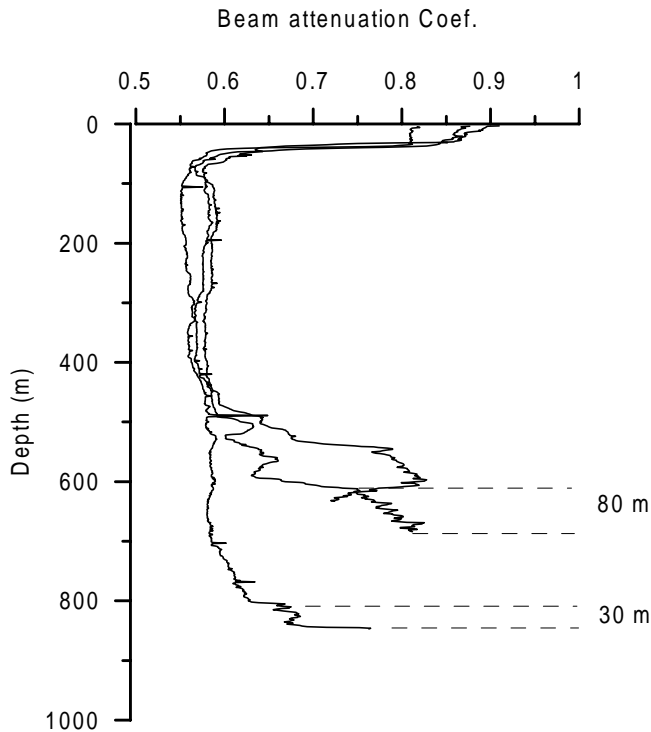
Fig. 14. Beam attenuation coefficient profiles on the Shetland continental slope as an indicator of turbidity (higher coefficient indicates higher turbidity). The higher turbidity near the bottom determines the benthic boundary layer thickness that varied at time of deployment in spring between 30 m and 80 m.

Synthesis

Our results on the DSi fluxes in the water column and at the sediment-water interface suggest that silica refuelling may occur in the FSC at a relatively high rate. Dissolution of settling $BSiO_2$ in an area where the siliceous production is quite low and the settling time quite short appears not necessary to account fully for that. Furthermore, silica refuelling seems to take place mainly in bottom waters and particularly at mid-slope where

the fluxes from the sediment are higher, due to accumulation of relatively labile biogenic silica, than on the rest of the channel and where resuspension of bottom material was seen to occur permanently during a 5 months observation period. The data presented here suggest that particle resuspension can enhance DSi regeneration to the water column when associated with turbulent conditions in the BBL. Hence, the DSi enrichment observed in the FSC appears to be mainly due to input from $BSiO_2$ dissolving at the sediments surface and partly from $BSiO_2$ dissolving in resuspended material, the contribution from settling $BSiO_2$ being minor at the time we investigated the study site. Enhanced fluxes at mid-slope may be the consequence of focusing of relatively labile material, possibly coming from up-stream or from the channel axis, due to the combination of strong currents, intermittent upwelling favorable conditions (Hosegood and van Haren, 2003) and confined to depth greater than ~600 m due to the strong pycnocline. Furthermore, the data show that DSi flux in the water column (benthic efflux, dissolution during settling and flux from resuspended particles) is not balanced by the input of $BSiO_2$ from settling from the photic zone and imply lateral advection of particulate $BSiO_2$ (Fig. 15).
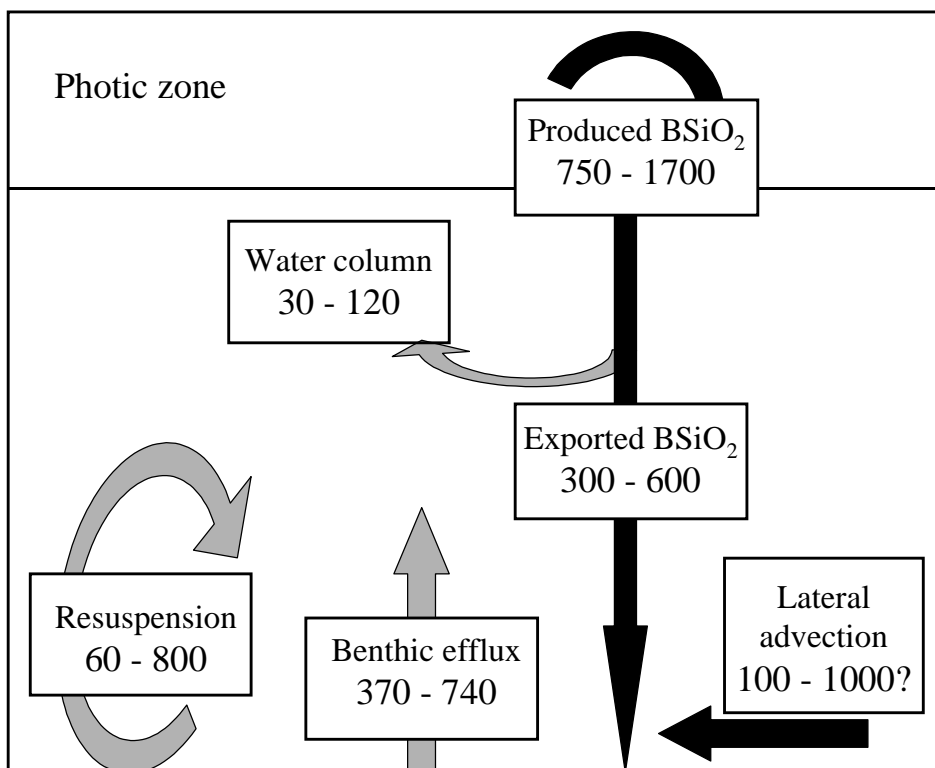
Fig. 15. *Diagram showing the different compartments of the silica budget and the ranges of the fluxes from each of these compartments and their contribution to the enrichment of silicic acid in the deep water of the FSC. The black arrows represent fluxes of particulate $BSiO_2$ and the grey arrows, fluxes of dissolved silicic acid. All fluxes are given in $\mu mol\ m^{-2}\ d^{-1}$.*

CONCLUSIONS

We showed that mid-slope benthic regenerated DSi fluxes from the surface sediments and to a lesser extent DSi fluxes from resuspended sediment in a turbulent region may be responsible of stepwise DSi enrichment of the deep waters of the FSC. We suggest that repetitive resuspension of bottom particles and the resulting focussing on the slope can substantially contribute to the dissolved silica flux to the water column. This is particularly true in a bottleneck like the FSC where due to the combination of strong bottom currents, strong pycnocline and a funnel shape channel, sediments are focussed on a narrow band on the slope, leading to trapping of $BSiO_2$ at mid-slope. Such zonation in the DSi fluxes across the slope contrasts with open ocean conditions where most of the dissolution of settling $BSiO_2$ would take place in the water column before particles reach the bottom and where sediments would be advected off the slope.

Strong bottom currents in the FSC flushing the water away towards the Wyville-Thomson Ridge and the Iceland Basin may explain why the bottom water in the FSC never reaches high levels of DSi. Furthermore, we believe that the combination of these strong currents with a strong stratification may prevent the enriched water to reach the euphotic zone where the DSi concentration remains low (1-5 μmol l^{-1} on the Shetland side before the bloom). This may partially explain why the assemblages of the primary producers in the FSC in July 1999 was dominated by calcareous species (Prymnesiophyceae) instead of diatoms (Riegman and Kraay, 2001).

ACKNOWLEDGEMENTS

REFERENCES

Alldredge, A. L., Gotschalk, C., 1988. In situ settling behavior of marine snow. *Limnology and Oceanography* 33, 339-351.

Aller, R.C. and Benninger, L.K., 1981. Spatial and temporal patterns of dissolved ammonium, manganese and silica fluxes from bottom sediments of Long Island Sound, U.S.A. *Journal of Marine Research* 39, 295-314.

Andrews, D. and Bennett, A., 1981. Measurements of diffusivity near the sediment-water interface with a fine-scale resistivity probe. *Geochimica and Cosmochimca Acta* 45, 2157-2169.

Barnett, P.R. Watson, O.J. and Connelly, D., 1984. A multiple corer for taking virtually undisturbed samples from shelf, bathyal and abyssal sediments. *Oceanologica Acta* 7, 399-408.

Berelson, W.M., 2002. Particle settling rates increase with depth in the ocean. *Deep-Sea Research II* 49, 237-251.

Berger, W.H. and Herguera, H., 1992. Reading the sedimentary record of the ocean's productivity. In: Falkowski, P.G., Woodhead, A. (Eds.), Primary productivity and biogeochemical cycles in the sea. Plenum, New York, pp. 455-486.

Bett, B.J., 2000. Benthic ecology of the Faeroe-Shetland Channel, Section 4.3.1 in Environmental Surveys of theSeafloor of the UK Atlantic Margin, Atlantic Frontier Environmental Network [CD-ROM, 53 pp]. Geotek Limited, Daventry, Northants NN11 5EA, UK.

Bonnin, J., Van Raaphorst, W., Brummer, G.-J. A., Van Haren, H. and Malschaert, H., 2002. Intense mid-slope resuspension of particulate matter in the Faeroe-Shetland Channel: short-term deployment of near-bottom sediment traps. *Deep-Sea Research I* 49, 1485-1505.

Broecker, W.S., and Peng, T.-H., 1982. Tracers in the Sea. Eldigio press, Colombia University. Palisades, New York, 690 pp.

Brzezinski, M.A., 1985. The Si:C:N ratio of marine diatoms: interspecific variability and the effect of some environmental variables. *Journal of Phycology* 21, 347-357.

Brzezinski, M.A. and Nelson, D.M., 1995. The annual silica cycle in the Sargasso Sea near Bermuda. *Deep-Sea Research I* 42, 1215-1237.

Calvert, S.E., 1983. In: Silicon Geochemistry and Biogeochemistry, S.R. Aston, Ed. Academic Press, London, 143-186.

Dixit, S., 2001. Dissolution of Biogenic Silica: solubility, reactivity and the role of aluminum. Ph.D. Thesis, Georgia Institute of Technology, USA, 197 pp.

Fanning, K.A., Carter, K. L. and Betzer, P.R., 1982. Sediment resuspension by coastal waters: a potential mechanism for nutrient re-cycling on the ocean's margins. *Deep-Sea Research* 29, 953-965.

Gardner, W.D., 1985. The effect of tilt on sediment trap efficiency. *Deep-Sea Research* 32 (3), 349-361.

Gargett, A.E., 1984.Vertical eddy diffusivity in the ocean interior. *Journal of Marine Research* 42, 359-393.

Gehlen, M., Malschaert, H and Van Raaphorst, W., 1995. Spatial and temporal variability of benthic silica fluxes in the southeastern North Sea. *Continental Shelf Research* 15, 1675-1696.

Gehlen, M. and Van Raaphorst, W., 2002. The role of adsorption-desorption surface reactions in controlling interstitial $Si(OH)_4$ concentrations and enhancing $Si(OH)_4$ turn-over in shallow shelf seas. *Continental Shelf Research* 22, 1529-1547.

Grasshoff, K., Ehrhardt, M. and Kremling, K., 1983. Methods of seawater analysis, Verlag Chemie, Weinheim, Germany.

Hansen, B. and Østerhus, S., 2000. North Atlantic-Nordic Seas exchanges. *Progress in Oceanography* 45, 109-208.

Hosegood, P. and Van Haren, H., 2003. Ekman-induced turbulent mixing over the continental slope in the Faeroe-Shetland Channel. *Deep-Sea Research I* 50, 657-680.

Hosegood, P., Bonnin, J. and Van Haren, H. Solibore-induced sediment resuspension over the continental slope in the Faeroe-Shetland Channel. Submitted to *Nature*.

Hurd, D.C., 1973. Interactions of biogenic opal, sediment and seawater in the central equatorial Pacific. *Geochimica and Cosmochimica Acta* 37, 2257-2282.

Knappertsbusch, M. and Brummer, G.-J.A. 1995. A sediment trap investigation of sinking coccolithophorids in the North Atlantic. *Deep-Sea Research I* 42, 1083-1109.

Koning, E., Brummer, G.-J, Van Raaphorst, W., Van Bennekom, A.J., Helder, W. and Van Iperen, J., 1997. Settling, dissolution and burial of biogenic silica in the sediments off Somalia (northwestern Indian Ocean). *Deep-Sea Research II* 44 (6/7), 1341-1360.

Koning, E., Epping, E. and Van Raaphorst, W., 2002. Simultaneous dissolution of silica and aluminum: an accurate method to analyze biogenic silica in marine sediments. *Aquatic Geochemistry* 8, 37-67.

Kuijpers, A., Troelstra, S.R., Wisse, M., Heier Nielsen, S. and Van Weering, T.C.E., 1998. Norwegian Sea overflow variability and NE Atlantic surface hydrography during the past 150 000 years. *Marine Geology* 152, 75-99.

Kuijpers, A., Hansen, B., Hühnerbach, V., Larsen, B., Nielsen, T. and Werner, F., 2002. Norwegian Sea overflow through the Faeroe-Shetland gateway as documented by its bedforms. *Marine Geology* 188, 1-18.

Li, Y.-H. and Gregory, S., 1974. Diffusion of ions in sea water and in deep-sea sediments. *Geochimica and Cosmochimica Acta* 38, 703-714.

McManus, J., Hammond, D.E., Berelson, W.M., Kilgore, T.E., DeMaster, D.J., Ragueneau, O.G. and Collier, R.W., 1995. Early diagenesis of biogenic opal: Dissolution rates, kinetics and paleoceanographic implications. *Deep-Sea Research II* 42, 871-903.

Meile, C., Koretsky, C., M. and Van Cappellen, P., 2001. Quantifying bioirrigation in aquatic sediments: An inverse modeling approach. *Limnology and Oceanography* 46 (1),164-177.

Müller, P.J. and Schneider, R., 1993. An automated method for the determination of opal in sediments and particulate matter. *Deep-Sea Research I* 40, 425-444.

Nelson, D.M., Tréguer, P., Brzezinski, M.A., Leynaert, A. and Quéguiner, B., 1995. Production and dissolution of biogenic silica in the ocean: revised global estimates, comparison with regional data and relation ship to biogenic silica sedimentation. *Global Biogeochemical Cycles* 9, 359-372.

Pilskaln, C.H., Lehmann, C., Paduan., J.B. and Silver, M.W., 1998. Spatial and temporal dynalics in marine aggregate abundances, sinking rate and flux: Monterey Bay, central California. *Deep-Sea Research II* 45, 1803-1837.

Rabouille, C., Gaillard, J.-F., Tréguer, P. and Vincendeau, M.-A., 1997. Biogenic silica recycling in surficial sediments across the Polar Front of the Southern Ocean (Indian sector). *Deep-Sea Research II* 44 (5), 1151-1176.

Ragueneau, O., De Blas Varela, E., Tréguer, P., Quéguiner, B. and Del Amo, Y., 1994. Phytoplankton dynamics in relation to the biogeochemical cycle of silicon in a coastal ecosystem of Western Europe. *Marine Ecology Progress Series* 106, 157-172.

Ragueneau, O., Tréguer, P., Leynaert, A., Anderson, R.F., Brzezinski, M.A., DeMaster, D.J., Dugdale, R.C., Dymond.J., Fischer, G., Francois, R., Heinze, C., Maier-Reimer, E., Martin-Jézéquel, V., Nelson, D.M. and Quéguiner, B., 2000. A review of the Si cycle in the modern ocean: recent progress and missing gaps in the application of biogenic opa as a productivity proxy. *Global and Planetary Change* 26, 317-365.

Ragueneau, O., Gallinari, M., Corrin, L., Grandel, S., Hall, P., Hauvespre, A., Lampitt, R.S., Rickert, D., Stahl, H., Tengberg, A. and Witbaard, R., 2001. The benthic silica cycle in the northeast Atlantic: seasonality, annual mass balance and preservation mechanisms. *Progress in Oceanography* 50, 171-200.

Rickert, D., 2000. Dissolution kinetics of biogenic silica in marine environments. Berichte zur Polarforschung 351. Ph.D. Thesis, Alfred Wegener Institut, Germany, 211 pp.

Riegman, R. and Kraay, G.W., 2001. Phytoplankton community structure derived from HPLC analysis of pigments in the Faeroe-Shetland Channel during summer 1999: the distribution of taxonomical groups in relation to physical/chemical conditions in the photic zone. *Journal of Plankton Research* 23 (2), 191-206.

Rutgers van der Loeff, M.M. and Boudreau, B.P., 1997. The effect of resuspension on chemical exchanges at the sediment-water interface in the deep-sea – A modelling and natural radiotracer approach. *Journal of Marine Systems* 11, 305-342.

Schink, D.R., Fanning, K.A. and Pilson, M.E.Q., 1974. Dissolved silica in the upper pore waters of the Atlantic Ocean floor. *Journal of Geophysical Research* 79, 2243-2250.

Schlitzer, R., Ocean Data View, http://www.awi-bremerhaven.de/GEO/ODV, 2002.

Schlüter, M. and Sauter, E., 2000. Biogenic silica cycle in surface sediments of the Greenland Sea. *Journal of Marine Systems*. 23, 333-342.

Strickland, J.D.H. and Parsons, T.R., 1968. A practical handbook of seawater analysis. *Fisheries Research Board of Canada*, Bulletin 167, 1-311.

Tahey, T.M., Duineveld, G.C.A., Berghuis, E.M. and Helder, W., 1994. Relation between sediment-water fluxes of oxygen and silicate and faunal abundance at continental shelf, slope and deep-water stations in the northwest Mediterranean. *Marine Ecology Progress Series* 104, 119-130.

Tréguer, P., Nelson, D.M., Van Bennekom, A.J., DeMaster, D.J., Leynaert, A. and Quéguiner, B., 1995. The silica cycle in the world ocean: a reestimate. *Science* 268, 375-379.

Turrell, W.R., Slesser, G., Adams, R.D., Payne, R. and Gillibrand, P.A., 1999. Decadal variability in the composition of Faeroe Shetland Channel bottom water. *Deep-Sea Research I* 46, 1-25.

Van Aken, H.M and Eisma, D., 1987. The circulation between Iceland and Scotland derived from water mass analysis. *Netherlands Journal of Sea Research* 21, 1-15.

Van Aken, H.M., 1988. Transports of water masses through the Faeroese Channels determined by an inverse method. *Deep-Sea Research* 35, 595-617.

Van Bennekom, A.J., 1985. Dissolved silica as an indicator of Antarctic Bottom Water penetration, and the variability in the bottom layers of the Norwegian and Iceland Basins. *Rit Fiskideildar* 9, 101-109.

Van Beusekom, J.E.E., Van Bennekom, A.J., Tréguer, P. and Morvan, J., 1997. Aluminum and silicic acid in water and sediments of the Enderby and Crozet basins. *Deep-Sea Research II* 44 (5), 987-1004.

Van Cappellen, P. and Qiu, L., 1997. Biogenic silica dissolution in sediments of the Southern Ocean: I. Solubility. *Deep-Sea Research II* 44 (5), 1109-1128.

Van der Zee, C., Van Raaphorst, W. and Epping, E., 2001. Absorbed Mn^{2+} and Mn redox cycling in Iberian continental margin sediments (northeast Atlantic Ocean). *Journal of Marine Research* 59, 133-166.

Van Raaphorst, W., Kloosterhuis, H.T., Cramer, A. and Bakker, K.J.M., 1990. Nutrient diagenesis in the sandy sediments of the Dogger Bank Area, North Sea: pore water results. *Netherlands Journal of Sea Research* 26, 25-52.

Van Raaphorst, W., Malschaert, H., van Haren, H., Boer, W. and Brummer, G.-J., 2001. Cross-slope zonation of erosion and deposition in the Faeroe-Shetland Channel, North Atlantic Ocean. *Deep-Sea Research I* 48 (2), 567-591.

Walsh, I., Fisher, K., Murray, D. and Dymond, J., 1988. Evidence for resuspension of rebound particles from near-bottom sediment traps. *Deep-Sea Research* 35 (1), 59-70.

Wollast, R., and Garrels R.M., 1971. Diffusion coefficient of silica in seawater. *Nature* 229, 94.

World Ocean Atlas, 1998. http://ingrid.ldgo.columbia.edu/SOURCES/.NOAA/.NODC/.WOA98

CHAPTER 5

Geochemical characterization of resuspended sediment on the SE slope of the Faeroe-Shetland Channel

ABSTRACT

Inductively Coupled Plasma Mass Spectrometry (ICP-MS) analyses were carried out on surface sediments and resuspended material. A statistical analysis was performed on the multi-elemental concentrations to identify the source area of the resuspended material collected in the sediment traps from the SE slope of the Faeroe-Shetland Channel. Results indicate that the material intercepted by the traps has a composition similar to that of surface sediments from depths greater than 550 m. This suggests that particles advected on the slope do not originate from the upper slope or the shelf edge but from a deeper area and that local resuspended material is deposited deeper than 550 m. Multi-elemental and grain size analysis of trap samples from distinct intense resuspension events illustrate differences among samples. These differences were interpreted as a result of the varying intensity of the resuspension mechanism although separate source areas or different resuspension mechanism cannot be excluded. The identification of the source area of resuspended material is tempered by the homogeneity of the surface sediments in the region, due to the uniform glacial debris deposits, the high-energy currents and the lack of clearly identifiable continental input sources.

INTRODUCTION

During the last 2 decades, extensive interdisciplinary investigations carried out on continental margins have revealed that sediment input on the slopes is mainly due to lateral advection of material originating from the shelf edge or upper slope.

The results of the SEEP programme in the Middle Atlantic Bight, indicated that preferential deposition occurred in a region characterized by minimal current intensity, the so-called depocenter (Walsh, 1988; Biscaye et al., 1994). This zone of preferential deposition was fuelled for ~50% by aged and refractory material from relict sources on the shelf (Biscaye and Anderson, 1994; Anderson et al., 1994) and enhanced respiratory activity in the depocenter suggested that labile organic matter was deposited as well (Rowe et al., 1994). For the study area of the SEEP experiments, a more or less steady transport of particles to the deposition area was suggested (Biscaye and Anderson, 1994) despite the intermittent nature of the source of material (Churchill et al., 1994; Brunner and Biscaye, 1997). Intermediate nepheloid layers (INLs), detaching from the shelf edge or upper slope where material is temporarily stored, and spreading off the slope may account for transport down the slope at a more or less constant rate. Data collected during the OMEX project at the Goban Spur however, revealed that cross slope (down-slope) transport mainly occurred within persistent benthic nepheloid layers (BNL) and probably less via INLs (McCave et al, 2001).

Results from near-bottom sediment traps deployed on the SE slope of the Faeroe-Shetland Channel (FSC) during the PROCS programme have shown that sediment resuspension was taking place at depths greater than 471 m (Bonnin et al., 2002). Current velocities were strong enough to enable resuspension of phytodetritus aggregates that had already been in contact with the seabed, the so-called "rebound" material (Walsh, 1988). Massive and abrupt resuspension events have also been observed at mid-slope, entraining, in addition to the rebound particles, coarse and aged sediments in suspension in the water column over 2 tidal cycles at least. From a detailed analysis of near-bottom current meters, Hosegood et al. (submitted) demonstrated that this massive sediment resuspension was facilitated by strongly enhanced vertical velocity created by a hydraulic jump at the leading edge of internal solitary waves travelling up the slope. Furthermore, ^{210}Pb inventories from surface sediments on the SE slope of the FSC showed enhanced sediment deposition in a band between 550 and 850 m water depth (Van Raaphorst et al., 2001). This depth interval corresponds to the zone of major resuspension as measured by sediment traps (Bonnin et al., 2002) and suggests that a large amount of the resuspended material is re-deposited locally. Although it seems evident that enhanced erosion-resuspension-deposition loops take place at mid-slope in the FSC, the source of the resuspended material is still uncertain. Assessing this source area of resuspended material appears particularly interesting since the hypothesis of an upslope transport in the FSC is challenging and may alter the view on lateral advection and particle transport on continental slopes.

In this study, carried out within the framework of the PROCS programme, grain size and multi-elemental analyses were performed in combination with total organic carbon (TOC) analyses on surface sediment as well as on sediment trap material from the SE slope

of the FCS. The main objectives were: 1) to identify the cross-slope zonation of erosion-deposition zones on the slope, 2) to better characterize the geochemical composition of resuspended material over the slope and 3) to identify the source of resuspended material on the slope.

MATERIALS AND METHODS

Study Area

The Faeroe-Shetland Channel (60°N, 6°W - 63°N, 1°W) connects the Norwegian Sea with the Atlantic Ocean. The channel has a maximum depth of 1500-2000 m at the northeastern entrance and is about 600-650 m deep at the Wyville-Thomson Ridge in the south (Fig. 1). The upper 200-500 m of the water column is composed of two distinct water masses, North Atlantic Water (NAW) flowing northward along the West Shetland shelf and
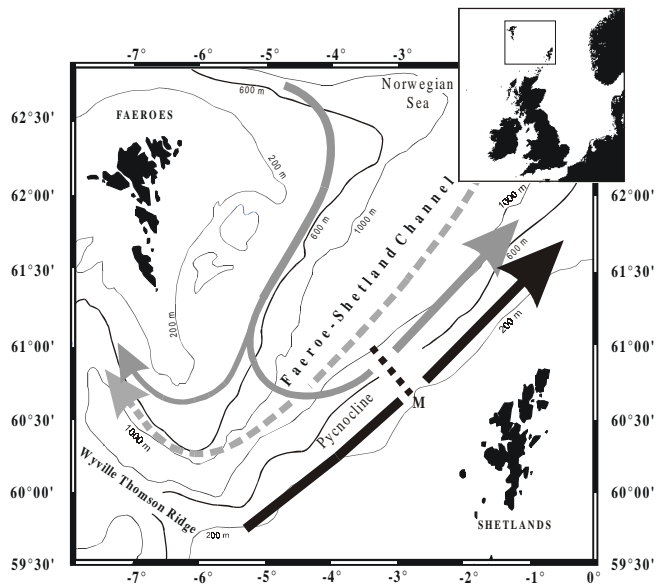
Fig. 1. *Map of the study area with position of the mooring transect (M) and of the main water masses in the Faeroe-Shetland Channel. The 5 water masses described by Turrell et al. (1999) are grouped here into 3 according to direction of flow. Black arrow: NAW (North Atlantic Water), grey arrow: MNAW (Modified North Atlantic Water) and AI/NIW (Arctic Intermediate/North Icelandic Water), and dashed arrow: NSAIW (Norwegian Sea Arctic Intermediate Water) and FSCBW (Faeroe-Shetland Channel Bottom Water). For more details on the location of the moorings, see Table 1.*

Modified North Atlantic Water (MNAW) flowing southward across the Faeroe Shelf and upper northwestern slope. This MNAW turns around in front of the Wyville-Thomson ridge and then runs northward parallel to the NAW along the central axis of the Channel. Deep water (> 500 m; FSCBW) comes from the Norwegian Basin and flows southward towards the Wyville-Thomson Ridge and further. The morphology and hydrography of the margin are described in detail by Stoker et al. (1993) and Turrell et al. (1999).

Samples

Samples were collected during two cruises on the SE slope of the FSC. PRO1 was conducted in spring 1999 (April 14th – May 5th) and PRO2 in fall 1999 (September 21st – October 13th). During each cruise a number of moorings, all equipped with 2 near-bottom sediments traps, were deployed at the seabed along a transect perpendicular to the slope at depths between 470 m and 1000 m (Fig. 1). During the cruise PRO1, 4 moorings: C3, C4, C6 and C8 were deployed at 471 m, 700 m, 777 m and 1000 m, respectively. During PRO2, 5 moorings were deployed: C1, C3, C4, C6 and C8 at 550 m, 700 m, 800 m, 900 m and 1000 m, respectively. In between the two cruises, 2 long-term mooring were deployed: D3 and D5 at 800 m and 1050 m, respectively, covering a time period of ~5 months (PRO LT). A summary of the sediment traps, their position and water depth is given in Table 1.

Table 1. *Sediment traps name, position, water depth and the TMF averaged for the whole deployment interval.*

Trap	Position	Water depth (m)	Average TMF ($g\ m^{-2}\ d^{-1}$)
PRO1-C3-30	60°48.48'N-02°59.34'W	441	0.14
PRO1-C3-2	-	471	0.42
PRO1-C5-30	60°55.36'N-03°05.88'W	670	13.74
PRO1-C5-2	-	700	25.53
PRO1-C6-30	60°56.91'N-03°13.22'W	747	24.02
PRO1-C6-2	-	777	59.67
PRO1-C8-30	61°00.09'N-03°18.39'W	970	5.20
PRO1-C8-2	-	1000	5.66
PRO2-C1-30	60°52.48'N-03°00.51'W	520	1.51
PRO2-C1-2	-	550	8.78
PRO2-C3-30	60°56.80'N-03°07.02'W	670	2.98
PRO2-C3-2	-	700	5.43
PRO2-C5-30	60°58.99'N-03°09.94'W	770	1.81
PRO2-C5-2	-	800	2.76
PRO2-C6-30	61°00.46'N-03°12.52'W	870	2.82
PRO2-C6-2	-	900	5.28
PRO2-C8-30	61°01.71'N-03°14.44'W	970	2.15
PRO2-C8-2	-	1000	4.24
PRO LT-D3	60°57.41'N-03°14.25'W	800	14.89
PRO LT-D5	61°00.83'N-03°19.47'W	1050	10.87

All moorings consisted of a buoyancy package at the top and a weight at the bottom fastened to two acoustic releases. The sediment traps were positioned with their apertures at 2 and 30 meters above the bottom (mab), except for PRO LT where traps were deployed at 2 mab only. For each mooring, the trap at 2 mab was mounted on a NIOZ-designed anchor frame, which allowed the sediment trap to be as close as possible to the seabed. The frame, with a total weight under water of 800 kg, including bottom weight and acoustic release system effectively reduced the motion of the line. To allow sampling in the high-energy regime of the FSC, all traps were modified from their conventional conical shape to a cylindrical shape by adding a 1.5-m long PVC cylinder with baffled aperture (10 mm hexagons). The resulting total length of the effectively cylindrical traps was 2 m and the collecting area on the top of the trap is 0.042 m^2 (aspect ratio 8:1). The sediment trap settings, sample processing and details of tilt effect on trapping efficiency are given in Bonnin et al. (2002).

For each deployment period (PRO1, PRO2) the traps are hereafter identified by the number of the mooring followed by the height above the bottom at which they stand, for instance C5-2 and C5-30 for traps mounted on mooring C5 at 2 and 30 mab, respectively.

Surface sediment samples were collected using a multicorer (Barnett et al., 1984) at different stations on a section perpendicular to the Shetland slope from 300 to 1228 m water depth (Fig. 1). The corer was equipped with 12 polycarbonate tubes, which normally collected undisturbed cores of 20-35 cm long with clear overlying water. For this study only the top layer of each sediment core was used. The sediment slices were freeze-dried, homogenized and ground using an automated carborundum ball-mill and kept in clean glass vials until analysis.

Particle size analysis and sediment size fractions

Particle size was measured with a Coulter LS230 laser particle-sizer as described by Konert and Vandenberghe (1997). Approximately 500 mg of freeze-dried material was suspended in ~10 ml water and placed in the ultrasonic bath for 15 minutes. Before putting the material into the Coulter, the suspension was sieved over 1 mm. The suspensions in the Coulter were diluted to an obscuration of 10% before the measurements were performed. During the measurements all samples were ultra-sonicated internally. Grain size distributions were corrected for the weight retained on the 1 mm sieve. A similar method was used for particle size analysis of trap samples (when sufficient amount of material was present), using ~200 mg of freeze-dried material. Swimmers were handpicked before processing of the samples so that no sieving was necessary.

Splits of the sediment top layer of all stations were fractionated into three size fractions (< 63 µm, 63-250 µm and > 250 µm) by dry sieving. Approximately 1-2 g of freeze-dried material was used for sieving. The size fractions were checked microscopically for the presence of aggregates. The coarser size fractions (63-250 µm and > 250 µm) did not contain aggregates of smaller particles and/or faecal pellets after sieving.

^{234}Th activity

The ^{234}Th activity was measured directly after the cruise in 15 g of ground freeze-dried samples either by counting the 92 keV gamma emissions with a high-resolution planar germanium GC3019 detector or by counting the 63 keV and 92 keV gamma emissions with a low energy GL1020R detector after Buesseler et al. (1992). Samples from a single core were measured with the same detector. Calibration was performed using an external ^{238}U standard in a silicate matrix, and supported activity was measured after four months. Excess ^{234}Th activity, the difference between the initial count and the supported activity, was corrected for the time elapsed between samples collection and counting.

Total Organic Carbon (TOC) and CaCO$_3$

Freeze-dried, homogenized and ground sediment trap and sediment samples were analyzed for total carbon and TOC on a Carlo-Erba 1500 elemental analyzer following the procedure of Verardo et al. (1990) and modified after Lohse et al. (1998, 2000). For TOC determination, carbonates were removed by progressive and controlled acidification with sulphurous acid. The CaCO$_3$ content was calculated as follows:

$$CaCO_3 = Total\ Carbon - TOC \times (100/12)$$

Multi-elemental analysis

Splits of surface sediment samples and sediment trap high TMF samples were size fractionated by wet sieving on a 50-µm nylon mesh. Both fine fraction (< 50 µm) and bulk fraction were analyzed with an inductively coupled plasma mass spectrometer (ICP-MS) in order to determine the elemental composition of the following elements: Mg, Al, K, Ca, Ti, Mn, Fe, Zn, Sr, Zr, and Ba. Samples were partly prepared and measured at the NIOZ and partly at the geochemistry department of the Utrecht University.

NIOZ- Between 5 and 20 mg of dry sample (for traps and surface sediment samples, respectively) was accurately weighed in a Teflon bomb. A mixture of 9 ml HNO3 (suprapur) acid and 3 ml HF acid was added and left to digest for 3 hours in a microwave. After digestion, 2 ml of perchloric acid (HClO$_4$) were added and the bombs were placed on a hot plate (95°C) until complete evaporation. Once the bombs had cooled down, the solid residue was diluted in 1M Teflon grade HNO$_3$ until a final dilution of ~2×10^4. The diluted samples were analysed using a Finnigan MAT Element 2 High Resolution Inductively Coupled Plasma–Mass Spectrometer (HR ICP-MS). The accuracy and precision of the overall procedure were estimated by analysing standard reference materials MAG1 (US Geological Survey) and GBW 07309A (China Centre for certified Ref. Mat.). Accuracy was better than 6 % and precision better than 3%.

Utrecht- Between 3 and 39 mg of dried sample (for traps and surface sediment samples, respectively) was weighed in a Teflon digestion vessel. A mixture of 2.5 ml of HF and 2.5 ml mix acid ($HCLO_4$:HNO_3=3:2) was added and closed vessels were put on a hotplate for at least 12 hours at 90°C. The vessels were opened and put on the hotplate at 150°C for about 4 hours until incipient dryness after which 25 ml 4.5% HNO_3 was added. The vessels were closed again and put on a hotplate for at least 4 hours at 90°C. The diluted samples were analysed using an Agilent 7500a ICP-MS. Accuracy and precision of the overall procedure were estimated by analysing standard reference materials MM91 (Utrecht Geochemistry lab standard) and SO1 (University of Mining and Metallurgy). Accuracy was better than 4% and precision better than 6%.

Statistical treatment of the elemental data

In order to account for the cross-slope and temporal distribution of the chemical elements in surface sediments as well as on near-bottom trap samples, multivariate analysis was performed on element concentration. The co-variability between elements (TOC, Mg, Al, K, Ca, Ti, Mn, Fe, Zn, Sr, Zr, and Ba) was examined by means of Principal Component Analysis (PCA) that was performed on the correlation matrices of element concentrations by using the SYSTAT software (Wilkinson, 1988).

RESULTS

Sediment traps

The Total Mass Flux (TMF) and TOC in sediment trap samples from near-bottom traps of PRO1 were described in detail in Bonnin et al. (2002) and are just summarized briefly here. At 471 m fluxes were low (0.07 to 0.9 g m^{-2} d^{-1}) during the entire deployment time, while at 700 and 777 near-bottom TMF increased sharply on day 112 (Fig. 2), and decreased to reach its background value after day 115. During this period, TMF at 1000 m water depth was one order of magnitude lower and remained so during the whole trapping period. TMF and TOC in sediment traps from PRO2 and PRO LT are shown in figures 3 and 4, respectively. As observed for PRO1, TOC content in traps samples decreased when TMF increased indicating that during high TMF the organic matter is diluted by lithogenic material. Bonnin et al. (2002) showed that the TOC content for PRO1 trap samples collected during the high flux period was similar to the TOC content of the surface sediment. Similar results were also found for PRO LT but not for PRO2 where the TOC content of high TMF samples was always higher than 2.2%, which is much higher than TOC content of surface sediments.
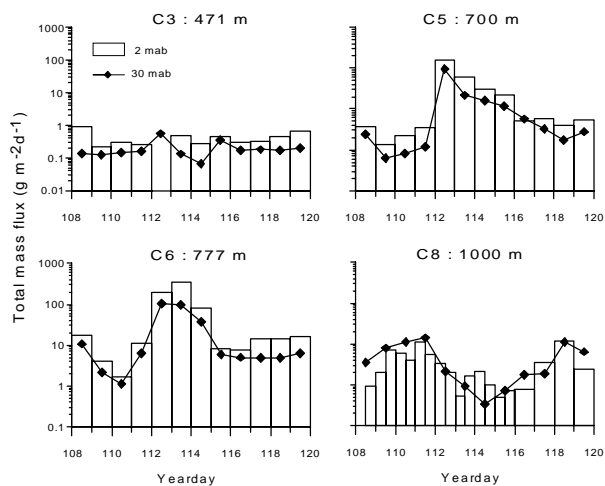
Fig. 2. *Total mass flux (TMF) measured from sediment traps from PRO1 positioned at 30 and 2 mab (diamonds and bars, respectively). TMF is plotted on a logarithmic scale for a better comparison between fluxes from all depths. Note the large differences between the upper slope and the mid-slope with maximum TMF of 350 g m^{-2} d^{-1} at 777 m on day 112. For TOC content we refer to Fig. 6 in Chapter 2.*
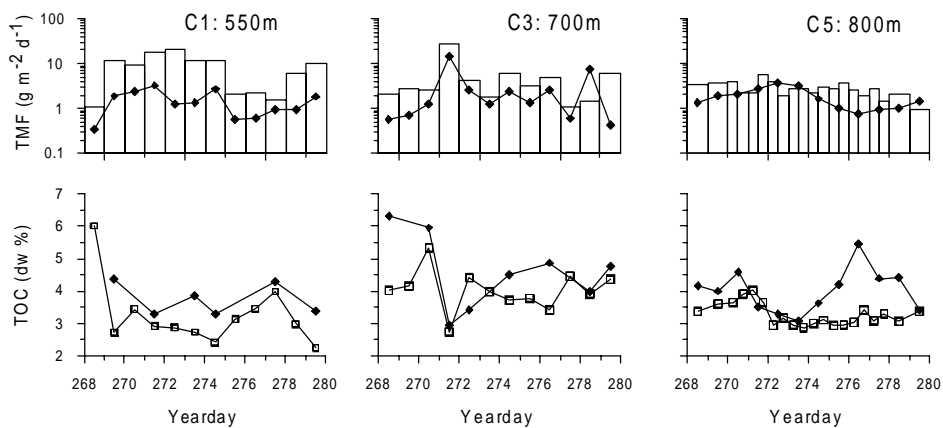
Fig. 3. *TMF at 30 mab (diamonds) and 2 mab (bars) are shown on the upper panels and the corresponding total organic carbon (TOC) content is shown on the lower panels for the PRO2 deployment. For the lower panels, the diamonds and squares represent TOC at 30 and 2 mab, respectively.*
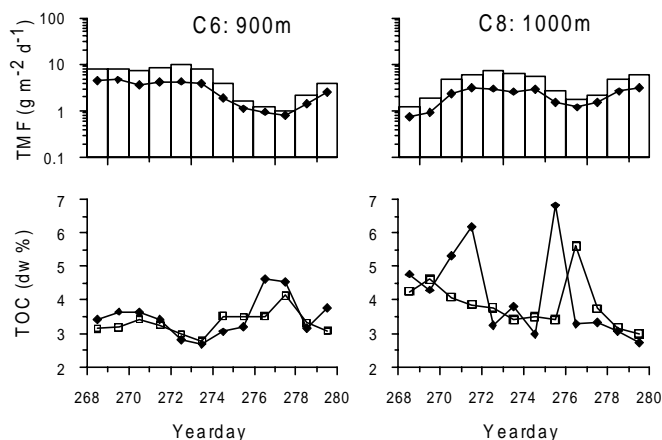
Fig. 3. Continued.
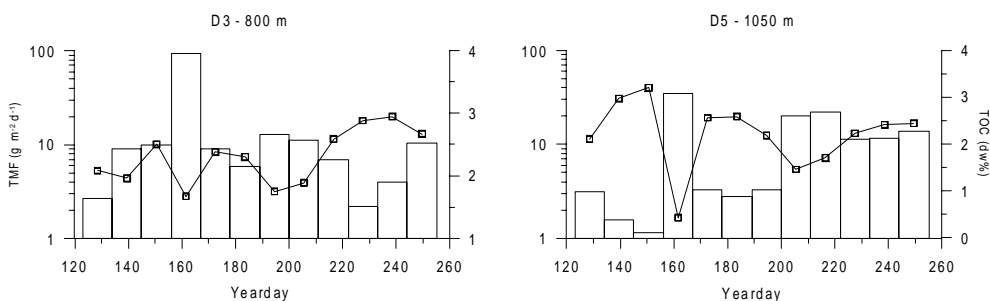
Fig. 4. TMF (bars) and TOC (squares) from PRO-LT at 2 mab from 800 and 1050 m water depth.

The multi-elemental composition for trap samples is given in Table 2. As shown for the trap deployed at 1050 m water depth during PRO LT, the concentrations of major and trace elements in the samples generally followed the same pattern. All the elements shown, except K, show similar behaviour: concentrations increase with increasing TMF up to a TMF value ~15 g m^{-2} d^{-1} and decrease when TMF exceeds this threshold value, which suggests dilution by other element(s). The correlation of K with TMF indicates that K could be one of the diluting elements during the high flux event although concentration of K in high TMF samples is not significantly high as compared to Ca, Al or Fe and suggests that additional unmeasured element(s) exert(s) dilution effect during high TMF (Fig. 5).
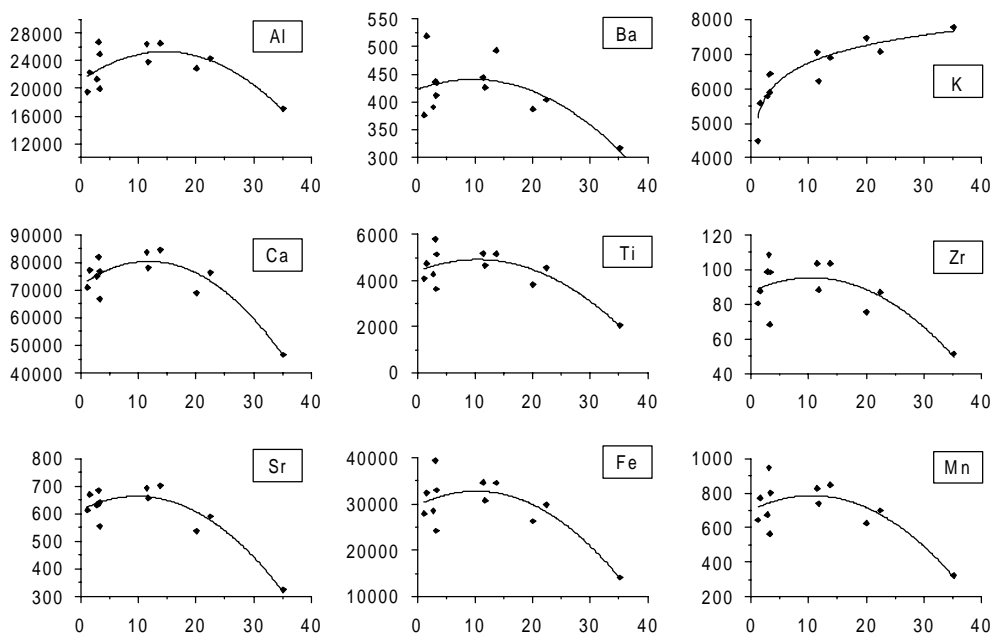
Fig. 5. *Concentration of major and trace elements in sediment trap samples from PRO-LT D5 plotted versus TMF. The black line corresponds to the power fit.*

Surface sediments

Sediment grain size- Visual inspection of the sediment cores showed that on the upper slope the sediment consisted of light brown clays overlaid by ~5 cm of greyish-brown coarse sand. Deeper down the slope at 750 m water depth clay was not present in the upper 10 cm, and on the lower slope clay was observed only below 9 cm. The transition from clay to coarse sands was interpreted as the transition from glacial to interglacial conditions (Stoker et al., 1991) and illustrates that since the early Holocene sediment accumulation was more pronounced on the lower slope than on the upper slope. The average median grain size for the top layer of surface sediment (Fig. 6a) decreased from ~500 µm at 375 m to ~150 µm at 600 m and remained constant deeper down the slope, which is close to the values measured for the lower slope by Van Raaphorst et al. (2001). The grain size of surface sediment on the upper slope is certainly underestimated due to the presence of large drop stones of glacial origin that can be several centimetres in diameter.
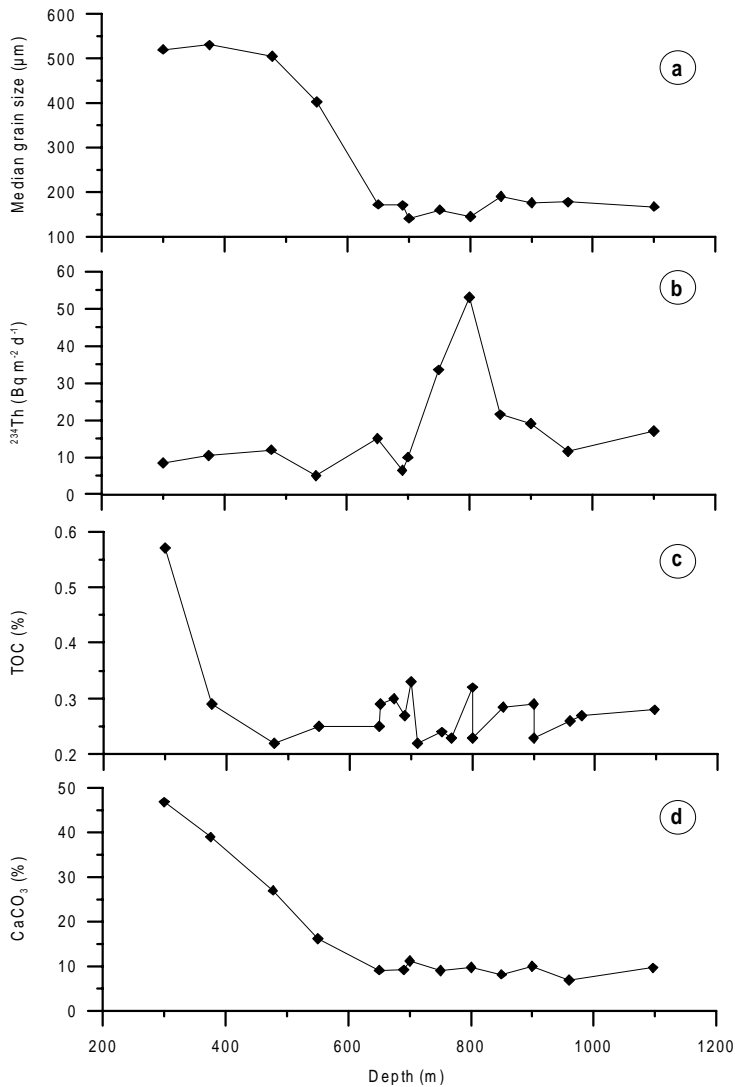
Fig. 6. *Median grain size (a), ^{234}Th inventories (b), TOC content (c) and CaCO$_3$ content (d) of surface sediment across the SE slope of the FSC.*

For selected stations at various depths on the slope, weight percentages of the size fractions < 63µm, 63-250 µm and > 250 µm are shown in figure 7. At the shallow station the fraction < 63 µm increased down-core while the > 250 µm fraction decreased. At mid-slope, the distribution is more or less constant with depth, with the 63-250 µm fraction being most abundant. At the deepest station the < 63 µm fraction increased with depth to nearly 100%. The increase in the fine fraction to > ~75% at the shallow and deep stations (at 5 and 9 cm, respectively) corresponds to the clay layer underlying the sand.

Size fractions (weight %)
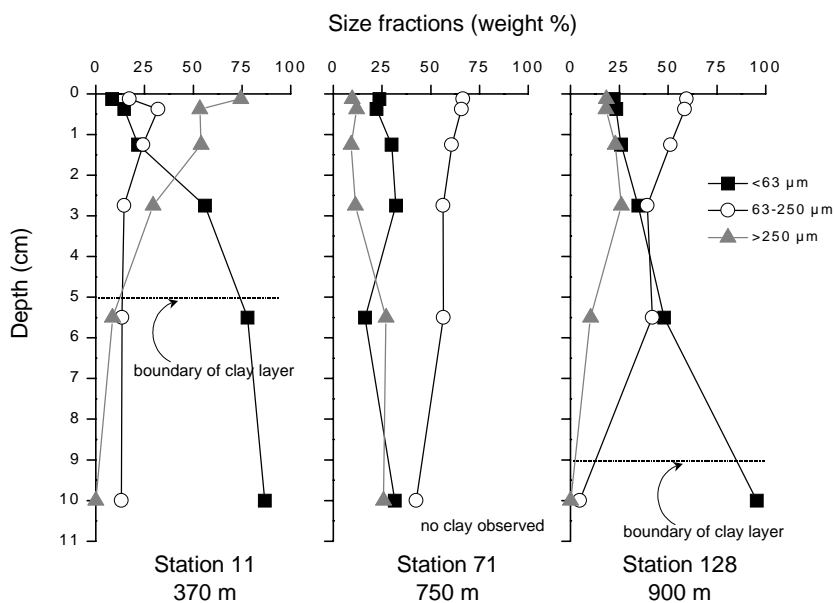
Fig. 7. Sediment size fractions in weight percentages, as obtained from particle size analysis in the upper 10 cm of sediment at 370, 750 and 900 m water depth across the FSC. Here only the cumulative weight percentages for the < 63 μm, 63-250 μm and > 250 μm fractions are shown. The dashed lines denote the transition from the sand to clay layer, based on the increase of the < 63 μm fraction as well as on visual observations.

Cross-slope variations in ^{234}Th, CaCO$_3$, and TOC content- ^{234}Th profiles reached their background concentration within the upper centimeter of the sediments at all stations. The inventory of ^{234}Th in the upper centimeter increased almost five-fold from 250 mBq cm^{-2} at 300 m to almost 1200 mBq cm^{-2} at 750 m and subsequently decreased to ~700 mBq cm^{-2} at 850 and 900 m depth (Fig. 6b). The highest calcium carbonate content was found on the upper slope (47%) and contents decreased to 10% at the lower slope (Fig. 6d). The TOC content of the surface sediment did not vary significantly across the slope. The values on the upper slope however were higher than those on the rest of the slope (Fig. 6c).

Major and trace elements- For both the fine and the bulk fractions, concentrations of some major elements are given versus water depth in figure 8. Most elements (Ti, Al, Fe, Mg, Ba) do not show a clear distribution across the slope. Ca content, however, shows a clear decrease from the upper to the lower slope. This is in good agreement with CaCO$_3$ data (Fig. 6c) and suggest that most of the Ca is associated with CaCO$_3$. Except for Ca no relation emerges between elemental content of the bulk material and grain size composition. For the fine fraction a distinct manganese peak is found at ~700 m while Ba, K and Al show a clear minimum at 550 m (Fig. 8). Similar cross-slope distributions of element concentrations are not observed in the bulk sediment.

Principal Component Analysis (PCA)

A total of 4 PCA were performed on elemental concentrations of sediment trap samples and surface sediments. Previous studies have shown that multivariate analysis is a valuable tool to correlate elements with similar behavior in geochemical studies (Araújo et al., 2002). A first PCA performed on the bulk sediment trap material from all 3 deployment periods (PRO1, PRO2 and PRO LT) revealed that three principal components (PC) account for more than 88% of the total variance observed in the data set (Table 2). Al, Ti, Fe, Mg, and Mn score high on the first principal component (PC1) indicative of their relative importance while K has a fairly high negative score. TOC, Ca and Sr score high on PC2. Finally, Ba has a high score on PC3.

Table 2. *Scores of the elements on the first 3 PCs from the PCA performed on bulk sediment trap samples.*

	Factor 1	Factor 2	Factor 3
Fe	**0.984**	-0.133	0.036
Ti	**0.965**	-0.174	-0.099
Mg	**0.964**	0.171	0.068
Mn	**0.935**	-0.280	0.167
Al	**0.933**	0.106	0.254
Zr	**0.822**	-0.122	0.117
TOC	-0.057	**0.967**	0.074
Ca	0.053	**0.880**	0.196
Sr	0.469	**0.787**	-0.181
Ba	-0.136	0.549	**0.780**
K	-0.600	0.417	0.469
Var (%)	42	34	12

Similarly, a second PCA was performed on trap samples from the mooring PRO-LT D5. The first two PCs explain more than 83% of the total variance (Table 3). Again, Fe, Mg, Ti, Mn, Al in addition with Zr, Sr, Ca score high on PC1 while only K scores high on PC2.

Table 3. *Scores of the chemical elements from the PCA performed on sediment trap samples from PRO-LT D5. Note that PC3 accounted for less than 1% and is therefore not shown here.*

	Factor 1	Factor 2
Fe	**0.982**	0.074
Mg	**0.975**	0.002
Zr	**0.955**	0.047
Ti	**0.947**	0.199
Mn	**0.943**	0.199
Sr	**0.911**	0.327
Al	**0.824**	-0.513
Ca	**0.765**	-0.377
Ba	**0.697**	0.401
K	0.060	**-0.920**
Var (%)	64	20

A third PCA was performed on the fine fraction of the high sediment trap flux samples only. The first two PCs explain more than 85% of the total variance (Table 4). Al, Ti, Fe, Mg, Mn in addition with Zr, Ca and score high on PC1 while Ba, Sr and Th have high scores on PC2.

Table 4. *Scores of the elements on the 2 PCs from the PCA performed on the fine fraction (<50 μm) of sediment trap samples with high TMF.*

	Factor 1	Factor 2
Fe	**0.979**	-0.058
Mg	**0.959**	0.082
Ti	**0.957**	-0.143
Al	**0.940**	0.182
Zr	**0.954**	-0.018
Mn	**0.931**	-0.138
Ca	**0.909**	0.240
K	**0.705**	0.269
Ba	-0.479	**0.789**
Sr	0.353	**0.784**
Var (%)	66	19

A final PCA was realized on the fine fraction of surface sediments and trap samples material (bulk and fine). Three PCs account for 84% of the variance (Table 5). Al, Ti, Mn, Fe and Mg score high on PC1 and Zr and K have high score on PC2. Ca scores high on PC3.

Table 5. Scores of the elements on the first 3 PCs from the PCA performed on sediment trap samples and surface sediment (< 50 µm).

	Factor 1	Factor 2	Factor 3
Fe	**0.980**	-0.118	0.037
Ti	**0.969**	-0.109	0.132
Mg	**0.956**	-0.002	-0.067
Mn	**0.923**	-0.172	0.008
Al	**0.885**	0.051	-0.100
Zr	0.152	**0.762**	0.458
K	0.006	**0.672**	0.232
Ba	-0.260	0.553	-0.511
Sr	0.314	0.498	-0.559
Ca	0.104	0.095	**-0.950**
Var (%)	54	17	13

DISCUSSION

Enhanced sediment deposition deeper than 600 m

The grain size distribution across the SE slope of the Faeroe-Shetland Channel shows a clear zonation with coarse sediment on the upper slope and finer material deeper than 550 m (Fig. 6a) and suggests that no net deposition of recent sediments takes place on the upper slope. From side scan sonar imagery, seabed photography and surface sediment sampling, Masson (2001) concluded that there was a lack of deposition at depth < 450 m as well, which he attributed mainly to the intense boundary currents flowing north-eastwards (NAW, Fig. 1) and to low input of modern sediments.
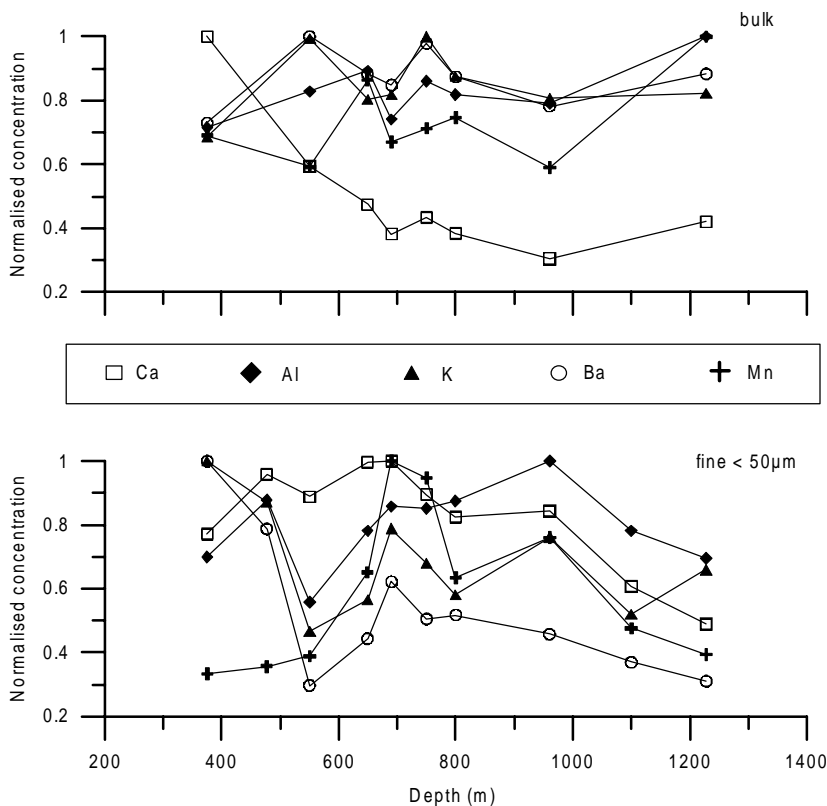
Fig. 8. Concentration of selected elements (Ca, Al, K, Mn, Ba), from bulk surface sediment (upper panel) and fine fraction (< 50 μm, lower panel), normalized to their highest value and plotted versus water depth across the slope.

The size fraction analysis of surface sediments (Fig. 7) shows that the depth of the glacial clay layer, that marks the changeover from weak bottom currents during glacial period to vigorous hydrodynamic regime during the interglacial, varies with water depth. The layer was observed at ~5 cm depth on the upper slope (370 m), ~9 cm depth at 900 m but was not observed at mid-slope (750 m) down to 10 cm within the sediment column. This is probably because our corer could not penetrate the sediment deep enough to meet this clay layer, although we cannot completely rule out the hypothesis of the absence of the clay at mid-slope. The thickness of the modern deposit layer would suggest that, since the last glacial, preferential deposition takes place at mid-slope relatively to other depths on the slope. This hypothesis of enhanced deposition at mid-slope is further confirmed by the higher [234]Th inventories of the sediment around 700 - 800 m water depth (Fig. 6b). Although [234]Th inventories only reflect the conditions during the past few weeks, this is in good agreement with the findings of Van Raaphorst et al. (2001) who observed that [210]Pb

flux on surface sediment at depths greater than 550 m was higher than the theoretical input expected from atmospheric deposition and production from decay of ^{226}Ra in the water column.

Elemental analysis of the fine fraction of the sediment revealed a manganese peak around 700 m. Manganese is redox sensitive and coupled to organic matter oxidation (Myers and Nealson, 1988). Thus, focusing of labile organic matter at this depth is not likely since accumulation of labile organic matter would favor reducing conditions and dissolution of the solid manganese phase. Low TOC content in core tops at mid-slope is consistent with this result. Furthermore, Grutters et al. (2001) have shown an increase of total hydrolysable amino acid (THAA) concentrations and amino acids mole percentages at ~750 m and they attributed this increase to enhanced bacterial activity in surface sediment and not to settling or advection of fresh organic matter from the upper slope or shelf. The manganese peak could then be due to accumulation of reworked and refractory material.

Origin of the trap material

A visual inspection of high flux trap samples under the binocular revealed that quartz and feldspar grains as well as planktonic and benthic foraminifera are in overwhelming amounts present in high TMF samples. Grain size analysis of some high flux samples from PRO1 showed the presence of these large particles in the traps. The particle size analysis showed a bimodal distribution with the dominant mode of ~100 µm during day 112 (Fig. 9). With passing time the dominant mode shifted from ~100 µm to ~8 µm illustrating the succession from fast settling of the coarse particles (within 2 days for particles > 100 µm) to the slow settling of fine clayish particles. Note the presence of some particles larger than 200 µm in trap C6-2 on day 113 that corresponds to the highest TMF (350 g m^{-2} d^{-1}).

Table 6. *Relative quantitative mineralogy measured by XRD of the lithogenic fraction of high TMF trap samples (S. Van der Gaast). The number of crosses (+) indicates the relative abundance of minerals in a given sample and (-) indicates absence.*

Sample	Quartz	Feldspar	Calcite	Mica/illite	Vermiculite	Chlorite	Pyrite
Pro1 C3-B	+++++	++	++++	+	+	+	++
Pro1 C5-B5	++++++	+++	+++++	+	+	+	+
Pro1 C6-B6	+++++	+++	++++	++	++	+	+
Pro1 C8-A4	+++++	+++	+++	+	++	+	-
Pro2 C1-B2	+++++	++	++++	++	++	++	-
Pro2 C3-B4	++++	+++	++++	++	++	++	-
ProLT D3-4	++++	+++	+++	++	++	+	-
ProLT D5-4	++++++	++++	+++	++	++	+	-

Both the grain size distribution in trap samples and visual observation of foraminifer and quartz and feldspar grains indicate a true sedimentary origin for mid-slope trap material during high flux events. Mineralogical analysis of some trap samples (Table 6) performed by X-ray powder Diffraction (Van der Gaast, 1991) gave semi-quantitative mineralogy of the trap samples and revealed the dominance of minerals such as quartz, calcite and feldspar and coarse clay minerals: micas/illite, vermiculite and chlorite (Van der Gaast, pers. comm.) and the quasi absence of fine particles (< 2 µm) in most of the trap samples.
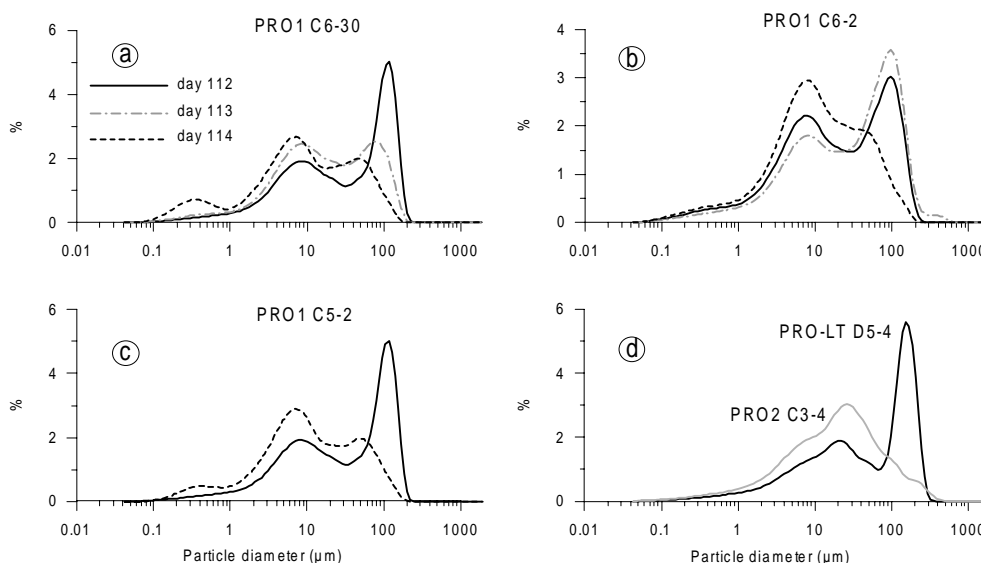
Fig. 9. *Grain size spectra of high TMF samples from PRO1 (C6-30, C6-2 and C5-2, plots (a), (b), (c), respectively), PRO-LT (D5-4, plot (d) black line) and PRO2 (C3-B4, plot (d) grey line) for days, 112, 113 and 114 (PRO1), 158-169 (PRO-LT) and 272 (PRO2). Note the shift in the dominant mode from day 112 (day of major resuspension event) to day 114, which clearly shows the settling of the coarse particles. The data also show that coarser particles collected during maximum resuspension of PRO2 were smaller (~30 µm) than those collected during maximum resuspension during PRO1 (~100 µm), while particles intercepted during PRO-LT were larger (~200 µm).*

The benthic origin of trap samples as suggested above, is further confirmed by the PCA performed on element concentrations of sediment trap material. Factor loadings of the first 2 PCs of elemental concentrations of bulk sediment trap material from all three deployment periods is shown in figure 10. Ti, Al, Fe, Mn and Mg score high on PC1 and suggest that samples having high loading on PC1 are characterized by their heavy mineral content which is the case for the mid flux samples. One would expect the amount of heavy
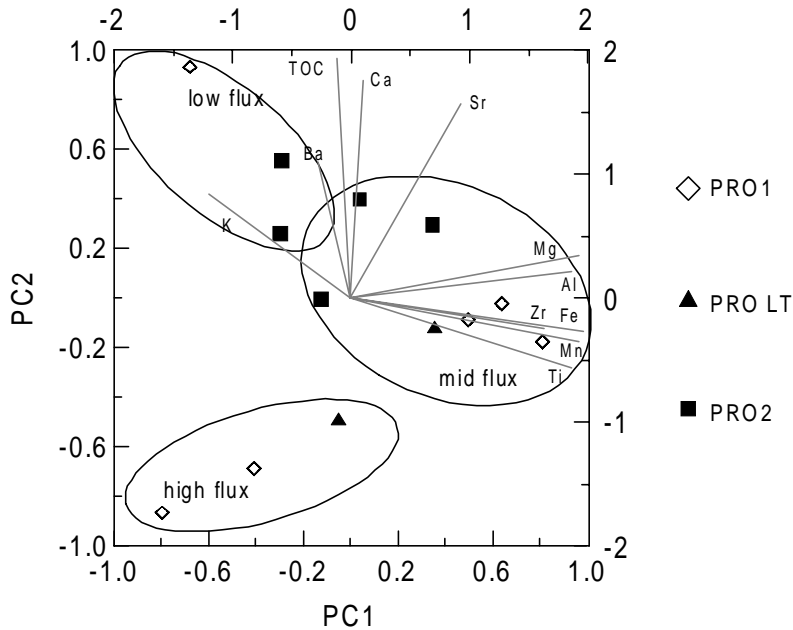
Fig. 10. *Element scores (vectors, bottom and left axis) and sample loadings (symbols, top and right axis) from the PCA applied on bulk trap samples from all 3 deployment periods*

lithogenic elements to be positively correlated with increasing TMF (which in our case reflects sediment resuspension). Such relation is not observed here. Low flux samples are well correlated with TOC, Ca and Ba and indicate a pelagic origin. The correlation with K is more difficult to explain, however it is clear that K does not belong to the heavy elements group (Fe, Zr…). High flux samples do have negative loading on PC1 and on PC2 but is correlated with none of the elements. The only possible explanation is that there is, in the high TMF samples, a diluting component as mentioned earlier, which we believe to be silicon that could not be measured with ICP-MS due to the destruction method (use of HF). Furthermore, high TMF samples have a negative loading on PC2 while low TMF samples have a strong positive loading. We saw that TOC and Ca score high on PC2 and that low flux samples are much less influenced by resuspension. This suggests that TOC and Ca are associated with the pelagic input due to settling from the upper water column. As shown in Table 3, barium scored low in PC1 and not as high on PC2 as TOC and Ca but was the only element to score high on PC3. It is not straightforward to assign a clear source for Ba since the mechanism of barite formation in the marine environment is still poorly understood (seawater is undersaturated with respect to $BaSO_4$). It is generally accepted however that barite crystals form primarily in microenvironments such as aggregates and faecal pellets, where the concentration of soluble $BaSO_4$ is exceeded due to decay of organic matter (Dehairs et al., 1980; Bishop, 1988). Furthermore, a good correlation between particulate barium and organic carbon was observed in several studies on sediment traps (Dymond et

al., 1992; Francois et al., 1995) and also indicate a close relation between barium and organic matter in the marine environment. Dehairs et al. (2000) from analysis of barium in traps moored at several depths in the Bay of Biscay have observed an increase of the barium content of trap samples with increasing water depth, which can be due to precipitation of barite crystals in settling aggregates. McCave et al. (2001) proposed that this increase of barium near the bottom could be due to lateral input and that the flux of biogenic barium could not be straightforwardly related to primary productivity of the overlying waters. As lateral input is dominant in our traps a clear relation between barium concentration and primary production is unlikely. However, our data set does show a good correlation between the barium and the TOC flux in the near-bottom traps (Fig. 11). The good regression coefficient ($r^2 = 0.897$) might be partly explained by the magnitude of the flux, which overprints the barium and TOC signals. However, since barium was observed in larger proportions in the PRO2 traps than in the PRO1 traps (up to 1200 ppm during PRO2 compared to 600 ppm during PRO1) and since PRO2 was characterized by much lower fluxes, we do consider barium content as an indicator of settling flux of aggregates stemming from the upper layer of the water column.
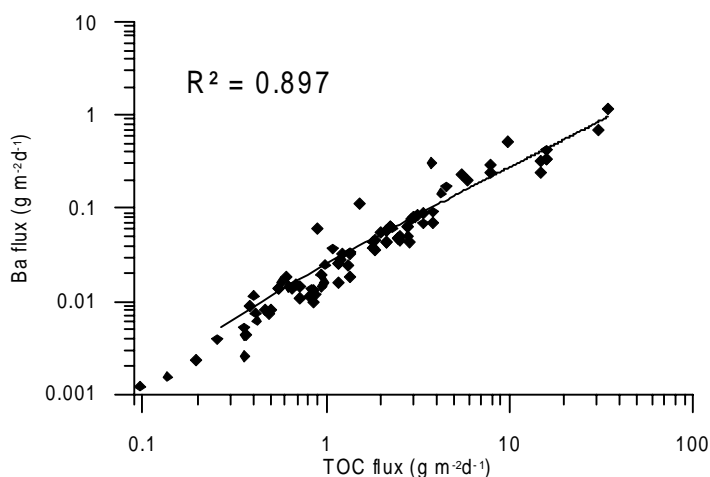
Fig. 11. *Ba flux plotted vs. TOC flux from all near-bottom trap samples.*

The 2nd PCA performed on trap samples from mooring PRO-LT D5 (Fig. 12) shows that high and low bulk samples have different loading on PC1 and PC2. Given the factor scores (Table 3) it is likely that mid flux and the fine fraction of high flux samples are characterized by the heavy mineral elements and K. This PCA also shows that the bulk material and the fine fraction from the same high flux sample (D5-4) have different loading on the first 2 PCs (mainly on PC1). The fine fraction has a strong positive loading on PC1

while the bulk sample has a negative loading, which indicates that the coarse fraction of the sample has a different chemical composition than the fine one (no or less heavy elements). Furthermore, the mineralogical analysis show that quartz is very abundant in high flux trap samples where coarse particles contribute largely to the TMF (Fig. 9). Furthermore, high TMF samples have different loading on PC2 than low TMF samples. Therefore, we believe that the elements associated with the coarse fraction (e.g., Si) explain the difference in loadings on PC1 between the bulk and fine fraction of the same sample.
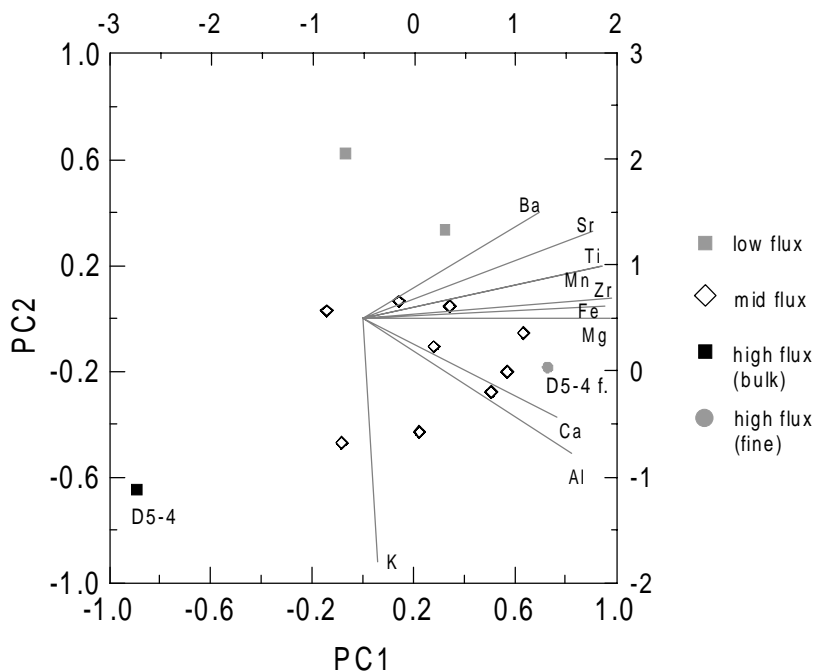
Fig. 12. *Element scores (vectors, bottom and left axis) and sample loading (symbols, top and right axis) from the PCA applied on trap samples from mooring PRO-LT D5.*

The results of the 3rd PCA performed on the fine fraction of the high TMF samples (700 and 777 m water depth) from the 3 deployment periods show that samples from the different sampling periods have different factor loadings (Fig. 13) and suggest that during high resuspension flux events, material intercepted at different periods had different geochemical signatures. Barium concentrations were higher in the PRO2 traps samples than in the PRO1 ones. This may partly explain why material intercepted in sediment traps during high flux intervals at different periods of the year have different composition. It also suggests that during the PRO2 period contribution to the intercepted flux by pelagic particles is higher.
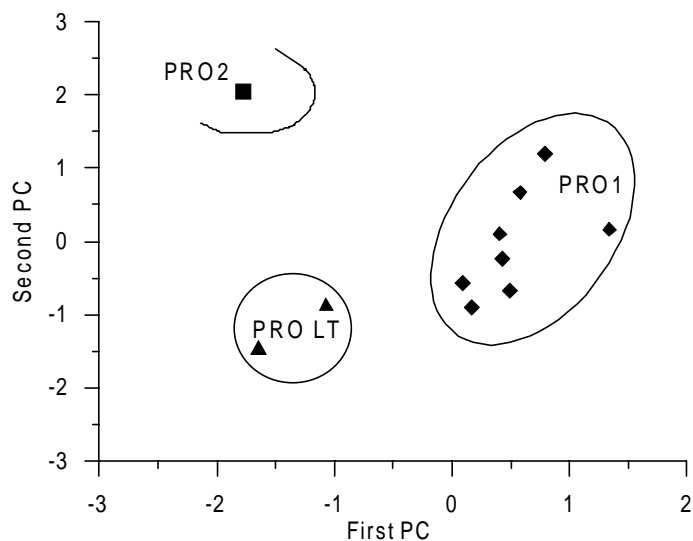
Fig. 13. *Loading of the first 2 PCs from the second PCA performed on the highest TMF samples from the 3 deployment periods.*

Source area of resuspended sediments

Earlier in this discussion it has been suggested that the upper slope is a zone of erosion or non-deposition. However, this appears to be in contradiction with the intense resuspension fluxes measured at 700 and 777 m if we assume that material supplied to the slope is advected from the upper slope or the shelf edge, as shown for other continental margins (Biscaye et al., 1994; Van Weering et al., 1998; McCave et al., 2001). The particularly low resuspension flux observed at 471 m during PRO1 indicates that resuspended material does not originate from the shelf or shelf edge and spreading off slope within intermediate nepheloid layers detaching from the shelf edge. If this would be the case, it would be difficult to explain how coarse sediments that arrive in massive amounts at mid-slope and are advected to the lower slope are not observed on the upper slope. Furthermore, the paucity of detrital carbonates (bryozoans, echinoderm, molluscs) in trap samples inferred from visual inspection under the binocular also tends to exclude a coastal source area although we cannot completely rule out that such biogenic debris may have been transported away by the strong currents.

The outcome of the PCA performed on surface sediments and trap samples (Fig. 14), shows that surface sediment from depths shallower than 477 m cluster separately from surface sediments from deeper on the slope and from trap material from all sampling intervals. This indicates that a boundary in the elemental composition of surface sediment exists around 500 m. It suggests that low TMF and PRO2 samples are less clearly associated with surface sediment than other trap samples and suggests a larger proportion of

pelagic input. Factor loadings of the fine fraction of high TMF samples from PRO1 and surface sediment from 649 to 960 m are fairly close, which suggests that a deep source area for the resuspended material during high flux events is plausible. Since water mass at this depth is flowing from the NE, long distance longitudinal transport of fine particles originating from the northerly entrance of the channel or the Norwegian Sea is likely.
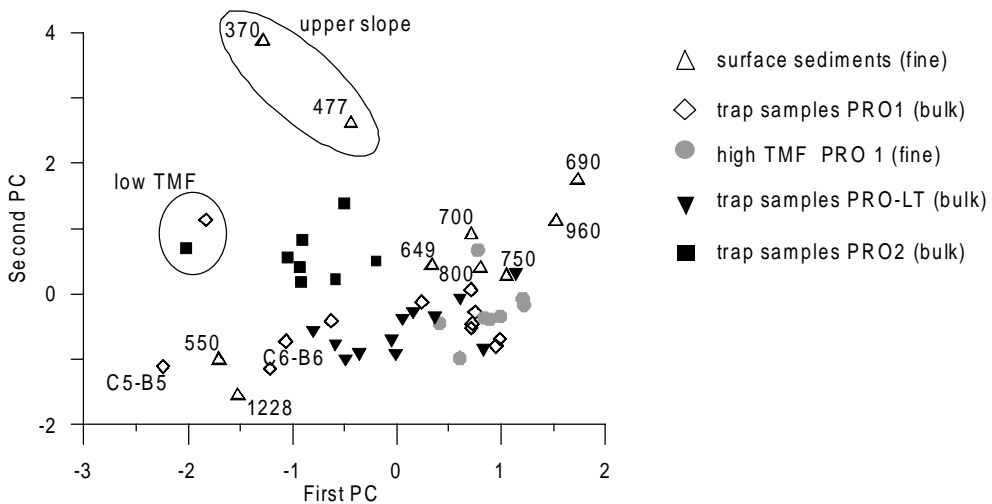
Fig. 14. *Loading of the first 2 PCs from the third PCA performed on surface sediment (< 50 μm) and trap material. The numbers next to the symbols indicate the depth (m) of surface sediments.*

Results from near-bottom current meters and acoustic Doppler current profiler deployed in the study area during PRO1 have revealed that massive sediment resuspension at mid-slope was facilitated by non-linear internal waves traveling up the SE slope of the FSC (Hosegood et al., submitted) pointing at a source area for resuspended material as deep as 700 or 800 m.

Abundant coarse quartz and feldspar grains present in the high TMF samples are of angular shape and hence suggest minimal abrasion. It indicates that the resuspended coarse particles have not been subject to intensive bottom transport prior to resuspension and exclude long distance longitudinal transport for these particles. Hosegood et al. (submitted) have shown that the mechanisms that facilitate sediment resuspension is associated to a sudden drop in the temperature of ~4.5 °C at 471 m water depth that occurred within a few minutes evidencing the abruptness of the resuspension. Such abrupt mechanism is not compatible with a remote source but more likely indicates a nearby origin for the resuspended material. The fact that the source area for the resuspended material

corresponds to the deposition zone also indicates that most of the sediment resuspended during major events is redeposited locally.

Sediments, resuspended during the highest flux event of each the 3 different deployment periods had a different geochemical composition and this difference may be partly explained by the timing of the bloom in the Faeroe-Shetland Channel. Another possible explanation is that resuspended sediments can have different source areas. Van Raaphorst et al. (2001) have shown that under normal stratification conditions, the SE slope of the Faeroe-Shetland Channel was critical for internal tidal waves between 350 and 550 m, where the major pycnocline meets the sloping bottom. The authors estimated that increased turbidity around 700 m could be due to the breaking of internal waves impinging where the slope is critical and sustaining down-slope particle transport in a permanent benthic nepheloid layer and intermittent intermediate nepheloid layers. The mechanism is described by Hosegood et al. (submitted) and implies that a source area as deep as 800 m is strongly related to down-slope depression and up-slope relaxing of the thermocline. A similar observation was made at 700 m during PRO2 at time of the major resuspension on day 271. Hence, the depth on the slope involved in sediment resuspension seems to depend strongly on the intensity of the depression of the thermocline. This depression can be caused by energetic eddies and meanders resulting from shear produced by topographic steering of the slope current and merging of the warm North Atlantic water with cold Nordic waters (Oey, 1998). Likewise in the Gulf of Lions, bottom-trapped topographic waves propagating with a ~7-day period along the continental slope have been evoked to explain fluctuations of the along slope currents (Flexas et al., 2002). During PRO1, the thermocline was depressed down to 700 or 800 m during ~4 days (Hosegood et al., submitted) thereby generating resuspension of surface sediments from this depth. During PRO2 conditions may have been less favorable for down-slope migration of the thermocline involving a shallower source area. The high variability of the temperature at 550 m water depth confirms that the major thermocline impinges on the slope at this depth. The large differences between the TMF in the traps at 30 and 2 mab (a factor of 5 on average) suggests that most of the resuspended particles do not reach the upper trap but are confined in the benthic nepheloid layer within which they can be advected further down the slope.

Mineralogical analysis on trap material has revealed the presence of pyrite crystals in samples corresponding to highest TMF from PRO1 (Table 6). Since pyrite is originating from reduction of sulfate this suggests that at least part of the material collected in traps originates from the reduced layer, which can be several centimeters deep in the sediment. However, it is not possible to say whether the reduced layer has been eroded by one single event like the one observed during PRO1 or whether this is the result of recurrent short-term resuspension events. Furthermore, the erosion rate may be higher than the pyrite oxidation rate and may expose pyrite crystals on sediment surface. The absence of pyrite in samples from PRO2, when the intensity of resuspension was lower, tends to support the idea of a rather deep origin in the sediment for the pyrite. It demonstrates that the resuspension mechanism in the FSC can be extremely energetic. This suggests that the

observed different chemical composition of trap samples could also be explained by the intensity of the mechanism that results in the resuspension of sediments.

Synthesis

Sediment transport on the SE slope of the FSC may be facilitated by non-linear internal waves originating from the deep part of the basin and traveling up the slope or by internal tidal waves impinging on the upper slope, between 350 and 550 m and facilitating down-slope advection of resuspended material (Van Raaphorst et al., 2001). Grain size and ^{234}Th analysis showed enhanced sediment deposition on the slope between 550 and 850 m water depth but no increase of the TOC content. Thus, this deposition zone on the slope appears to be present due to the combination of convergent resuspension fields and lower averaged current speed at this depth (Van Raaphorst et al., 2001; Bonnin et al., 2002).
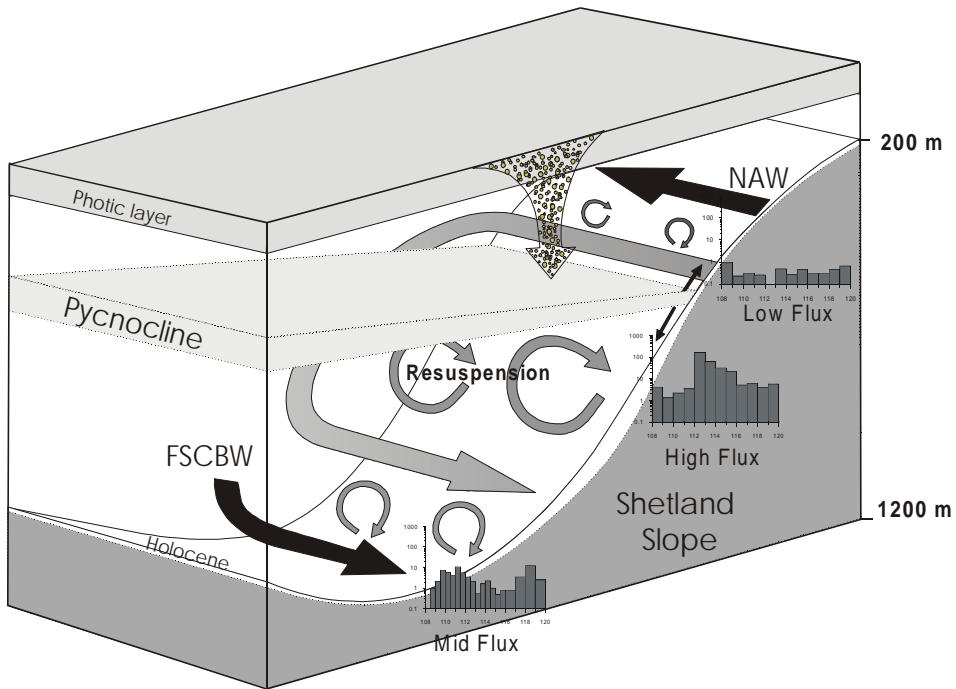
Fig. 15. *Diagram illustrating the different mechanisms acting on the distribution of sediments on the SE slope of the FSC and the relation with the near-bottom fluxes observed during PRO1. The surface water (NAW) and deep water (FSCBW) masses are indicated bye the black thick arrows. Hypothesised fine particles pathway in the FSC is schematised by the large grey arrow.*

Surface sediments and sediment trap data suggested that seabed material from the shelf or the upper slope cannot sustain the particle flux in the deeper regions of the slope which can be due to intense bottom currents flowing north-eastwards and a strong temperature-salinity front at ~550 m (Van Raaphorst et al, 2001; Bonnin et al., 2002). It is also clear that coarse particles captured by mid-slope traps have a nearby source and do not originate from the upper slope or shelf edge. Since fine particles could not be advected from the shelf to the deeper parts of the channel, the question remains where the fine material on the lower slope is coming from? One hypothesis is that under the action of the strong currents flowing north-eastwards on the outer shelf and upper slope, most of the settling fine particles are winnowed and transported away towards the entrance of the channel. Here, a different current regime may favor particle settling and advection to the deeper part of the channel where the vigorous FSCBW can transport them south-westwards (Fig. 15). This would result in ageing of the particles along their route towards the deepest part of the channel and explain why the sediments at all depth across the slope have a relatively low TOC content. Recurrent resuspension and mixing of surface sediments will favor mixing of the slope sediments, which limits the identification of the source area of the resuspended material, based on a comparison of the elemental concentrations of trap material and core tops.

ACKNOWLEDGEMENTS

REFERENCES

Anderson, R.F., Rowe, G.T., Kemp, P.F., Trumbore, S. and Biscaye, P.E., 1994. Carbon budget for the mid-slope depocenter of the middle Atlantic Bight. *Deep-Sea Research II* 41, 669-703.

Araújo, M.F., Jouanneau, J.-M., Valério, P., Barbosa, T., Gouveia, A., Weber, O., Oliveira, A., Rodrigues, A. and Dias, J.M.A., 2002. Geochemical tracers of northern

Portuguese estuarine sediments on the shelf. *Progress in Oceanography* 52, 277-297.

Barnett, P.R. Watson, O.J. and Connelly, D., 1984. A multiple corer for taking virtually undisturbed samples from shelf, bathyal and abyssal sediments. *Oceanologica Acta* 7, 399-408.

Biscaye, P.E., Flagg, C.N. and Falkowski, P.G., 1994. The Shelf Edge Exchange Processes experiment, SEEP-II an introduction to hypotheses, results and conclusions. *Deep-Sea Research II* 41, 231-252.

Biscaye, P.E. and Anderson, R.F., 1994. Fluxes of particulate matter on the slope of the southern Middle Atlantic Bight: SEEP-II. *Deep Sea Research II* 41, 459-509.

Bishop, J.K.B., 1988. The barite-opal-organic carbon association in oceanic particulate matter. *Nature* 331, 341-343.

Bonnin, J., Van Raaphorst, W., Brummer, G.-J. A., Van Haren, H. and Malschaert, H., 2002. Intense mid-slope resuspension of particulate matter in the Faeroe-Shetland Channel: short-term deployment of near-bottom sediment traps. *Deep-Sea Research I* 49, 1485-1505.

Bonnin, J. and Van Raaphorst, W., Dissolved silica enrichment in the deep waters of the Faeroe-Shetland Channel. Submitted to *Deep-Sea Research I*.

Brunner, C.A. and Biscaye, P.E., 1997. Storm-driven transport of foraminifers from the shelf to the upper slope, southern Middle Atlantic Bight. *Continental Shelf Research* 17, 491-508.

Buesseler, K.O., Cochran, J.K., Bacon, M.P., Livingstone, H.D., Casso, S.A., Hirschberg, D., Hartman, M.C. and Fleer, A., 1992. Determination of Thorium isotopes in seawater by non-destructive and radiochemical procedures. *Deep-Sea Research I* 39, 1103-1114.

Churchill, J.H., Wirick, C.D., Flagg, C.N. and Pietrafesa, L.J., 1994. Sediment resuspension over the continental shelf east of the Delmarva Peninsula, *Deep-Sea Research I* 41, 341-363.

Dehairs, F., Chesselet, R. and Jedwab, J., 1980. Discrete suspended particles of barite and the barium cycle in the open ocean. *Earth and Planetary Science Letters* 49, 528-550.

Dehairs, F., Flagel, N., Antia, A.N., Peinert, R., Elskens, M. and Goeyens, L., 2000. Export production in the Bay of Biscay as estimated from barium barite in settling material: a comparison with new production. *Deep-Sea Research I* 47, 167-186.

Dymond, J., Suess, E. and Lyle, M., 1992. Barium in deep-sea sediment: a geochemical proxy for paleoproductivity. *Paleoceanography 7*, 163-181.

Flexas, M.M., Durrieu de Madron, X., Garcia, M.A., Canals, M. and Arnau, P., 2002. Flow variability in the Gulf of Lions during the MATER HFF experiment (March – May 1997). *Journal of Marine Systems* 33-34, 197-214.

Francois, R., Honjo, S, Manganini, S.J. and Ravizza, G.E., 1995. Biogenic barium fluxes to the deep sea: implications for paleoproductivity reconstruction. *Global Biogeochemical Cycles* 9, 289-303.

Grutters, M., Van Raaphorst, W., Boer, W., Malschaert, H. and Helder, W., 2001. Mid-slope accumulation of amino acid-rich organic matter across the Faeroe-Shetland Channel. Geologica Ultraeictina, 213, PhD Thesis, 96 pp.

Hosegood, P., Bonnin, J. and Van Haren, H. Solibore-induced resuspension in the Faeroe-Shetland Channel. Submitted to *Nature*.

Konert, M. and Vandenberghe, J., 1997. Comparison of laser grain size analysis with pipette and sieve analysis: a solution for the underestimation of the clay fraction. *Sedimentology* 44, 523-535.

Lohse, L., Helder, W., Epping, E.H.G. and Balzer, W., 1998. Recycling of organic matter along a shelf-slope transect across the NW European Continental Margin (Goban Spur). *Progress in Oceanography* 42, 77-110.

Lohse, L., Kloosterhuis, R.T., de Stigter, H.C., Helder, W., Van Raaphorst, W. and Van Weering, T.C.E., 2000. Carbonate removal by acidification causes loss of nitrogenous compounds in continental margin sediments. *Marine Chemistry* 69, 193-201.

Masson, D., 2001. Sedimentary processes shaping the eastern slope of the Faeroe-Shetland Channel. *Continental Shelf Research* 21, 825-857.

McCave, I.N., Hall, I.R., Antia, A.N., Chou, L., Dehairs, F., Lampitt, R.S., Thomsen, L., Van Weering, T.C.E. and Wollast, R., 2001. Distribution, composition and flux of particulate material over the European margin at 47°-50°N. *Deep-Sea Research II* 48, 3107-3139.

Myers, C.R. and Nealson, K.H., 1988. Bacterial manganese reduction and growth with manganese oxides as the sole electron acceptor. *Science* 240, 1319-1221.

Oey, L.Y., 1998. Eddy energetics in the Faeroe-Shetland Channel: a model resolution study. *Continental Shelf Research* 17, 1929-1944.

Rowe, G.T., Boland, G.S., Phoel, W.C., Anderson, R.F. and Biscaye, P.E., 1994. Deep-sea floor respiration as an indication of lateral input of biogenic detritus from continental margins. *Deep-Sea Research II* 41, 657-669.

Stoker, M.S., Hitchen, K. and Graham, C.C., 1993. The geology of the Hebrides and West Shetland shelves, and adjacent deep-water areas, United Kingdom Offshore Regional Report. British Geological Survey, London.

Turell, W.R., Slesser, G., Adams, R.D., Payne, R. and Gillibrand, P.A., 1999. Decadal variability in the composition of Faeroe Shetland Channel bottom water. *Deep-Sea Research I* 46, 1-25.

Van der Gaast, S. 1991. Mineralogical analysis of marine particles by X-ray powder diffraction. In: Marine particles: analysis and characterization. Geophysical Monograph 63, Eds: D.C. Hurd and D.W. Spencer. 472 pp.

Van Raaphorst, W., Malschaert, H., van Haren, H., Boer, W. and Brummer, G.-J., 2001. Cross-slope zonation of erosion and deposition in the Faeroe-Shetland Channel, North Atlantic Ocean. *Deep-Sea Research I* 48 (2), 567-591.

Van Weering, T.C.E., McCave, I.N., De Stigter, H.C., Hall, I. and Thomsen, L., 1998. Recent sediments, sediment accumulation and carbon burial at Goban Spur, N.W. European continental margin. *Progress in Oceanography* 42, 5-35.

Verardo, D.J., Froelich, P.N. and McIntyre, A., 1990. Determination of organic carbon and nitrogen in marine sediments using the Carlo Erba NA-1500 analyzer. *Deep-Sea Research* 37 (1), 157-165.

Walsh, I., Fisher, K., Murray, D. and Dymond, J., 1988. Evidence for resuspension of rebound particles from near-bottom sediment traps. *Deep-Sea Research* 35 (1), 59-70.

Wilkinson, L., 1988. SYSTAT, the system for statistics. SYSTAT.

Concluding remarks

STATUS OF SEDIMENT RESUSPENSION ON CONTINENTAL SLOPES

Continental slopes have long been considered to play an important role in the transfer of particulate matter from the shallow and productive shelf seas to the deep ocean. Resolving the uncertainties in these exchanges of particulate matter in general and organic carbon and biogenic elements in particular requires knowledge of the fluxes and processes involved in particulate matter erosion and transport. Therefore, it is not surprising that continental margin areas have received particular attention in the last decade. However, most of the studies carried out on continental slopes have mainly concentrated on the long-term processes (such as erosion by strong boundary currents) and the role of short-term processes on sediment resuspension and transport is still to be better understood.

Short-term processes such as heavy storms over the outer shelf (Churchill et al., 1994; Brunner and Biscaye, 1997), internal waves impinging on the slope (Cacchione and Drake, 1986; Dickson and McCave, 1986; Thorpe and White, 1988; Atzetsu-Scott et al., 1995) and a combination of these processes have also been invoked for to explain the resuspension of seabed particles and the creation of nepheloid layers at the shelf edge or upper slope. Increased turbulence above the slope and the resulting resuspension of sediments and formation of nepheloid layers is generally attributed to critical internal wave reflection. The highest degree of sediment mixing and transport may be also governed by short and intermittent energetic events. However, because of the difficulty to observe and resolve these short-term processes on continental slopes, understanding their role on particles resuspension and cross-slope distribution is still poor.

THIS STUDY

This thesis is the outcome of the sedimentology and geochemistry component of the PROCS programme that was carried out on the south-east continental slope of the Faeroe-Shetland Channel. It benefited from the unique combination of fast sampling near-bottom current meters, optical backscatter sensors, temperature sensors and sediment traps deployed during 2 short intervals of 12 days and a longer period of 5 months. The work presented here also greatly benefited from the close collaboration between the department of Marine Chemistry and Geology and the department of Physical Oceanography of the

Royal NIOZ. This collaboration has permitted a unique understanding of the physical processes taking place in the near-bottom boundary layer and their impact on sediment resuspension and distribution across the slope. This study particularly focused on the short-term and highly energetic mechanisms and has highlighted several points concerning resuspension of seabed material and transport of particles on the continental slope:

Resuspension of sedimentary particles was observed at all times at depths greater than 471 m and was related to the elevated bottom current speeds. The resuspension is variable both in time and in space, with higher resuspension observed at mid-slope and with peak resuspension fluxes reaching up to 350 g m^{-2} d^{-1} on day 113 at 777 m water depth. At water depths less than 471 m, little or no resuspension took place due to the consolidated nature of the seabed, although strong bottom currents were observed. Our results also indicated that massive sediment resuspension, to which coarse and aged sediment proper can contribute up to 70% of the total mass flux, can occur repeatedly in the investigated area. The presence of coarse material indicates a local source for resuspended material during this particular event. During this intense resuspension event, strong along-slope bottom current velocity appears not to be the trigger mechanism.

Physical data, based on fast sampling near-bottom instruments (ADCP, Thermistor strings, FLY) deployed at various depth on the slope, showed that such massive and abrupt resuspension was associated with a sudden drop in the temperarure and reversal of the bottom current occurred within a minute and was related to the passage of internal non-linear solitary waves ('solibore') travelling up the slope. Sediment resuspension at least 30 m up in the water column was attributed to the rotor formed at the leading edge of the waves characterized by increased vertical velocity.

The surge of the water mass as clearly shown by temperature profiles is directed upslope and therefore indicates an origin from deeper than 700 m. Furthermore, the observation of such a phenomena on the continental slope is unique as so far it has only been observed in shallower environments. It is particularly interesting here as it appears as an additional and potentially dominant mechanism for transporting sediment over continental slopes.

Results based on biogenic silica analysis in surface sediments, near-bottom sediment traps samples and suspended matter in the water column as well as dissolved silica fluxes calculated at the sediment-water interface and in the water column indicated that silica enrichment observed in the deep waters of the Faeroe-Shetland Channel was mainly due to active refuelling from the sediments with a small contribution from the dissolution of pelagic settling biogenic silica debris. The data efflux of dissolved silica was particularly intense between 600 and 850 m water depth, which coincides with the depth zone of major sediment resuspension and suggests that the mechanisms responsible for sediment resuspension also have a strong impact of the distribution and recycling of nutrients. This further points at the recurrence of the observed phenomena and related resuspension mechanism. This study also revealed the importance of the basin geomorphology and its interaction with strong stratification and high-speed currents, which enable sediment deposition at mid-slope as shown by the increased concentration of radioactive isotopes.

Finally, statistical analysis performed on multi-elemental concentrations from surface sediments and resuspended material indicates that a shallow source for the resuspended material intercepted at mid-slope is unlikely in the study area. On the contrary, the data suggest and that the material untercepted by the near-bottom traps originates from a location deeper than 550 m and shallower than 1228 m, which confirm the findings from the detailed study of the hydrodynamic showing the occurance of up-slope transport of sediments in this particular slope environment. However, the homogeneity of the surface sediments, mainly due to uniform glacial debris deposits and high-energy currents makes the identification of the source area of resuspended material a particularly difficult task in the Faeroe-Shetland Channel.

PERSPECTIVES

Our study on the SE slope of the Faeroe-Shetland Channel showed the impact of short-term processes on remobilisation, mixing and transport of surface sediments in a high-energy environment and the potential importance of these processes in the recycling of biogenic elements on the continental slope. Regarding the key role of short-term processes on the distribution and recycling of biogenic particles on the slope, it appears particularly interesting to conduct similar research on other continental margins. Those having a similar channel-like geomorphology like the Mozambique Channel, Rockall Throug where internal waves have been shown to occur, as well as open slope systems where the export of organic matter is high (e.g., coastal upwelling areas or regions influenced by strong continental input). This would be particularly interresting when combining surface water, water column, resuspended particles and surface sediment analyses (geochemical, sedimentological, physical) with near-bottom current measurement (current meters, ADCP) and in situ observation of particle (benthic vehicules, camera). Such investigations of other margin systems would contribute to assess the role of short-term processes on a global scale.

The results of the PROCS programme have demonstrated however the limitations of 2D investigations, particularly in high-energy environments were lateral advection is strong. Deployment of moorings equipped with synchronous fast-sampling near-bottom current meters, ADCP, turbidity and temperature sensors and sediment traps on several parallel sections across the slope is a pre-requisite to both quantify the lateral advection and assess the fate of resuspended sediments on the slope.

Effects of turbulence and sediment resuspension on benthic organisms and ecosystems may be quite important as the organisms have to overcome the ecological problems due to turbulence such as nutrient and particle dynamics. These effects on biological activities and community structure have the potential to strongly modify the quantity and/or quality of particulate matter and therefore have consequences for biogeochemical fluxes. Investigations on the effects of turbulence on the organisms, community and ecosystem levels appear therefore of utmost importance.

In the recent years, it became apparent that our knowledge of processes that regulate dissolution (and preservation) of biogenic silica in the water column and at the sediment-water interface is limited. Understanding these processes appear of major interest since siliceous phytoplankton play a major role in the "biological pump" that is expected to be important in reguating the atmospheric CO_2 concentration. Effects of turbulence on dissolution of diatoms (i.e., increased residence time in the water column and mechanical friction with the surrounding water, disturbance of benthic communities and bacteria that facilitate dissolution by removing the organic coatings, input of DSi in the mixed layer due to higher vertical diffusion, or decrease of the DSi concentration in the bottom water due to disturbance of the benthic boundary layer) may be minor but the fact that our knowledge on these effects is still extremely poor should stimulate future research in order to better constrain silica remineralisation in the oceans which is a crucial part of the global cycle of silica and carbon.

Finally, more detailed knowledge on short-term and potentially very active mechanisms enabling sediment resuspension and transport off and along the slopes appears particularly interesting in areas that receive much attention for paleo-environmental studies. Indeed, high-energy processes as described in Chapter 3 certainly lead to major perturbations of the sedimentary signal. Ignoring massive resuspension-redistribution of surface sediments would probably lead to erroneous interpretation of proxy data (forams, biomarkers, isotopic ratios etc…) since the sedimentary signal may be strongly perturbed (e.g., due to lateral advection or re-mobilisation onto the sediment surface of older material). Integration of the effects of these short-term processes in paleo-environmental studies requires a better understanding of the mechanisms involved in sediment resuspension on continental margins and slopes.

ACKNOWLEDGEMENTS

CURRICULUM VITAE

Jérôme Bonnin was born on 10 June 1973 in Libourne, south-west France. After his "Baccalauréat" passed in 1992 in the "Lycée Michel Montaigne" in Bordeaux, he integrated the University of Science of Bordeaux where he studied Earth Sciences. He passed his Bachelor in Geology and Oceanography in 1997 after a semester spent at the Southampton Oceanographic Centre, where he developed a strong affection for international working atmosphere. After his military service duty, spent in the French air force, he started his Masters in Marine Environments and Paleo-environments in 1998 at the university of Bordeaux I. His graduation research was carried on "High resolution benthic foraminifer successions around Mediterranean sapropels S5, S4 and S3" under supervision of Dr. Frans Jorissen. In August 1999 he started a PhD position at the Royal Netherlands Institute for Sea Research within the PROCS programme. He is now temporarily "resuspended and transported" to Bremen in Germany by the strong current of love and aims at settling down permanently in France when "turbulent" conditions of a postdoc situation will have calmed down.

Achter de computer

Werken in de zomer voelt nietecht als werken, vindt Jerome Bonnin. Het is een stuk ontspannender en daar boft de Fransman bij. De hele zomer moet hij doorbuffelen om zijn proefschrift op tijd af te krijgen. Vóór september moet de tekst bij zijn promotoren zijn.

Bonnin werkt als onderzoeker op de afdeling Mariene Chemie en Geologie van het Koninklijk Nederlands Instituut voor Onderzoek der Zee (NIOZ). Het NIOZ ligt verscholen tussen de duinen en de dijk op Texel, op een steenworp afstand van de veerboothaven. Op het instituut is de vakantietijd al begonnen. De lange, halfduistere gangen liggen er verlaten bij, in de kantine is het praktisch uitgestorven.

De deur van Bonnins werk-

'Niemand valt je lastig 's zomers'

kamer is volgeplakt met Franse cartoons. Aan de muur hangt een vrolijk gekleurd strandset te, compleet met schepte, vormpies en zeefje, als was het de standaarduitrusting van iedere zeebodem-onderzoeker.

Een kleine vier jaar geleden kwam Bonnin naar Nederland. Hit had net zijn studie geologie afgerond aan de universiteit van Bordeaux. Een beurs voor promotieonderzoek kon hit in Frankrijk niet krijgen. Zijn afstudeerbegeleider in Bordeaux, de Nederlander Frans Jorissen, wees hem op een vacature ij het NIOZ. Bonnin solliciteerde en kwam op Texel terecht.

Voor het NIOZ doet hij onderzoek naar de opwerveling van slib op de oceaanbodem. Zeestromingen brengen het weinig bekend', zegt Bonnin in zijn uitstekende Engels.

Vanaf het speciale onderzoeksschip van het NIOZ deed hij ter plaatse onderzoek. Met apparatuur mat hij de snelheid van de stromingen, onderzocht hij de troebelheid van het water en keek hij naar de samenstelling van het slib. En dat allemaal om een verband te vinden tussen veranderingen in de zeestromingen en veranderingen in het sediment.

Het slib bevat onder meer informatie over vroegere klimaatveranderingen en de manier waarop de oceaan daarop reageerde. Het onderzoek van Bonnin kan daarom bijdragen aan een beter begrip van klimatologische veranderingen. 'Je kijkt maar naar een heel klein stukje, maar misschien helpt het om een beter beeld van het hele proces te krijgen. Dat isuiteindelijk toch waar het in de wetenschap om gaat.'

De zeestromingen kunnen in enkele uren veranderen. Een van de sleutelwoorden van Bonnins onderzoek is daarom 'korte termijn.' Hierin schuilt het vernieuwende van zijn research. Want andere onderzoekers keken juist naar de lange termijn, naar de manier waarop de zeestromingen in de loop van jaren veranderen en de bodemsamenstelling beïnvloeden.

Wetenschappers uit andere disciplines zijn bij Bonnins onderzoek betrokken. 'Dat is een van de grote krachten van het NIOZ, de mogelijkheid om samen te werken', zegt de Fransman. 'Er zijn hier onder anderen fysici, chemici en biologen. En van tijd tot tijd proberen we iets samen te doen. Zo goed en zo kwaad als dat gaat, want iedereen houdt natuurlijk zijn eigen agenda.'

Deze zomer staat Bonnin er echter alleen voor. Niet dat hij daartegenop ziet. 'De zomer is ideaal om een proefschrift te schrijven. Niemand valt je lastig en je kan je volledig op het schrijven concentreren.' Bonnin werkt wel vaker 's zomers door. 'Het is best *relaxed*. Je neemt eens wat vaker een pauze en geniet van het weer. En het mooiste is dat je weet dat je na de zomer nog op vakantie gaat.'

Dirk van Harten